Simulation Based Grid Energy Storage Optimization to Enhance Renewable Energy Storage in Iceland

Michael E. Sugar

Faculty of Industrial Engineering
University of Iceland
2014

Simulation Based Grid Energy Storage Optimization to Enhance Renewable Energy Storage in Iceland

Michael E. Sugar

60 ECTS thesis submitted in partial fulfillment of a *Magister Scientiarum* degree in Environment and Natural Resources

Advisors
Rúnar Unnþórsson, University of Iceland
Egill Benedikt Hreinsson, University of Iceland
Ivan E. Tornes, Battelle Memorial Institute, USA

Faculty Representative
Teitur Birgisson, Landsnet

Faulty of Industrial Engineering
School of Engineering and Natural Sciences
University of Iceland
Reykjavík, May 2014

Simulation Based Grid Energy Storage Optimization to Enhance Renewable Energy Storage in Iceland
60 ECTS thesis submitted in partial fulfillment of a *Magister Scientiarum* degree in Environment and Natural Resources

Department of Mechanical Engineering, Industrial Engineering, and Computer Science
School of Engineering and Natural Sciences
University of Iceland
Hjarðarhagi 6
107, Reykjavik
Iceland

Telephone: 525 4000

Bibliographic information:
Michael E. Sugar, 2014, *Simulation Based Grid Energy Storage Optimization to Enhance Renewable Energy Storage in Iceland*, Master's Thesis, Faculty of Industrial Engineering, University of Iceland. pp. 117

Printing: Háskólaprent
Reykjavík, Iceland, May 2014

University of Iceland

Masters Thesis

Simulation Based Grid Energy Storage Optimization to Enhance Renewable Energy Storage in Iceland

Author:
Michael Sugar
Faculty Representative:
Teitur Birgisson

Supervisors:
Rúnar Unnthórsson
Egill Benedikt Hreinsson
Ivan E. Tornes

60 ECTS thesis submitted in fulfilment of the requirements for the degree of Master of Science

with the

Environment and Natural Resources Program
Department of Mechanical Engineering, Industrial Engineering, and Computer Science

May 2014

Declaration of Authorship

I, Michael Sugar, declare that this thesis titled, 'Simulation Based Grid Energy Storage Optimization to Enhance Renewable Energy Storage in Iceland' and the work presented in it are my own. I confirm that:

- This work was done wholly or mainly while in candidature for a research degree at this University.
- Where any part of this thesis has previously been submitted for a degree or any other qualification at this University or any other institution, this has been clearly stated.
- Where I have consulted the published work of others, this is always clearly attributed.
- Where I have quoted from the work of others, the source is always given. With the exception of such quotations, this thesis is entirely my own work.
- I have acknowledged all main sources of help.
- Where the thesis is based on work done by myself jointly with others, I have made clear exactly what was done by others and what I have contributed myself.

Signed: _____

Date: _____

"As I get older, I get smaller. I see other parts of the world I didn't see before – other points of view. I see outside myself more."

Neil Young

"It is remarkable how many things you can explode. I'm lucky I still have all my fingers."

Elon Musk

UNIVERSITY OF ICELAND

Abstract

School of Engineering and Natural Sciences
Department of Mechanical Engineering, Industrial Engineering, and Computer Science

Master of Science

Simulation Based Grid Energy Storage Optimization to Enhance Renewable Energy Storage in Iceland

by Michael Sugar

Abstract – Renewable energy resources are contributing evermore to the generation mix worldwide, however, expanding grids in size and complexity have given rise to unforeseen complications such as frequency oscillations, voltage sags and spikes, and power outages. In 2013, nearly 100% of electricity generation in Iceland was from hydropower and geothermal sources; there is also high potential for wind and tidal energy, both options are being explored and would benefit from additional technologies to manage fluctuations and store energy surplus. Landsnet hf. is the sole transmission system operator (TSO) responsible for energy balance in Iceland. On the consumer side, load variations represent difficulties for utilities to meet ever-changing demand. Research indicates high-capacity electricity energy storage (EES) has the potential to be economically beneficial as well as carbon neutral, all while improving power and voltage quality, peak-shaving, reducing the number of grid failures and smoothing out natural fluctuations in renewable energy (RE) sources. Two complex resource deployment scenarios are modeled using GridCommand^{TM} Distribution: (1) large-scale EES at the transmission level, and (2) small-scale community energy storage at the residential level. These scenarios are demonstrated to behave harmoniously in the Icelandic power system. Results reveal 10 MWh capacity battery EES at a density of 60% in the transmission model provides optimal performance conditions. The residential model requires a lower EES density of 30% using 45 kWh capacity batteries. Optimal conditions are defined by EES performance metrics, and signify improvements in power quality, energy balance, and peak-shaving when electricity demand is at its highest. EES technologies are presented and tested at different locations across the Icelandic grid to predict which solutions are best for the future development of the electricity system. The role of EES integration into Iceland's electricity grid has been explored with primary focus on improving energy efficiency, grid optimization, transmission and distribution control, and maintaining infrastructure.

Acknowledgements

Before the first word written, and the last sentence finished, through every obstacle and opportunity, from the first glow of predawn until the inky fatigue of every night, at each step of the way, I have been blessed with tremendous support and strength from my friends and family. I would especially like to thank my incredible parents Gloria and Perry for their never-ending wisdom and guidance, my little sister Carly for making me smile, the Sugar, Socken and Ash families, the Lipszycs, Diana and the Whitcombs, the Di Tomassos, Clayton, Niklas, Kamil, Pat, the Vibe Tribe, Reynir, and my advisor, Rúnar.

The researchers would also like to sincerely thank Orkuveita Reykjavíkur (Reykjavík Energy) and Landsnet hf. for their significant contributions in datasets, technical support and valuable information pertaining to this project. Battelle and Pacific Northwest National Laboratories (PNNL) contributed modeling software GridCommand^{TM} Distribution and GridLAB-D^{TM} aid in parsing the data files from Reykjavík Energy and Landsnet. These services were instrumental in building an accurate Icelandic grid model with which to run simulations.

Last, but certainly not least, I would like to thank Landsvirkjun, Orkustofnun and all donors who helped fund this project on Experiment (the crowdfunding site formerly known as Microryza) – it would not have been possible without all of your generosities. Thank you all.

Contents

List of Figures

List of Tables

Abbreviations and Nomenclature

AC	**A**lternating **C**urrent
ASCII	**A**merican **S**tandard **C**ode for **I**nformation **I**nterchange
BES	**B**attery **E**nergy **S**torage
BMS	**B**attery **M**anagement **S**ystem
CAES	**C**ompressed **A**ir **E**nergy **S**torage
CES	**C**ommunity **E**nergy **S**torage
CSV	**C**omma **S**eparated **V**alue
DC	**D**irect **C**urrent
DER	**D**istributed **E**nergy **R**esources
DG	**D**istributed **G**eneration
DOD	**D**epth **O**f **D**ischarge
DOE	**D**epartment **O**f **E**nergy
DR	**D**emand **R**esponse
DSO	**D**istribution **S**ystem **O**perator
DVC	**D**ynamic **V**Ar **C**ompensator
ε	**E**psilon constant
EDLC	**E**lectric **D**ouble **L**ayer **C**apacitor
EES	**E**lectricity **E**nergy **S**torage
ES	**E**nergy **S**torage
ESA	**E**nergy **S**torage **A**ssociation
EVs	**E**lectric **V**ehicles
FACTS	**F**lexible **AC** **T**ransmission **S**ystem
FES	**F**lywheels **E**nergy **S**torage
G2V	**G**rid-to-**V**ehicle
GCD	**G**rid**C**ommand^{TM} **D**istribution

GLD	**G**rid**L**AB-**D**^{TM}
GLM	**G**rid**L**AB-D^{TM} **M**odel
GES	**G**rid **E**nergy **S**torage
GT&D	**G**eneration **T**ransmission and **D**istribution
GUI	**G**raphical **U**ser **I**nterface
HMI	**H**uman **M**achine **I**nterface
IL	**I**ndustrial **L**oad
J	**J**acobian
kV	**K**ilovolt
kW	**K**ilowatt
kWh	**K**ilowatt **h**our
LA	**L**ead **A**cid battery
Li-ion	**Li**thium-**ion** battery
L	**L**oad
MW	**M**egawatt
MWh	**M**egawatt **h**our
MVAr	**M**egavolt-**A**mpere **R**eactive
NaS	Sodium **S**ulfur battery
NEA	**N**ational **E**nergy **A**uthority (Orkustofnun)
NiCd	**N**ickel **C**admium battery
NR	**N**ewton-**R**aphson Method
O&M	**O**perations and **M**aintenance
OR	**O**rkuveita **R**eykjavíkur (Reykjavík Energy)
PHS	**P**umped **H**ydro **S**torage
PNNL	**P**acific **N**orthwest **N**ational **L**aboratory
PP	**P**ower **P**lant
PSS/e	**P**ower **S**ystem **S**imulator (Siemens)
PV	**P**hotovoltaic
P_i	Net real **P**ower **i**njected
P_G	Real **P**ower **G**enerated
P	Real Power
Q	Reactive Power
Q_i	Net Reactive Power injected

RE	**R**enewable **E**nergy
RFB	**R**edox **F**low **B**attery
RTE	**R**ound **T**rip **E**fficiency
SOC	**S**tate **O**f **C**harge
SMES	**S**uperconducting **M**agnetic **E**nergy **S**torage
SNG	**S**ynthetic **N**atural **G**as
SS	**S**ubstation
TOU	**T**ime **O**f **U**se
TSO	**T**ransmission **S**ystem **O**perator
TWh	**T**erawatt **h**our
TWh/a	**T**erawatt **h**our per **a**nnum
UPS	**U**ninterrupted **P**ower **S**upply
V2G	**V**ehicle-to-**G**rid
$\|V\|$	**V**oltage magnitude
θ	Voltage angle (Phase angle)
VAr	**V**olt-**A**mpere **R**eactive
VRB	**V**anadium **R**edox **B**attery
VVO	**V**olt-**V**Ar **O**ptimization

For my family, friends, and loved ones...

Chapter 1

Overview

1.1 Introduction and Background

With ageing infrastructure and renewable energy (RE) generation on the rise, there has never been a more urgent need for a modern electricity grid. Many envision this modernized smart grid based on its capacity to integrate RE sources, being virtually carbon neutral, featuring improved voltage control, demand response and supply flexibility. Currently, the leading technology for achieving these modifications rests in grid electricity energy storage (EES). The technology exists today, however the need now is to provide tactical solutions, not technologies.

Energy storage is not a new concept in itself. Since the early uses of biogas for energy production and the invention of the first electrochemical battery in 1800 by Alessandro Volta, energy storage has become common for many household and industrial applications (Yang *et al.*, 2011). It has also been an integral component of electricity generation, transmission and distribution (GT&D) systems for well over a century (ABB, 2012). Traditionally, the capacity for EES has been met by the physical storage of energy reserves in fossil fuels and harnessed by power plants, as well as through large-scale pumped hydro storage (PHS) plants (ABB, 2012). The power landscape has changed dramatically in recent years, bringing the proliferation of modern RE sources as a means to meet today's energy and environmental demands, albeit these changes have given rise to a surprising number of unforeseen obstacles. At the beginning of its development, RE generation technology focused more on harnessing the maximum power from renewable resources, ignoring the need for power system reliability and stability (Yang *et al.*, 2011). Output fluctuations from renewable energy sources otherwise known as intermittencies, which are common with wind, tidal and solar photovoltaic (PV) generation, lead to variability and uncertainty in electricity production to the grid (Lavine *et al.*, 2011; Yang *et al.*,

2011; Rahman *et al.*, 2012; ABB, 2012). Such fundamental changes in the design and controllability of the grid call for smart, efficient power GT&D networks, and energy storage solutions.

Assessing and planning for future changes to the Icelandic power system are best explored with advanced modeling tools. This study uses GridCommand^{TM} Distribution (GCD) and GridLAB-D^{TM} (GLD) softwares for its analysis of two complex resource deployment scenarios. Multiple configurations of EES technologies are tested at different locations across the Icelandic grid to predict which solutions are best for the future development of the electricity system with energy storage. Results underscore the intended motivations behind the research, highlighting improvements in Icelandic grid energy efficiency, maintaining infrastructure, dampening load variations, taking advantage of energy arbitrage, and sparking concepts for a smarter grid with greater transmission and distribution control. Landsnet has installed a very workable transmission network across the country; therefore the main goal here is assessing how best to implement EES devices for storing Iceland's annual energy surplus, as well as helping establish smart grids for better voltage control and distribution on the local scale. Goals and study relevance will be outlined next.

1.2 Smarter Grids: Goals, Relevance and Motivations

Electricity networks are in a continual state of change, propelled by many interconnected factors: ageing infrastructure, installation of distributed generators, increased alternative energy, regulatory incentives and the availability of new technologies. A smart grid intelligently integrates the actions of all connected users – producers, consumers and those that do both – in order to efficiently deliver sustainable, economic and secure electricity supplies as efficiently as possible (Wade *et al.*, 2010). Rollout of smart grid technology also implies a fundamental re-engineering of the electricity services industry. Generally speaking, technical infrastructure retrofits would be necessary in the Icelandic power system, however these additions would help tack on several years to the lifecycles of current infrastructure by alleviating stress-points across the grid. This research defines EES as a key component in smart technologies that contribute to energy efficiency, voltage control, reduced risk of oscillations, maintaining infrastructure, integrating intermittent energy sources, and energy balancing, which are all imperative research objectives. The data collected from the simulations are used to evaluate the impacts of new smart grid technologies.

According to Landsnet (2013A), *"power generated into the grid cannot be stored, therefore power must be consumed as soon as it is generated"*. In other words, electricity production equals consumption at any given time. Utilities must prepare detailed day-ahead schedules to ensure this delicate balance of electricity generation and consumption is met, deriving the second motive for investigating EES in Iceland. The power schedules state that the amount of electricity they intend to generate or purchase for the next day equals their intended sale to customers or other power companies.

In Iceland, generating companies and suppliers are referred to as Balancing Responsible Parties (BRPs). Although a BRP submits to Landsnet a schedule that is in balance for the next day, deviations often occur in practice because power consumption cannot always be predicted perfectly. An energy market equipped with energy storage and smart technologies could potentially integrate with utility and BRP demand response programs, engage in permanent load shifting, reduce peak demand and cope with distributed generation.

Another major goal of this thesis is to create a strategic and logical approach to grid optimization using energy storage solutions for the Icelandic utilities to consider moving towards 2020 and beyond. Achieving this formula for success involves two parts: conducting a detailed analysis of the Icelandic power system after increased EES capacity has been installed, and secondly communicating the results of these simulations in a manner that is constructive for an economically viable and environmentally beneficial outcome. Researching EES in Iceland offers tremendous upside, and should be viewed as a template by other countries for improving their existing grids. It is important for Iceland, a model country in renewable energies, to lead by example and set a precedent for developing its smart grid.

Should the Icelandic government agree to terms with the UK for subsea transmission of Iceland's renewable energy, EES is imperative to manage such a large change in the power system, one that would effectively alter Iceland's electricity market from a balanced islanded network to an unbalanced system. The environmental footprint of grid infrastructure has also come under increased criticism in recent years. Lessening environmental impacts and protection from the unpopular damming of scenic rivers and landscape for hydropower is another motivation for this thesis, and since EES allows for the efficient integration of the country's unrivaled potentials in alternative energy sources such as geothermal, wind, and tidal, the concept of planning a grid to accommodate these changes became apparent. Finally, the possibility to store 100% renewably sourced electricity derived the third motivation to investigate EES in Iceland. A grid capable of storing 100% renewable electricity and the roughly 10% annual energy surplus may alleviate concerns of rising electricity prices in the country through a better energy

arbitrage system. These research objectives fall in line with the Landsnet priorities of becoming a leader in the introduction of smart grid solutions focusing on renewable energy, to foster energy-market innovation through increased value creation and sustainability (Landsnet, 2011).

1.3 Research Questions

Six overarching questions govern the direction of this research project and how it seeks to achieve its goals:

1. What role does energy storage (ES) play for grid optimization, energy arbitrage and peak reduction?
2. Which of the following EES configurations are most efficient in terms of grid optimization:
   (a) Transmission level (large-scale storage);
   (b) Distribution level (small-scale, community energy storage);
   (c) Clustered versus evenly distributed storage.
3. Does GridCommand^{TM} Distribution allow for accurate representations of power flows (both real and reactive) in the grid, and can both complex resource deployment scenarios ensure grid storage optimization?
4. Will identifiable weaknesses within the Landsnet transmission system be improved or solved with the aid of EES integration in GridCommand^{TM}?
5. How will EES address concerns of rising electricity prices and energy arbitrage in Iceland?
6. What does the future hold in store for energy storage?

1.4 Scope of Study

1.4.1 Overall Thesis Structure

Once sufficient background has been provided on the Icelandic power system and its electricity market in chapter 2, technical aspects of energy storage are then covered in chapter 3. Next, this thesis will move on to its second phase by explaining the methodology (chapter 4), demonstrating the simulation results (chapter 5) and providing

a comprehensive analysis of significant findings (chapter 6). A base case representing the present day layout of the grid is shown, next the performance metrics section examines the impacts of EES by comparisons between the base case and the case with newly added technologies. Post-processing on all simulations appears in graphs and tables to better interpret the data, followed by recommendations for Iceland to consider moving towards 2020, the possibility for future studies, a summary of the findings and how they answer the research questions, and lastly concluding statements.

1.4.2 Resource Deployment Scenarios

Approaching the design and analysis of future grid alterations requires simulations to be created with specific scenarios in mind to refine the scope of models in the GCD program, which bears hundreds of possible analytical tools and options. Therefore, the plan for drafting scenarios with high priority needs for the Icelandic power system was imperative.

Grid energy storage and its optimization are the main focus of this thesis. It is intended to serve as a reference for power systems engineers, planners, and policymakers interested in improving energy efficiency and taking full advantage of the environmental and innovative stronghold Iceland is fortunate to possess. While the emphasis is on technology, this study also addresses the significant policy, market, and other non-technical factors that may encumber the proposed solutions. It will provide a short background of Iceland's electricity markets, a review of the country's power system from producer to consumer including the relevant companies in charge of GT&D, a technical and economic summary of leading-edge EES technologies, and the solutions to the following two (2) resource deployment scenarios:

1. Li-ion community energy storage (CES) of varied densities arranged in evenly distributed configurations; and
2. Sodium sulfur (NaS) electricity energy storage for the transmission system in Iceland, of varied densities and in both evenly distributed and clustered configurations.

Economic aspects of energy storage are identified in the EES review (chapter 3), though considered beyond the intended scope of this technical and simulation-focused thesis. Therefore, there is room for further exploration into the economic aspects of energy storage and grid optimization in Iceland. Explicit analysis of power system oscillations are excluded for two reasons: (a) small signal stability (SSS) analysis has already been conducted for the Icelandic grid, and (b) GCD intrinsically incorporates these calculations

of real and reactive (or "imaginary") power flows when running simulations. This project also excludes solar PV additions to the grid, as Iceland is not currently considering widespread PV installations.

Temporal or time series data are modeled with a 12-month time signature ranging from 00:00:00 of January 1, 2012 to 23:59:59 of December 31, 2012. Simulations with the addition of EES are conducted using a three-day timestamp from July 7 to July 9, 2012 to keep results consistent. Transmission-level and industrial loads used in GCD models are representative of 2012 with the same timeframe. More information on timestamps and time signatures in the data can be found in the methodology chapter.

The geospatial scope is limited to Iceland, which is modeled by identifying the geographic locations of infrastructure in the Icelandic power system. Latitude and longitude coordinates were obtained using Landsnet's single-line diagram of the grid (see Appendix), an interactive satellite map of the transmission system from Loftmyndir (Loftmyndir, 2013), and Google Maps for cross-referencing location coordinates to the third decimal place to match Icelandic networks. Residential feeders were adapted from generic residential feeders to match Icelandic residential networks, stressing the importance of scale and detail to ensure the accuracy of each model and its results.

1.5 Research Protocol

Preparations for this project began by reviewing scientific journals and past academic research papers to form the basis of interpreting existing information on the technical aspects of the Icelandic power system and its energy markets. Next, articles on grid optimization, management, and electricity energy storage with a largely international perspective. From here, focus was refined to drafting ideas and concepts tailored to Icelandic markets and infrastructure aimed towards developing a transmission and residential level smart grid. In order to achieve this, large and comprehensive datasets were required to gain a thorough understanding of the intricacies within the Icelandic power system and to build a model. Public and some private files were made accessible in the forms of digital Excel copies, raw text (ASCII) files, and comma-separated values (CSV) tables from Landsnet, Orkuveita Reykjavíkur (OR), and Landsvirkjun. Advanced modeling software GridCommand^{TM} and GridLAB-D^{TM} were sought to assist in analyzing the Icelandic grid with new EES features for areas that were deemed feasible and advantageous to the country.

1.6 Contributions

The research intends to contribute to the state of knowledge in power systems analysis for Icelandic utilities and academic institutions alike seeking to investigate grid energy storage optimization and smart grid technologies. By providing a framework for planning infrastructure proliferation as well as specifically detailing the benefits of energy storage to the Icelandic power system, it will contribute an innovative approach to improving grid efficiency, managing peak demand and ease Landsnet's efforts in energy balancing, reducing power outages and disturbances, and ensuring high power and voltage quality. Most importantly, in the spirit of GridLAB-D^{TM} and its open-source collaboration efforts, the codes developed for this study are openly available for any future studies under the *Creative Commons "CC BY 3.0"* license. Allowing for a meaningful re-interpretation of the grid provides the grounds necessary for addressing the proposed research questions and motivations of this thesis. Iceland is in a unique position when it comes to its energy future, and by exploring its electricity system in a manner that considers new technologies, other countries can potentially derive their grid developments and increase renewables penetration using a similar approach presented herein.

Chapter 2

The Icelandic Power System

To serve as a background for this thesis, a synopsis of the current power system in Iceland is provided while underlining the main goals and objectives of the research. The three largest companies generate 97% of total electricity produced and are active in the wholesale market. The dominant producer, Landsvirkjun, produces 74% of total electricity. Smaller producers either sell directly to their own retail division or enter 7-10 year contracts with retail sales companies (Orkustofnun, 2011).

2.1 Electricity Markets and Energy Reality

Iceland is rich in RE resources compared to the country's energy requirements and demands. In 2013, nearly 100% of electricity and energy for heating were generated from renewable hydropower and geothermal sources, along with small contributions from two wind turbines. Consequentially, this abundance of RE draws significant interest from energy-intensive industry and data centres, of which consume roughly 80% of total electricity, including 74% used by the aluminum industry alone in 2009 (Lochet *et al.*, 2012, Orkustofnun, 2011). Landsvirkjun and Landsnet (2013A) reported residential loads utilize only 5% of total electricity, and still per capita electricity consumption is the highest in all of Europe (Orkustofnun, 2011; Landsvirkjun 2013). This statistic is considered to be a misrepresentation inflated by the overwhelming electricity demand by power-intensive users.

Orkustofnun is the National Energy Authority (NEA) in Iceland, and together with the Icelandic Parliament, the Althingi, implemented a set of common rules governing the internal market of electricity known as the Electricity Act, no. 65/2003 in 2003 (Orkustofnun, 2011). The Act has been amended several times in the years since, and

is broad in scope, containing comprehensive legislation on the generation, transmission, distribution and supply (sale) of electricity all as part of a competitive market (Orkustofnun, 2011; Lochet *et al.*, 2012). Iceland's parliament also recently adopted *Master Plan for Hydro and Geothermal Energy Resources*, a blueprint for the utilization of natural resources in the near future. Any planning of the grid's future development must be based on the guidelines set out in the Master Plan as well as on projected economic and population development. Landsnet is the independently managed transmission system operator (TSO), and solely responsible for delivering electricity to the six main distribution system operators (DSO) and energy-intensive industry (Landsnet, 2013A). All DSOs have exclusive rights to distribute electricity in designated areas of operation, the six companies include: Reykjavík Energy, Rarik, HS Orka, HS Veitur, Orkusalan and Westfjords Power (Drevdal *et al.*, 2011; Orkustofnun, 2011). The NEA regulates the transmission and distribution companies, ensuring their delivery of high quality electricity and security of supply. Landsnet constantly monitors frequency and voltage quality in the entire transmission system with a target system frequency of 50 Hz implying satisfactory quality of electricity. According to Landsnet (2013A), under normal operating conditions the average operating frequency measured over 10 seconds must be within the following quality limits:

50 Hz ± 1% (i.e. 49.5−50.5 Hz) 99.5% of the time.
50 Hz + 4 / 6% (i.e. 47.0−52.0 Hz) 100% of the time.

Security of supply is defined as the reliability of the entire power system and encompasses all links of the value chain of electricity supply, including the generation of electric energy, distribution of electric energy, and trading and retail (Haarla *et al.*, 2011; Grave *et al.*, 2012). Utilities in Iceland must therefore ensure consumer demand for electric energy is covered at the present day and in the future in an uninterrupted and sustainable manner (Batlle and Rodilla, 2010; Landsnet, 2013A). The concept especially applies to supply security during peak hours, noting the ability of the electric system to withstand sudden disturbances or failures.

Electricity trading may now occur through bilateral contracts and is on the verge of changing the future of Iceland's energy markets (Orkustofnun, 2011; Lochet *et al.*, 2012). According to the stated objectives of the Electricity Act, it is intended to encourage an economical electricity system, thereby strengthening Icelandic industry as well as regional developments. To reach this goal, it was sought to create a competitive environment for the generation and sale of electricity, encourage efficient and cost effective transmission and distribution of electricity, ensure the security of the electricity system and interests of consumers, and promote utilization of RE resources (Landsvirkjun, 2013B). Since the grid is balanced with no connections to larger, unstable foreign markets and with high

controllability over geothermal and hydropower, energy balancing is relatively simple compared to North American and European markets. That means electricity is delivered in real-time with customer demand at a high security rate. However, due to the variation in river flows, customers in the Icelandic power system can negotiate to take out a certain amount of the total energy as secondary energy (METSCO, 2013). The secondary energy is then sold at a lower rate than the primary energy, but the delivery is only guaranteed up to a specific minimum amount. This represents another area EES can earn its keep, by improving energy reserves and arbitrage.

Energy arbitrage is the act of buying low and selling high (in terms of electricity pricing). Arbitrage involves purchasing inexpensive electricity when its demand and cost are low (i.e. at night); and then selling the electricity when demand and price are high during the day (ESA, 2013). Storage systems that operate in this market generally have the capacity to store large amounts of energy, interact with the power grid at the transmission level, and operate on a diurnal cycle of charge and discharge. Examples of this EES include pumped hydro plants, compressed air electricity storage facilities, and large battery installations. As a result, power intensive industries that have a certain flexibility to reduce consumption during dry spells in power supply can find it beneficial to take a part of the power at a lower price in the form of secondary energy.

The electricity system has an installed capacity of 2119 MW and is currently being increased in one location at Búðarháls power station (Landsnet, 2013A). Annual power consumption in Iceland increased from 16.3 TWh/a in 2009 to 17.7 TWh/a in 2013; see Table 2.1. Generation capacities are shown in Table 2.2. The increase in electricity demand from power intensive industries has called for considerable investments in the transmission system.

TABLE 2.1: *Electricity consumption and demand growth between 2009 and 2014 (projected) is expected to rise by 2.6 TWh, a 15.95% increment in the period (Landsnet, 2012B).*

	Energy 2009 [TWh/a]	Energy 2013 [TWh/a]	Energy 2014 [TWh/a]	Growth [%/a]	All time peak [MWh/h]	Peak 2014/15 [MWh/h]
Iceland	16.3	17.7	18.9	3.2%	2.108	2.411

TABLE 2.2: *Net addition in generation capacity (Landsnet, 2012B).*

	Hydro [MW]	Geothermal [MW]	Other [MW]	Installed capacity [MW]	Available capacity at peak [MW]
Installed capacity in 2011	1,842	542	100	2,484	2,344
Net addition until 2014	95	124	0	219	2,562

Electricity in Iceland is transmitted on to the national power grid, a circular pass-through system that is renowned to be one of the most secure and modern power grids in the world (Haarla *et al.*, 2011; Landsnet, 2012A). Electricity consumers can connect to the

power grid almost anywhere they wish, regardless of their energy supplier (Orkustofnun, 2011). Locations near power plants and with several connections offer the most secure transmission of electricity. The physical layout and technical aspects of the grid are detailed next.

2.2 Present Day Grid Infrastructure

The Icelandic power system is a balanced, isolated system with no present-day connections to other countries, although a submarine cable connecting the UK grid (Germany and Norway also being discussed) is being widely debated (Hreinsson, 2013). New infrastructure development requires extensive planning and consultation with numerous stakeholders, whose standpoints can vary immensely (Landsnet, 2011). Small structural and installed capacity changes to the grid are occurring at the time this thesis was written.

The transmission grid consists of 3,204 km of overhead transmission lines, while the length of the DSO network (sum of all DSO's cable infrastructure) is approximately 22,565 km (Landsnet, 2013A). The transmission system connects 72 substations, with 77 supply points, of which 19 are power plants, five are power-intensive industries, and 53 are supply points to the DSOs (Landsnet, 2013A). For example, Landsnet transfers electricity to Reykjavík Energy through 12 supply points (A1 to A12).

The transmission system operates at voltages of 33 kV, 66 kV, 132 kV and 220 kV – see Figure 2.1. For the most part, the 132 kV lines form a ring network around the whole of the country. Everything below the 33 kV voltages occurs at 11 kV, which is then finally brought down to 400 V or 230 V and supplied to residential and some commercial loads by the DSOs – see Figure 2.2. The main residential load centre is in the southwest part of the island in the Greater Reykjavík Area.

High-voltage AC (HVAC) overhead cables transmit electricity in Iceland on the transmission level. Landsnet's transmission towers are made of either timber or steel, incorporating design elements that allow infrastructure to tolerate high winds and icing events (Landsnet, 2013A). Another important infrastructure requirement applies to the distance of conductors from the ground, whereby line voltage is the main determinant for the height of transmission towers. As a general rule, the higher the voltage the greater the tower height will be (Landsnet, 2013A). For this reason, the towers for 220 kV lines are made of steel with concrete foundations. Therefore, weather and line voltage are the main determinants for building materials used in the grid.

FIGURE 2.1: *Geographic layout of Iceland's transmission system as of 2012. Each triangle denotes a power plant, all other objects pictured are power intensive industry (Landsnet, 2013A).*

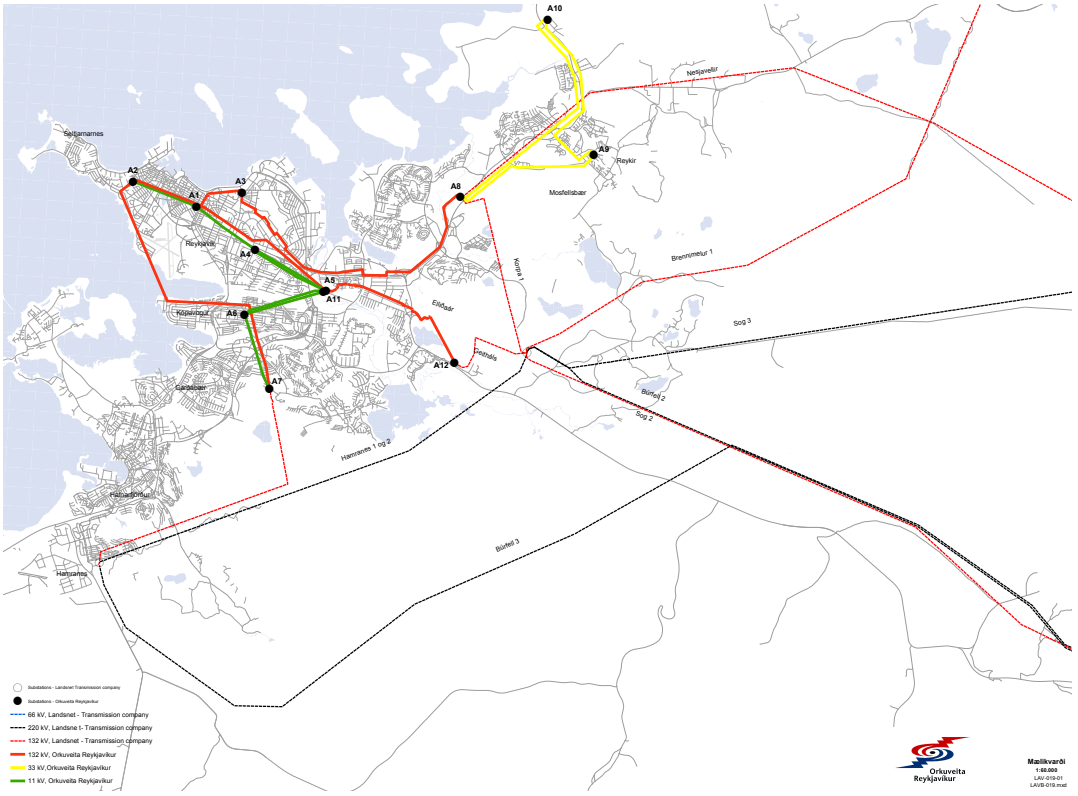

FIGURE 2.2: *Main transmission electric network supplying the DSO in the Greater Reykjavík Area at twelve major substations labeled A1 to A12 (Orkuveita Reykjavíkur, 2014B).*

There are currently no EES installations existing in Iceland, though the infrastructure is more than capable of integrating battery or other storage devices. The Icelandic power system does make use of dynamic VAr compensators (DVC) and other flexible AC transmission systems (FACTS) devices to control oscillations (such as harmonics and feedbacks that cause voltage sags or spikes, weakening power quality). For instance, one dynamic reactive power system unit is installed at the 132 kV Hryggstekkur substation in the east of Iceland, and connects to the Fljótsdalur substation at the Kárahnjúkar power plant, which is primarily supplying 540 MW power to the Alcoa aluminum plant (Guðmundsson *et al.*, 2006) (see Figures 2.3 and 2.4). There is also a reactive power compensator (for MVAr) that has recently come online at the Grundartangi industrial site at Klafastaðir. The compensator will increase the transmission capacity to Grundartangi and enable Landsnet to meet increased power demand without the need for additional power lines. Another benefit of this device is enhanced grid voltage control, having a predictable positive effect on power quality and the operation of the whole grid (Landsnet, 2013A). However, once electricity is in the grid, there is no current technology for its storage. The single-line diagram shown in Figure 2.3 is only a small portion of the entire Landsnet grid, where circular objects pictured denote generating units such as power plants, triangular objects denote load centres, thick lines show electrical buses and finally thin lines denote branches. Nominal line voltages are shown numerically beneath buses, while real powers (MW value) are given above branches and reactive powers (MVAr value) below the branch. Figure 2.4 illustrates the voltage and current control and monitoring abilities of the same Hryggstekkur DVC system shown in Figure 2.3.

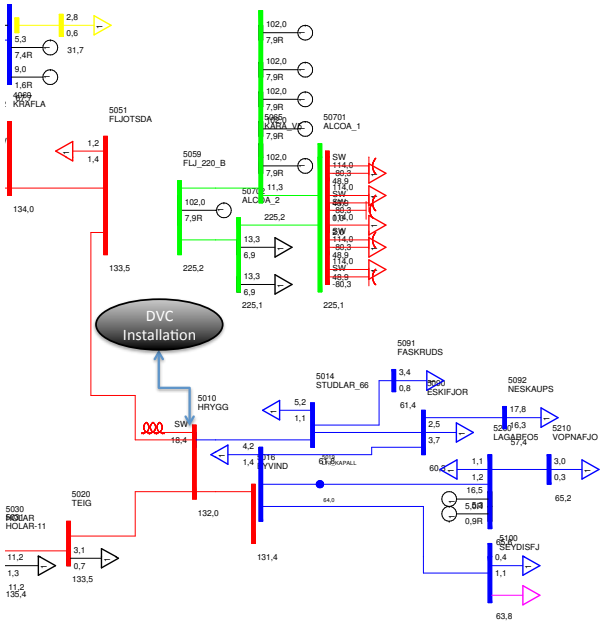

FIGURE 2.3: *Landsnet's DVC installation at Hryggstekkur substation shown in single-line diagram.*

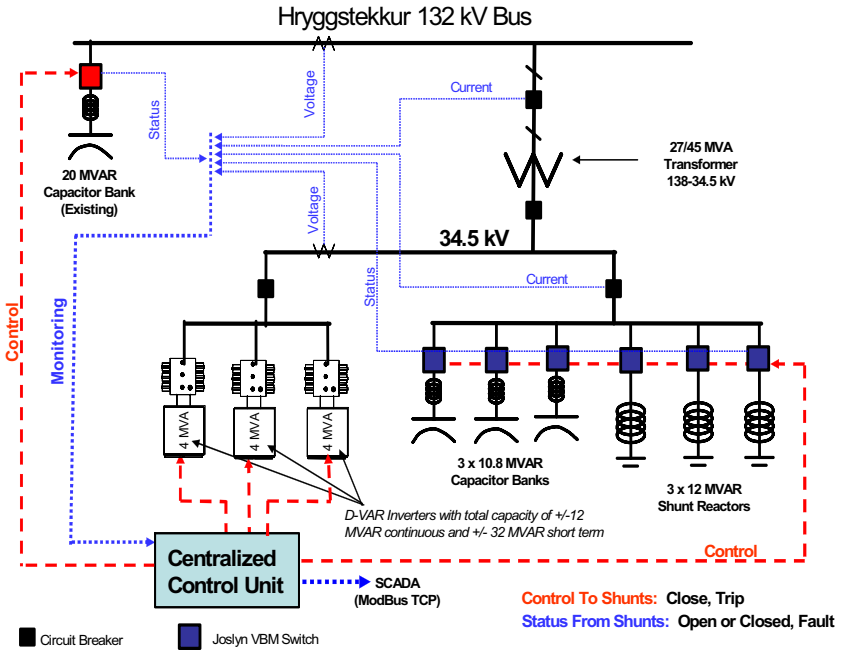

FIGURE 2.4: *A more detailed depiction of the DVC system layout at Hryggstekkur substation (Guðmundsson et al., 2006).*

Backup power generators are somewhat common too, especially for emergency power situations. Construction of a new backup diesel generator at Bolungarvík substation is currently underway with six power generating sets for prime power output of 1800 kW, up to 1500 RPM at 50 Hz (Landsnet, 2013A). Another generator located in Hafnarfjörður uses jet motors for provisions to the Alcan aluminum plant. However, these backup generators do not have remotely as much functionality as the EES solutions (Li-ion CES and NaS batteries) may offer the future grid, mainly because generators are unable to buffer small, rapid fluctuations in real and reactive power as efficiently as EES due to their discharge times as explained in the EES review chapter.

Another important consideration is the visibility of power infrastructure and the efforts that must be made to rethink Iceland's transmission routing and siting (Landsnet, 2012B). Landsnet seeks to construct fewer overhead, high-capacity transmission lines to lessen the number of lines across the country's landscape in the future, minimizing the grid's visual impact. It is significant to note that the current grid is not up to the task of connecting new power stations envisaged in the Master Plan (Landsnet, 2012B). At present, it only has enough capacity to connect the prospective power station on the lower Þjórsá river. Furthermore, heightened generation and thereby transmission demand calls for greater capacity and flexibility in the grid's operation, which will not be achieved without further strengthening the network. It is the author's opinion that wisely sited EES will offer a technical and aesthetic advantage in contrast to scarring the Icelandic landscape with more elaborate transmission networks, towers and cables, such

as the planned Skrokkaldalína line that would pass through the heart of the country's highlands and national park. Figure 2.5 shows Landsnet's vision for Iceland's future grid.

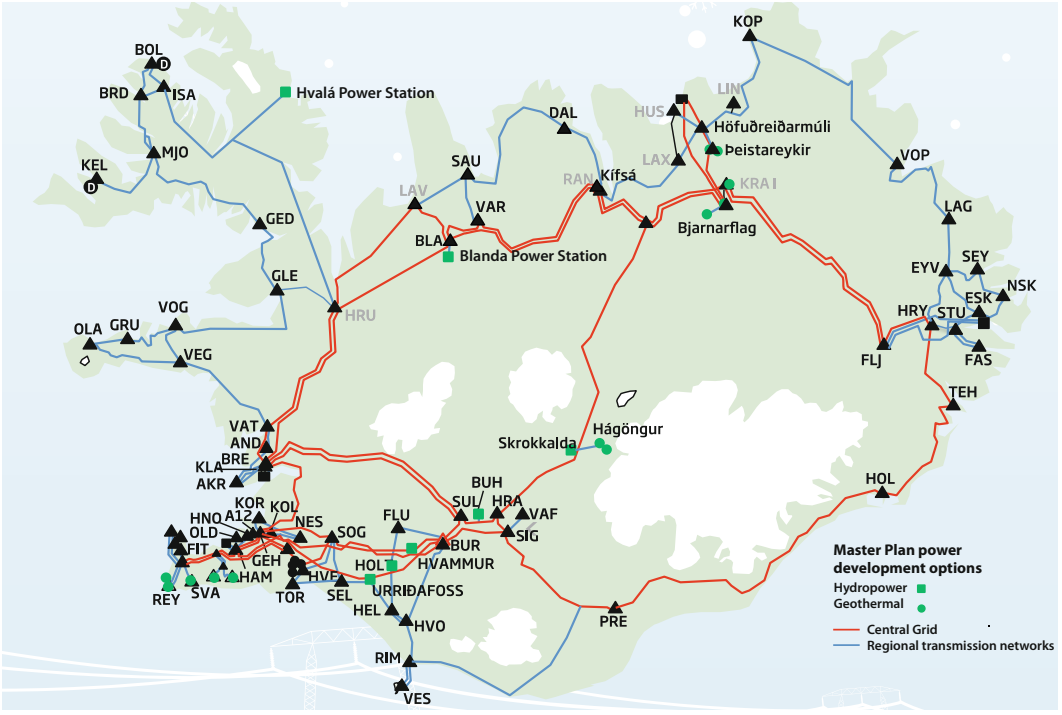

FIGURE 2.5: *Next generation of Landsnet prominently features new transmission line Skrokkaldalína crossing through the heart of the country's highlands and national park (Landsnet, 2013A).*

2.3 Grid Failures, Disturbances, and Power Outages

Although Landsnet operates a balanced, relatively modern grid in comparison to the size and complexity of many European and North American markets, there are still several inherent complications with its transmission and distribution. Most of the grid disturbances, however, are triggered by extreme Icelandic weather events. In fact, the year 2012 saw an unusually high occurrence rate of grid disturbances with severe storms acting as the prime culprit in every power outage (Landsnet, 2013B). Some cases even producing permanent damage to the grid, for instance, on January 10 and 11 the "Salty Storm" caused a number of transmission level failures in west Iceland. Heavy saline ocean spray was deposited on electrical equipment; the salt buildup eventually caused a substation in the Southwest called Brennimelur to explode and catch fire, leading to a four-hour transmission level power outage. This poses another area of perceived opportunity for energy storage in Iceland, for when several locally deployed NaS batteries can supply microgrids with power during transmission disturbances.

Two conflicting Landsnet reports (Performance Report, Landsnet (2013B); and Annual Report, Landsnet (2013A)) recount a total of 55 and 88 disturbances in 2012, respectively. These disturbances accounted for unsupplied energy to customers totaling 5703 MWh for the year, much higher than 4900 MWh from the preceding year (Landsnet, 2013B). Backup generators operated during disturbances in 2012 produced 1.174MWh. The main grid failure incidents were as follows:

- January 10, 11 storms triggered multiple transmission disturbances across the grid, particularly in west Iceland where saline build-up on electrical equipment produced a four-hour outage at the Brennimelur substation. This resulted in a substantial curtailment for power-intensive consumers at Grundartangi. Considerable flashovers also occurred in south and west Iceland. Energy not supplied to distributors (excluding power-intensive industries) measured 51.98 MWh (Landsnet, 2013B).

- February 22 failures at Fljótsdalur substation tripped large oscillations in east Iceland, including Fljótsdalur Line 3. Energy not supplied measured 126 MWh (Landsnet, 2013B).

- September 10, an intense northerly storm swept over the country with snow and ice buildup on power lines. Laxá Line 1 tripped, followed shortly by Kópasker Line 1 and Krafla Line 1. When the Blanda Line 2 tripped at midday, north Iceland was without power from Varmahlíð east to Krafla, including the towns of Sauðárkrókur, Akureyri and Dalvík. The weight of the ice and snow caused all damaged earth lines to sag down into the phase conductor, catastrophically damaging the transmission cables. Energy lost was recorded at 674 MWh (Landsnet, 2013B).

- November 1, another powerful northerly storm ripped through the country, triggering a number of serious trips in the distribution networks and other parts of the system. Most notably, the Fljótsdalur Line 2 tripped, quickly followed by the Sigalda Line 4/Prestbakki Line 1 (which both failed twice). Energy not supplied totaled approximately 38 MWh (Landsnet, 2013B).

- November 5, saline-saturated winds hit Iceland's Southwest region, causing massive large-scale outages in the Greater Reykjavík, which was without power for four hours. Energy not supplied was assessed at 74.5 MWh (Landsnet, 2013B).

- November 20-22, Tálknafjörður Line 1 tripped five times due to icing and a storm that swept through the Westfjords. Energy not supplied measured 87.8 MWh (Landsnet, 2013B).

- December 29, upon the arrival of the storm the Westfjords lost power first for a lengthy period, as did the town of Ólafsvík. The Ólafsvík Line was badly damaged, with a total of 67 towers broken. Towers on the Geiradalur and Mjólká Lines were also damaged. Minor failures occurred on the Breiðidalur and Tálknafjörður Lines. The Laxá Line suffered two breakdowns but was quickly repaired as the weather in the northeast was much more favourable than in the west. This storm caused extensive outages, with energy not supplied totaling 1911 MWh (Landsnet, 2013B).

Chapter 3

Potential EES Technologies

3.1 Terminology and Applications

The basic role of energy storage is to absorb energy when renewable energy output is high or while demand is low, and to discharge that energy during low RE output (i.e. low-wind days) or during peak-demand. Choice of storage technology is strongly influenced by the intended application to the grid and the duration for which the ES system may need to continuously charge or discharge. There is no single ES system that meets all grid applications. Three grid energy storage applications are summarized:

1. **Power quality**: Stored energy, in these applications, is only applied for milliseconds to minutes, assuring uninterrupted power supply (UPS) and voltage frequency regulation. Frequency regulation means maintaining a smooth voltage across the grid, preventing fluctuations in signals and reducing stress on transmission lines and power plants (Kaldellis and Zafirakis, 2007; Rahman *et al.*, 2012).

2. **Bridging power**: Stored energy used for minutes to hours, maintaining network continuity when switching from one source of energy generation to another or during transmission outages. This is also sometimes referred to as *spinning reserve* (Kaldellis and Zafirakis, 2007; Rahman *et al.*, 2012).

3. **Energy management**: Storage media in this application is used for many hours, to decouple the timing of generation and consumption of electric energy. Typically called *load leveling*, which is the charging of storage when electricity cost is low (Kaldellis and Zafirakis, 2007; Rahman *et al.*, 2012).

3.2 Direct and Enabling Technologies

The technologies deployed as part of the simulation's complex resource scenarios can be placed in one of two categories: direct and enabling. Direct technologies are those that provide direct benefit to the system. Enabling technologies are those that may not provide a direct benefit to the system, but they enable other beneficial technologies. As an example, a communications network does not provide any reduction in energy consumption, but it does enable demand response systems that create reductions in energy consumption (Schneider and Bonebrake, 2012).

3.2.1 Direct Technologies

The following technologies that will be specifically analyzed using GCD simulations are selected based on the motivations for this thesis and the technologies that are available within the GCD program for modeling. Direct technologies chosen for deployment in GCD include:

1. Energy storage (ES) – NaS and CES Li-ion for peak-shaving and voltage control;
2. Demand response (DR) – Time of use (TOU) with/without enabling technology.

3.2.2 Enabling Technologies

Despite their lack of direct benefits, these technologies form the foundation necessary for the technologies that do provide direct benefits to the system (Schneider and Bonebrake, 2012). These technologies are outlined in the following sections and include: (1) smart meters, (2) communication infrastructure, (3) human machine interfaces, and (4) battery management systems.

3.2.2.1 Smart Meters

Traditional electromechanical metering devices have proven to be accurate and reliable over multiple decades, but have the significant disadvantage of requiring manual data collection, which is a tedious, time-consuming task; there is no network connectivity. The deployment of new "smart meters" is the second largest component to future Icelandic grids (next to EES) as it enables the proper functioning of EES and improves demand response. These new meters allow one-way or bi-directional communications via a wired or wireless communications network. Communications to the customer can now include

time-based electricity rates or event-triggered signals, and allow the customer to read their meters quickly and more easily to adjust consumption patterns (Schneider and Bonebrake, 2012).

3.2.2.2 Communications Infrastructure

Communications infrastructure, both wireless and wired, is an excellent example of enabling technology, for it does not provide any direct benefit to the system. However, direct technologies, such as demand response, would not be possible without a supporting communications infrastructure (Schneider and Bonebrake, 2012). For the purpose of the conducted analysis that follows, it is assumed that the required communications infrastructure is available, but it will not be simulated in these experiments. Zero latency and infinite bandwidth is assumed.

3.2.2.3 Human Machine Interface

Human Machine Interfaces (HMI) can exist in many forms, but is strictly an enabling technology seen in residential networks. For instance, in a single-family residence, the HMI can range from a simple thermostat to a fully functional home energy management system. An HMI might also allow users to see the current price of electricity, adjust their consumption accordingly, or interact with an energy storage system (like an electric car). By providing an end-user with more information about the current price of electricity and the state of their consumption, the effectiveness of demand response opportunities is dramatically increased (Schneider and Bonebrake, 2012).

3.2.2.4 Battery Management Systems

Battery management systems (BMS) are centralized controller objects responsible for directing battery functions and communications in electricity networks. In GridCommand^{TM} and GridLAB-D^{TM}, the BMS controller monitors current and voltage from one or more battery cells and determines if the current is above or below a predetermined value. If for example the current is below the predetermined value (e.g. at nights), the BMS disconnects the battery cells from the load once the voltage falls below a voltage threshold (e.g. 11 kV). Once disconnected a reset signal is required to reconnect the battery cell(s) to the load. These BMS objects provide a host of other applications such as protecting batteries from operating outside its safe operating area, monitoring its state of charge, and even controlling its climate and environment.

For the Icelandic models retrofit with Li-ion and NaS batteries, the BMS technical specifications and system architecture are prudently defined using parametric analysis inside GCD. These parameters include charge setpoints, peak-shaving setpoints, charging and discharging rates, etc. All setpoint parameters can be referred to in the parameter tables from chapter 5.

3.3 Technical Considerations of EES

Performance requirements of EES are dependent on cycle life, state of charge (SOC) or depth of discharge (DOD), energy-to-power ratio, discharge times, and application. For example, to regulate frequency, the EES capacity may not need to be long lasting (minutes can be sufficient) but it must have a long cycle life because the system is likely to encounter multiple daily charge-discharge events. In comparison, energy management applications such as load leveling require systems with huge capacities (i.e. MWh or even GWh) that are capable of discharge durations for hours to days. For this application, preferred EES will have high round-trip efficiency (RTE) and a large DOD, along with low operation and maintenance costs. Below are some key terms, as well as Table 3.1 that categorizes EES based on these technical aspects.

- **Cycle life:** Number of complete charge-discharge cycles an energy storage system can perform before its nominal capacity falls below 80% of its initial capacity (Yang *et al.*, 2011). Key factors affecting cycle life are time (t) and the number of charge-discharge cycles completed (N). Lifetimes of 2000 to 4000 cycles are typical of most batteries, equating to around 8 to 15 years, respectively (ABB, 2012).

- **Depth of discharge:** DOD refers to the extent a storage device can discharge its total capacity. DOD affects cycle life, for instance, if the device is only partially discharged each cycle, then the cycle life will be much greater (Yang *et al.*, 2011). Also called state of charge (SOC).

- **Round-trip efficiency:** RTE is the standard measure of an electricity storage device's efficiency in the grid as the AC-to-AC RTE, written as AC $\mathrm{kWh_{out}}/\mathrm{kWh_{in}}$. However, this is not always the value reported, especially for devices that store DC energy such as capacitors and DC batteries (Denholm *et al.*, 2010). In some cases, the DC-to-DC RTE may be reported and additional losses in power conversion efficiencies must be considered if the device is to provide applications in the grid (Denholm *et al.*, 2010). The mean RTE for most ES devices is around 75% (Denholm *et al.*, 2010).

- **Discharge time:** Measured from milliseconds to hours, the suitability of an ES system for a specific application (i.e. power quality, bridging power, energy management) correlates to its energy-to-power ratio and is determined by two factors:
  - **Power density:** Indicates the ability to provide *instantaneous* power. High power density technologies can discharge large amounts of energy quickly, [kWh/kW]
  - **Energy density:** Indicates the ability to provide *continuous* energy over a period of time. High energy density technologies discharge for long periods, [Wh/kg]

TABLE 3.1: *Four categories of EES discharge times, their applications, energy-to-power ratios, and examples of potential EES technologies.*

Discharge Time	Applications and Description	Energy-to-Power Ratio	Examples
Short	-Resources discharge for milliseconds to minutes. -Provide instantaneous power quality, UPS, and voltage frequency regulation.	< 1	Superconducting magnetic energy storage (SMES), flywheels (FES), double layer capacitors (DLCs)
Medium	-Resources discharge for minutes to hours. -Provide power quality, UPS, and bridging power, consumer-side time-shifting, and generation-side output smoothing for mitigating RE's uncontrollable variability. -This category is predominantly batteries.	1 to 10	Lead acid (LA), nickel cadmium (NiCd), lithium ion (Li-ion), sodium sulphur (NaS), vanadium redox batteries (VRB)
Med-Long	-Resources discharge for hours to days. -Primarily for load leveling energy management, and can assist RE integration.	5 to 30	Hydrogen gas (H_2) and synthetic natural gas (SNG)
Long	-Resources discharge for days to months. -Useful for seasonal time-shifting and load leveling. Expensive and less efficient. -Strictly used for energy management.	> 10	Pumped hydro storage (PHS), compressed air energy storage (CAES), redox flow batteries (RFBs)

3.4 Potential EES Technologies

Energy storage systems are hereby classified as one of three (below) and compared using discharge times, rated power and system power ratings in Figures 3.1 and 3.2.

1. **Mechanical systems** (e.g. PHS, CAES, FES)
2. **Electrical systems** (e.g. capacitors and EDLCs, SMES)
3. **Chemical systems** (e.g. flow batteries, LA battery, Li-ion battery, NaS battery, NiCd battery, etc.)

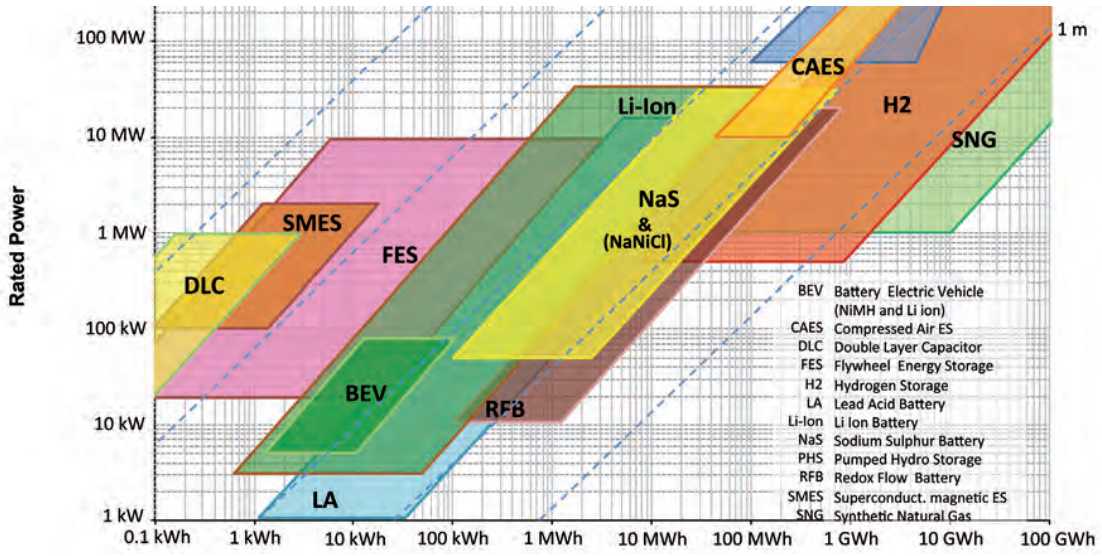

FIGURE 3.1: *Comparison of rated power, energy content and dicharge times of various EES technologies. Lower left area of figure denotes short discharge times strictly for power quality; the centre shows medium to long discharge times for bridging power; and the upper right area shows examples of long discharge time ES technologies for energy management (ESA, 2009).*

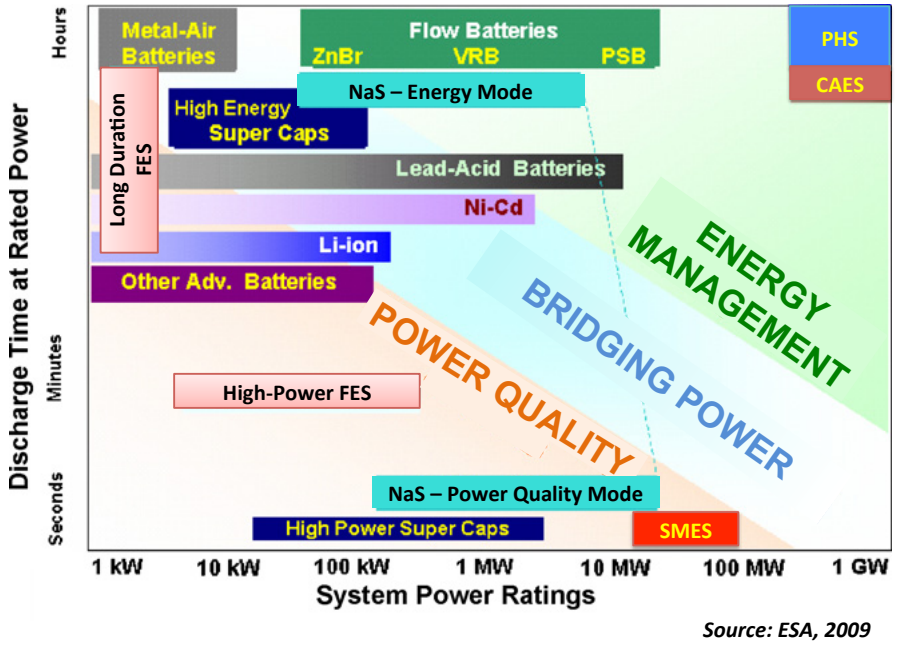

FIGURE 3.2: *Energy storage size and discharge times ranked according to the three applications: (1) power quality, (2) bridging power, (3) energy management.*

N.B. This paper focuses primarily on chemical systems. For the purposes of Icelandic transmission and distribution, battery energy storage devices offer the most promising option based on the technical and economic summaries.

3.4.1 Electrical Systems

Electrical EES devices are the only known technology to store electrical energy directly into electric current (Rahman *et al.*, 2012). Two systems are reviewed: (1) superconducting magnetic energy storage (SMES), and (2) electric double-layer capacitors (EDLCs).

1. *SMES systems* store electricity in the magnetic field created by flowing direct current (DC) in a superconducting coil that has been cryogenically cooled (Yang *et al.*, 2011; Rahman *et al.*, 2012). A diagram of a basic SMES system is shown in Figure 3.3. Once the superconducting coil is charged, the current will not decay and the energy can be stored almost indefinitely (Chen *et al.*, 2009; Rahman *et al.*, 2012). This stored energy can be released back to the grid simply by discharging the coil of its current. Of all EES technologies, SMES loses the least amount of electricity in the energy storage process; they are highly efficient, with a round-trip efficiency greater than 95% (Rahman *et al.*, 2012). Well suited for maintaining power quality and frequency regulation.

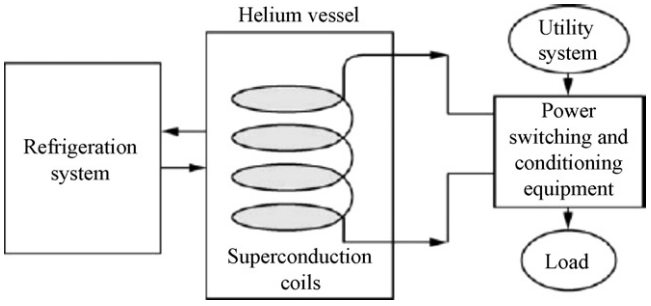

FIGURE 3.3: *Superconducting magnetic energy storage system.*

However, the major problems confronting the implementation of SMES units are the high capital cost of the superconducting units, energy requirements for supercooling the coils (refrigeration system) and the environmental issues associated with strong magnetic fields (Rydberg, 2011; Rahman *et al.*, 2012).

2. *EDLC systems*, also known as supercapacitors, are storage devices with unusually high power density compared to common capacitors. Sparing the complicated physics of how they maintain charge, supercapacitors applications are principally for power quality and UPS, given the high power energy outputs over a short duration.

3.4.2 Chemical Systems

The oldest method for storing electricity is in the form of chemical energy within batteries (ABB, 2012). Battery systems range from historically proven technologies (lead acid invented in 1859), to more modern inventions such as NiCd, NaS, Li-ion, and flow batteries (Electric Power Research Institute, 2010). New and exciting EES developments include graphene and magnesium-antimony (Mg||Sb) batteries (Sadoway *et al.*, 2012). Please note there has not been sufficient research conducted on graphene batteries for grid ES to include in this study. The following section outlines major EES high-powered batteries, and Table 3.2 summarizes the chemical systems based on technical data.

1. *Lead acid battery* (LA) consists of a positive electrode made of lead dioxide and a negative lead electrode, commonly separated by sulfuric acid electrolyte. Nominal cell voltage is measured at 2.0 V (Rahman *et al.*, 2012). LA batteries are a popular storage device for power quality, maintaining UPS, and other applications (Yang *et al.*, 2011). However, it has low cycle life (meaning it degrades quickly) and presents environmental issues when disposing of lead (Rahman *et al.*, 2012).

2. *Nickel cadmium battery* (NiCd) comprises a nickel hydroxide positive electrode plate and a cadmium hydroxide negative plate, separated by an alkaline electrolyte (Rahman *et al.*, 2012). Nominal cell voltage is 1.2 V (Rahman *et al.*, 2012). NiCd batteries are reliable, require low maintenance, and have high energy density (50 – 75 Wh/kg); disadvantages include low cycle life and difficulty disposing of cadmium, which is a toxic heavy metal (Yang *et al.*, 2011; Rahman *et al.*, 2012)

3. *Sodium sulfur battery* (NaS) consists of liquid sulfur at the positive electrode and liquid sodium at the negative electrode (see Figure 3.4). During discharge, the electrolyte allows Na^+ ions to flow through as electrons flow in the external circuit of the battery producing nearly 2.0 V (Rahman *et al.*, 2012). This process is reversible as charging causes the sodium ions to recombine as elemental sodium. 20% self-discharge occurs, and overall efficiency is 90% including heat losses. Initial capital cost is high, as is the operating temperature at over 300°C (Rahman *et al.*, 2012).

4. *Lithium ion battery* (Li-ion) stores electrical energy in electrodes made of Li-intercalation (reversible flow) compounds (Yang *et al.*, 2011). During charge and discharge, Li^+ ions transfer across an electrolyte (see Figure 3.5). Nominal cell voltage measures 3.2-3.7 V (ESA, 2009). Li-ion EES mitigates uncontrollable variability in RE generation output, offers reduced transmission costs, frequency regulation, and locational dependency challenges (wind farms tend to be far from load centers) of RE integration (Electric Power Research Institute, 2010).

5. *Vanadium redox battery* (VRB) consists of three major components: electrolytes, electrodes and membranes. The electrolyte is one of the most important components, being not only the conductor of the ions, but also the energy storage medium (Rahman *et al.*, 2012). Hence, the volume of the electrolyte determines the electricity storage capacity of the battery. Nominal cell voltage is between 1.15-1.55 V (ESA, 2009). Figure 3.6 illustrates a generic VRB, showing all 3 components.

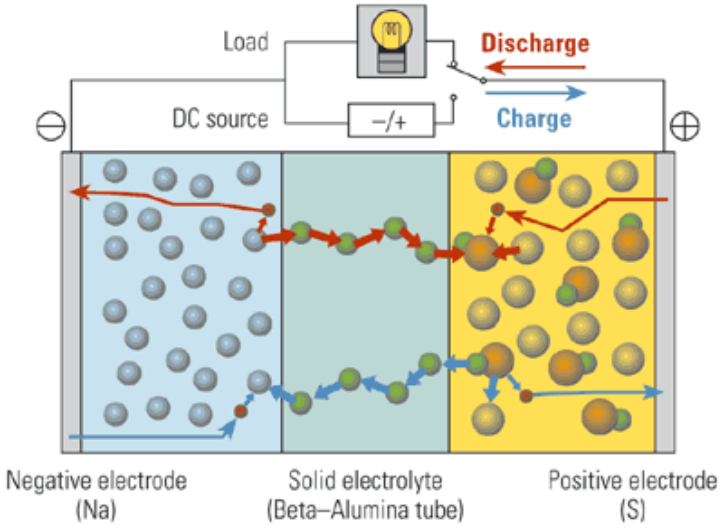

FIGURE 3.4: *Main features of NaS battery.*

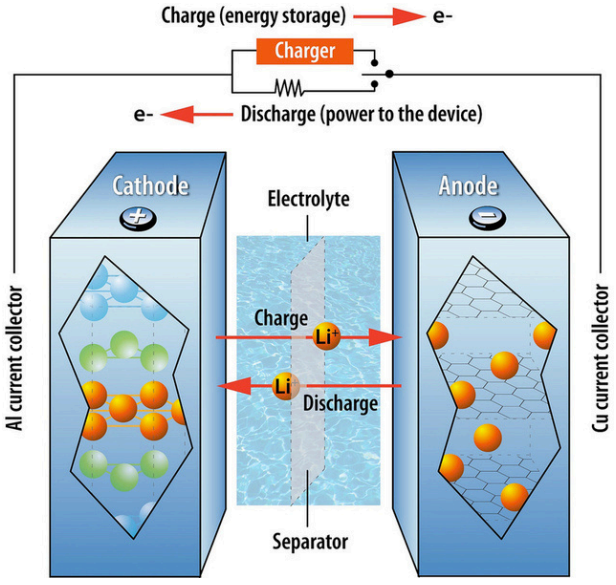

FIGURE 3.5: *Main features of Li-ion battery.*

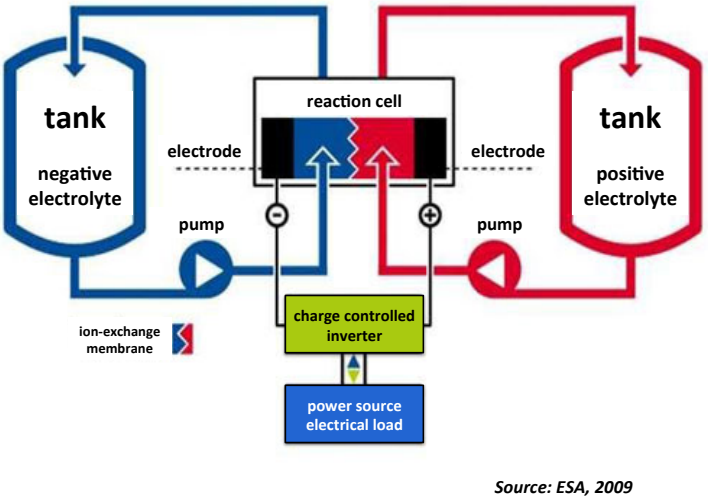

FIGURE 3.6: *Main features of a vanadium redox battery.*

TABLE 3.2: *Technical comparison of electrochemical systems for EES applications (Sources: Yang et al., 2011; Rahman et al., 2012.)*

Technology	Energy density (Wh/kg)	Operating temp (°C)	Discharge time	Self-discharge (% per month)	Cycle life (deep cycles)	RTE_{DC} (%)
LA	25 – 40	-40 – 60	up to 8 h	4 – 50	1000	50 – 75
NiCd	30 – 45	-10 – 45	up to 4 h	5 – 20	2500	55 – 70
NaS	150 – 240	300 – 350	4 – 8 h	negligible	4000	80 – 90
Li-ion	50 – 70	-25 – 40	up to 4 h	2	4000	94 – 99
VRB	10 – 20	0 – 40	4 – 12 h	3 – 9	5000	80 – 90

3.5 Economic Considerations of EES

For technically viable EES alternatives, economic comparisons may be made to find the best one. Cost represents the most fundamental issue of EES for achieving widespread market penetration (Yang *et al.*, 2011). Two important factors influence the feasibility of EES projects: (1) capital costs, and (2) life-cycle costs. Appendix A compares EES by capital costs and life-cycles.

1. *Capital costs* are typically expressed in terms of the unit cost of power ($/kW) for power applications (i.e. frequency regulation), or the unit cost of energy capacity ($/kWh) for energy applications (i.e. load leveling). The capital charge rate (also referred to as a fixed-charge rate or capital recovery factor) falls under capital costs and refers to the fraction of the total capital cost that is paid each year to finance the plant, including other required expenses such as permits and licenses. (Denholm *et al.*, 2010). It should be noted that this cost does not include any operation and maintenance (O&M) costs.

2. *Life-cycle costs* are expressed as the unit cost of energy ($/kWh), or power per-cycle over the lifetime of the unit. These costs are experienced continually over the useful life of the battery and any associated equipment, including O&M, salaries for labour, fuel and power costs, repair parts, costs of insurance and taxes, and associated overhead costs (Eyer and Corey, 2010; Denholm *et al.*, 2010).

Previous studies indicate the cost of electricity storage needs to be comparable to the cost of generating electricity to be competitive (Yang *et al.*, 2011). This equates to a life cycle cost for EES as low as 8 – 10 ¢/kWh per cycle (Yang *et al.*, 2011). Likewise, for capital costs to be competitive, the desired estimate assuming a life cycle of 15 years (or 4000 cycles, 5 cycles per week), 80% RTE and minimal O&M (5-10%) would be around $1300/kW (Yang *et al.*, 2011). Beyond the life cycle cost is the social cost that considers environmental impacts, such as the cost associated with reducing CO_2 emissions by deploying RE sources and advanced storage systems.

3.6 Summary of EES Technology

The serious challenges electrochemical storage technologies face was found to include: cycle life, depth of discharge, reliability, efficiency and economics (Rahman *et al.*, 2012). Electrical EES systems (i.e. SMES) are deemed far too costly for widespread market penetration in Iceland's energy storage sector. Therefore, it appears to be two low cost EES systems that are most suitable: Lithium-ion batteries and NaS batteries. While results indicate VRBs are the "most promising" option among other batteries considered, GridCommand^{TM} and GridLAB-D^{TM} do not support this battery type for parametric analysis at this time. Therefore, the first and second battery options, Li-ion and NaS respectively, are selected because GCD and GLD do contain program packages for modeling these batteries. The models used in this thesis incorporate Li-ion for community energy storage and NaS batteries for transmission level storage of 1 MW and greater. Results from this EES review chapter elucidate which battery storage technologies would be most suitable for the intended applications of maintaining power quality, real and reactive power peak-shaving and voltage control in Iceland. Table 3.3 gives a technical and economic summary of potential EES technologies, and Table 3.4 further supports why Li-ion and NaS batteries are ideal for renewable energy storage in Iceland.

TABLE 3.3: *Advantages and disadvantages of the technical and economic aspects of EES for RE integration.*

Technology	Advantages	Disadvantages	Application	Commercial Maturity	Cost	Remarks
1) Electrical EES						
SMES	High power	Low energy density and high production, operational costs	Power quality management	Medium	High production and operational cost	Suitable for short durations in sec or min
EDLC	Long cycle life, high efficiency	Low energy density	Power quality management	Medium	High production cost	Suitable for short durations
2) Chemical EES						
LA	Low cost	Limited cycle life, environmental concerns in disposal	Bridging power and energy management	High	Low capital cost	Renewables integration
NiCd	High power density, high efficiency	High cost, low RTE and low cycle life	Power quality and bridging power	High	High cost	Renewables integration
NaS (Energy mode)	Lower costs	Low power density	Energy management	Medium	Low cost	Renewables integration
NaS (Power mode)	Lower costs	Low energy density	Power quality and UPS	Medium	Low cost	Suitable for heavy-industry
Li-ion	High power density, high efficiency	High cost	Power quality and bridging power	Medium	High capital cost	Power quality management
VRB	Lower costs, good efficiency	Low energy density	Bridging power and energy management	Medium	Low cost	Renewables and power plants

TABLE 3.4: *Main features of most suitable EES technologies for renewable energy storage in Iceland (Source data: Rahman et al., 2012). VRB batteries are found to be most favourable here, however are not available in GCD or GLD.*

Technology	Li-ion	NaS	VRB	SMES	NiCd
Efficiency (%)	97	85	85	99	63
Cycle life charge/discharge	4,000	4,000	5,000	7,500	2,500
Size range (MW)	1–100	0.15–10	0.5–100	0.001–10	1–10
Operation temp (°C)	–25–40	300–350	0–40	–50	–10–45
Energy density (Wh/kg)	60	85	20	Low	38
Self discharge (losses)	Negligible	20% per day	Small	Small	0.6% per day
Environmentally safe	Yes	Yes	Yes	No	No
Disadvantages	High cost	High temp system, losses	Low energy density	Very high cost	Heavy metal Cd recycling issues
Top Choice	First	Second	Most promising	--	--

Chapter 4

Methodology and Materials

This chapter provides an overview of the two softwares GridCommand^{TM} Distribution and GridLAB-D^{TM}, computational calculations using the Newton-Raphson solver method, its function in power systems simulations, and describes the residential and transmission models used for parametric analysis. The processes for data acquisition, conversion, programming the model into the software, and mathematical derivations used for obtaining results are also outlined.

To analyze a power system and achieve accurate results, a detailed model with representative data is critical for reproducing a digital recreation that fully encompasses the complexities and dynamics of the system. Advanced software was called on for envisioning a future grid with powerful distributed energy resource modeling tools for effective planning, testing and resource allocation. Two relatively new computer programs were essential: GridLAB-D^{TM} (GLD) and GridCommand^{TM} Distribution (GCD).

Icelandic utilities Landsnet and OR store their data in formats not directly compatible with GCD and GLD, therefore, addressing this issue required unique data conversions into a format readable by the programs. This thesis models the infrastructure present in the real national grid and at the residential level. Examining the impacts of new technologies in the complex resource deployment scenarios is done using (1) a custom-built transmission network for Iceland and (2) a prototypical residential distribution feeder with minor adjustments to match Icelandic feeders for the distribution level analysis. By utilizing representative technologies and prototypical distribution feeders, which are generic residential networks configured to represent Icelandic residential loads, power infrastructure and technology, it will be possible for this study to estimate the feeder level impact of each new technology added, such as community energy storage, or CES, for instance. Once the impact of the technologies has been evaluated on the residential

level, the study then explores the impacts associated with deploying energy storage technology on a national level. This approach is similar to the methodology in the DOE's (2012) *Evaluation of Representative Smart Grid Investment Grant Project Technologies: Distribution Automation*. With one exception, while the residential feeders deploy Li-ion battery CES, the transmission model attaches NaS large-scale energy storage devices capable of storing upwards of 1 MW.

4.1 GridLAB-D™

GridLAB-D™ (GLD) is the adaptable simulation environment that passes third-party data and scripted commands to generate output files for analysis in grid management projects (Carlon, 2012). Therefore, it was used almost exclusively for data input of the raw and ASCII text files received from Landsnet and OR. The GLD algorithm calculates millions of states for independent devices (for example residential or industrial loads, energy storage devices, etc.), each described by models and equations relevant to the specific grid's power flows. At its simplest, GLD examines the interplay of every part of a power system. It was used for scripting the main transmission model, which was later passed to GridCommand™ to produce the grid for testing future scenarios with NaS energy storage. GLD is also an open-source tool, thus the code written for this thesis is made available online.

GridLAB-D™ accepts files with the extension .GLM (stands for GridLAB-D model) for processing, each simulation being run several times over the course of many days to generate output files with extensions .CSV (comma separated value). The resulting .CSV files were finally loaded into GridCommand™ for post-processing in order to create the plots and graphs seen in the results chapter. Figure 4.2 shows succinctly how this data conversion and processing works across different programming platforms.

The advantages of GLD's algorithm over traditional finite difference-based simulators are: (1) it handles unusual situations more accurately; (2) it accepts widely incongruent time scales, ranging from sub-seconds to many years; and (3) it integrates with new modules and third-party systems easily. For this project, partial datasets from Landsnet and OR were either incomplete or incompatible with the programs; GLD accounted for these issues with presets designed to work without the use of reduced-order models for the aggregate behavior of electrical systems. Therefore, GLD is able to avert the danger of erroneous or misapplied assumptions (Carlon, 2012).

4.2 GridCommand™ Distribution

GridCommand™ Distribution (GCD) is the second simulation environment with a graphic user interface that was developed by Battelle Memorial Institute as part of the DOE Smart Grid program, using algorithms developed with Pacific Northwest National Laboratory (PNNL). PNNL was also behind the creation of the GLD algorithm, which is what makes these two programs so harmonious. The software is a front-end for the open-source GLD.

GCD parsed the GLD code written for this project and compiled it into a detailed planning model for the parametric analysis of electricity networks, deploying smart grid technologies that encompass a wide array of devices and operating policies such as EES systems, distributed generation (DG), line configurations, transformers, demand response tariffs, volt-VAr optimization (VVO), PHEVs, and so on. GCD objects can be displayed down to the individual household level with remarkable detail; see Figure 4.1.

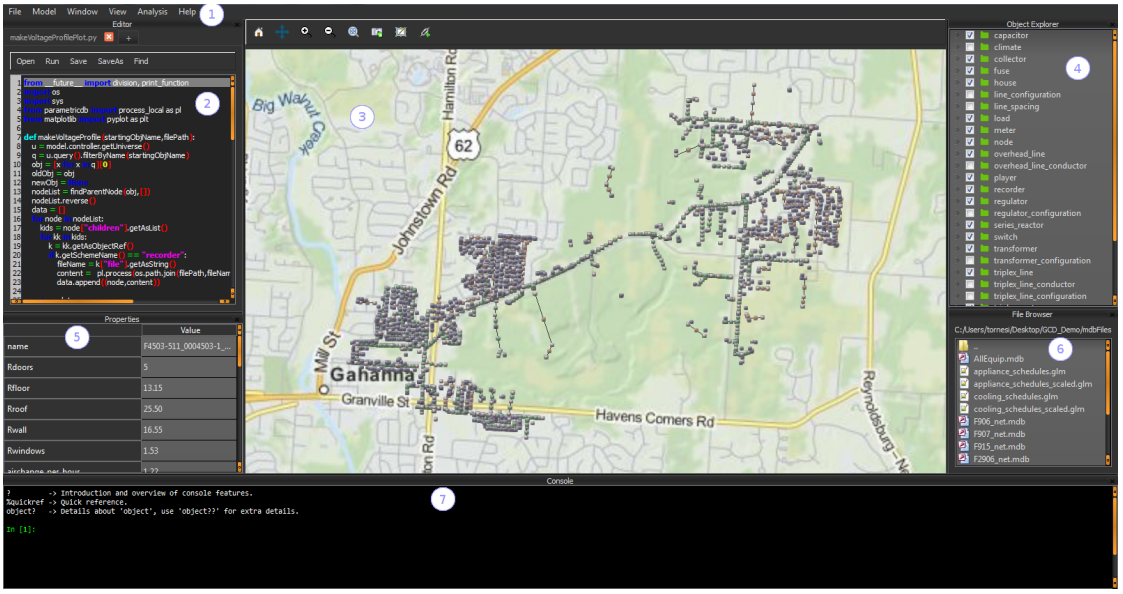

FIGURE 4.1: *Graphical user interface (GUI) in the GridView feature of GCD software.*

In summary, GCD is the software responsible for adding EES technologies to the circuit models built within GLD, allowing for the additions of multiple device configurations, assessing complex resource deployment scenarios, and providing insight into grid sensitivity and capacity under changing conditions. Power flow calculations were performed in GLD, and post-processing analysis was performed in GCD's plotting interface.

4.3 Data, Data, and Data

4.3.1 Data Acquisition

Identifying the geospatial location of infrastructure in the Icelandic power system was crucial for maintaining model accuracy. Latitude and longitude coordinates were obtained using Landsnet's single-line diagram of the grid (see Appendix B), an interactive satellite map of the transmission system from Loftmyndir (Loftmyndir, 2013), and Google Maps for cross-referencing location coordinates to the third decimal place. Geospatial data for each point can be seen in Appendix C, along with variables for bus voltage, real power, and reactive power. From the transmission system data shown in Appendix C, 33 major loads are defined in Iceland; five of which are power-intensive industries: Alcoa, Becromal, Century Aluminum, Elkem, and Rio Tinto Alcan. The remaining 28 are major distribution feeders to municipalities, residential areas, and external commercial activity. Substations are denoted with (SS), loads (L), industrial loads (IL), and power plants (PP).

Time signatures for baseline power flows span the period from January 1, 2012 to December 31, 2012, as specified in the scope of this thesis. Three-day simulations from July 7 to July 9, 2012 were run for comparing baseline models to models with EES added. Temporally, the data ranges from seconds, minutes, hours, days, and months on an annual basis. Reykjavík Energy provided basic residential load flow data, however Landsnet was unable to disclose power flows for their substations and power-intensive customers, declaring it private, sensitive information.

4.3.2 Data Entry and Conversion

Each object within the grid was assigned a corresponding `node` or `link` definition; `node` objects include substations, transformers, capacitors, industrial loads and power plants, `link` objects connect `node` objects together and include overhead power-lines, underground lines, and conductor specifications.

Landsnet operates its power systems planning and conducts analysis using a program called PSS/e, which is modeling software with different code formatting to GridLAB-D^{TM} .GLM files. PSS/e data was extracted as rich text, parsed using Python scripting language, and power values then compiled for every load and generator bus in the Landsnet grid (refer to tables in Appendix C). Once all geospatial data was compiled for each object in the grid, the script for the Icelandic power system was written inside GridLAB-D^{TM} to be later used as an input file for parametric analysis (addition of new technology)

within GridCommand™. Next, the resulting .GLM file from GridCommand™ is passed back to GridLAB-D™ to generate output files in .CSV format, and finally these .CSV files added to the plotting interface in GridCommand™ to produce the final results.

This file conversion and data entry process across different programming platforms is illustrated in Figure 4.2, which is organized by placing the software platform in the blue upper blocks, while the lower blocks show points that are separated into three parts: the first bullet denotes the platform process, the middle points are platform inputs, and the last bullet denotes the platform outputs. This creates a flow of inputs and outputs across the programming softwares.

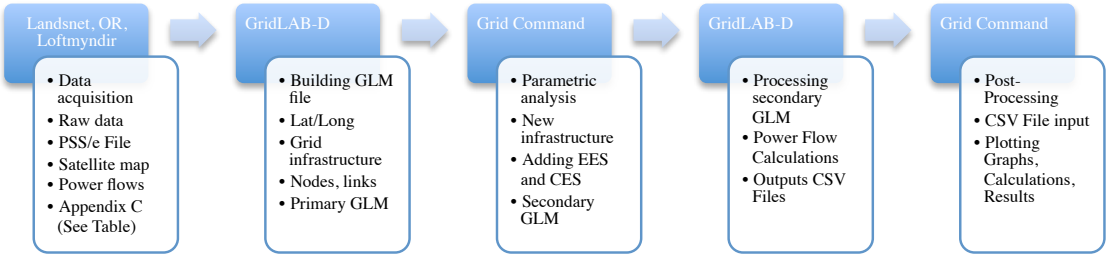

FIGURE 4.2: *Data conversion process across multiple programming platforms.*

4.4 Power Flow Model Calculations

First, a little history to help visualize the *bus concept* – the electrical bus derives its name from old transit buses with overhead bars for its passengers without a seat to hang on to during motion. One can then imagine these long handlebars as the electrical buses that carry electricity, and the passengers as the loads. Hence, the philosophy of a bus bar with terminated conductors feeding their respective loads. Electric grids contain specific information at each load bus and generator bus. A bus without any generators connected is called a load bus, whereas a bus with one or more generators is a generator bus. Lastly, a slack bus is any randomly selected bus that has a generator (Mork, 2000).

The goal of any power flow study is obtaining complete phase angle and voltage magnitude information for each bus in the power system, where,

$$\theta = phase\ angle \tag{4.1}$$

$$|V| = voltage\ magnitude \tag{4.2}$$

In a power flow model, it is assumed real power (P) and reactive power (Q) are known for each load bus (refer to P and Q values in Appendix C). For this reason, load buses

are also known as PQ buses. Generator buses assume real power (P_{G}) and voltage magnitude ($|V|$) are known. For the slack bus, it is assumed voltage magnitude ($|V|$) and voltage phase angle (θ) are known. Datasets obtained from Landsnet and OR provide this information on PQ power, phase angles and magnitudes, which are incorporated into the models.

For any system with N buses and R generators, there are then *2(N−1)−(R−1)* unknowns. Therefore, to avoid the simulation from incorporating any new unknown variables there must be *2(N−1)−(R−1)* equations to prevent additional unknowns. Power balance equations can now be called on for calculating real and reactive power for each bus. These equations are written as follows:

$$0 = -P_i + \sum_{k=1}^{N} |V_i||V_k|(G_{ik}cos\theta_{ik} + B_{ik}sin\theta_{ik}) \tag{4.3}$$

$$0 = -Q_i + \sum_{k=1}^{N} |V_i||V_k|(G_{ik}cos\theta_{ik} - B_{ik}sin\theta_{ik}) \tag{4.4}$$

Where P_i is the net real power injected at bus i, conversely Q_i the net reactive power injected at bus i, G_{ik} is the real power admittance corresponding to the ith row and the kth column, B_{ik} is the reactive or imaginary part of the element, and finally θ_{ik} represents the difference in phase angle between two buses (Mork, 2000).

4.5 The Newton-Raphson Method

The Newton-Raphson method, or NR method, is the algorithm used for solving power flow analyses run in every simulation for this experiment. Simply thought of as a linear approximation for nonlinear systems, when properly used it provides exceptional accuracy in replicating power systems.

Performing power flow studies of this nature require linear programming for calculating optimal power flows before and after the addition of EES to the residential and transmission models. Optimal conditions are herein determined by the EES densities and configurations that 'solve' threshold setpoints, which is deemed the most energy efficient EES arrangement in terms of PQ reductions and voltage regulation. This means of analyzing optimization is explained further in chapter 5.1. The NR method estimates any unknown variables in the power system, such as voltage magnitudes and angles at load buses, and phase angles at generator buses. Next, for each of the power balance

equations given above, the result of a linearized power system can be expressed as the following matrix:

$$\begin{bmatrix} \Delta\theta \\ \Delta|V| \end{bmatrix} = -J^{-i} \begin{bmatrix} \Delta P \\ \Delta Q \end{bmatrix} \tag{4.5}$$

Where J is a matrix of partial derivatives known as a Jacobian, (J),

$$J = \begin{bmatrix} \frac{\delta\Delta P}{\delta\theta} & \frac{\delta\Delta P}{\delta|V|} \\ \frac{\delta\Delta Q}{\delta\theta} & \frac{\delta\Delta Q}{\delta|V|} \end{bmatrix} \tag{4.6}$$

Now we can rearrange equations 4.5 and 4.6 for the relation in equation 4.7:

$$[J] \begin{bmatrix} \Delta\delta \\ \Delta|V| \end{bmatrix} = \begin{bmatrix} \Delta P \\ \Delta Q \end{bmatrix} \tag{4.7}$$

If real power (P) and reactive power (Q) are calculated, it follows that ΔP_i and ΔQ_i can be found using a rearranged form of the power balance equations (4.3, 4.4) called the mismatch equations:

$$\Delta P_i = -P_i + \sum_{k=1}^{N} |V_i||V_k|(G_{ik}cos\theta_{ik} + B_{ik}sin\theta_{ik}) \tag{4.8}$$

$$\Delta Q_i = -Q_i + \sum_{k=1}^{N} |V_i||V_k|(G_{ik}cos\theta_{ik} - B_{ik}sin\theta_{ik}) \tag{4.9}$$

All terms in the Jacobian and in the mismatch equations are evaluated using present values for V, θ and δ. Convergence is finally determined by monitoring the mismatch vectors of equations 4.8 and 4.9. Testing for $|\Delta P_i| \leq \varepsilon$ at all PQ buses, and testing for $|\Delta Q_i| \leq \varepsilon$ at all PQ buses is performed with $\varepsilon = 0.001$ per unit. Typically, the Q mismatches are greater than P mismatches, thus convergence often depends on ΔQ (Mork, 2000).

4.6 GCD Transmission Model of Iceland

The culmination of data entry, conversions, and .GLM file input into GridCommand^{TM} can be seen in Figure 4.3. The graphical user interface shows the GCD programming environment for simulations and its GridView mapping feature. From here, the model is

run through parametric analysis for the computer-assisted addition of new EES technologies (large-scale NaSfor the transmission model) with manually controlled parameters. This forms the basis of answering the research questions of this paper and addressing one of the two complex resource deployment scenarios. We refer to this new transmission system in Figure 4.3 as the 'IceOpt' model, the five red objects demarcate the most power-intensive industrial loads in Iceland.

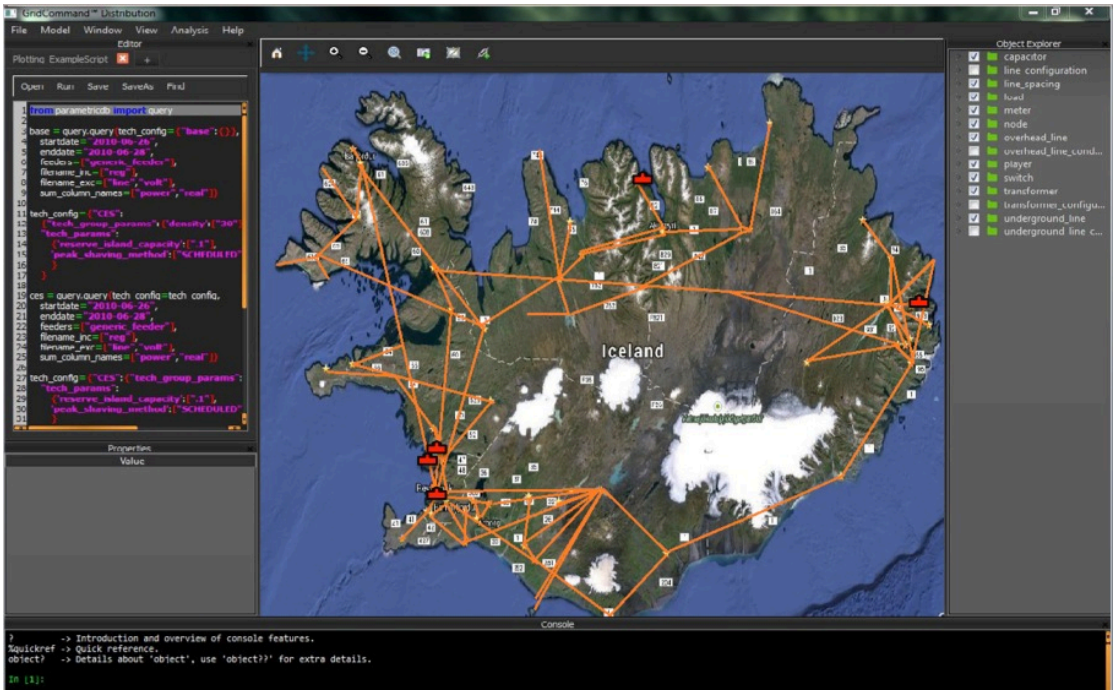

FIGURE 4.3: *Enhanced screenshot of the final transmission model seen in GridView of GCD.*

4.7 The Quadrant Concept

Four areas of potential weakness in the Icelandic power system are identified. Due to the size and scale of this project, sectioning the grid into quadrants would help with organizing parametric analysis and is intended to inject additional clarity into the organization and discussion of results. Ideally, because the entirety of the grid forms a ring network stretching around the perimeter of the country with no transmission lines crossing through its interior mainland, the quadrant concept would place high-capacity (10 MWh) NaS energy storage in the following designated areas: (I) Northwest quadrant [Case0]; (II) Northeast quadrant [Case1]; (III) Southeast quadrant [Case2]; (IV) Southwest quadrant [Case3]. Figure 4.4 represents these four areas as four distinct cases labeled Case 0 to Case 3 to be modeled in GCD.

Installing large MW-scale energy storage units at specific substations in each of these quadrants (four attachment sites total) are expected to yield greatest energy efficiency and grid EES optimization given the right configuration. Two attachment points for EES in each quadrant were tested; the EES configuration (or arrangement) that achieves greatest peak power and voltage reduction is deemed to be the best configuration for energy storage in Iceland's national grid. In total, eight attachment sites leads to many possible combinations to simulate. However, using Landsnet performance reports from the past three years we were able to narrow this number of possible combinations to just four configurations based on documented transformer weaknesses and transmission system failures. It may be worth investigating all possible combinations in future studies. The rationale for selecting the sites is discussed later in this chapter. Refer to Table 4.1 for the breakdown of each case's potential EES connection points.

TABLE 4.1: *Each case with two potential EES connection sites tested in GridCommand™*

Option A	Mjolka	Hryggstekkur	Holar	Brennimelur
Option B	Hrutatunga	Fljótsdalur	Prestbakki	Hamranes

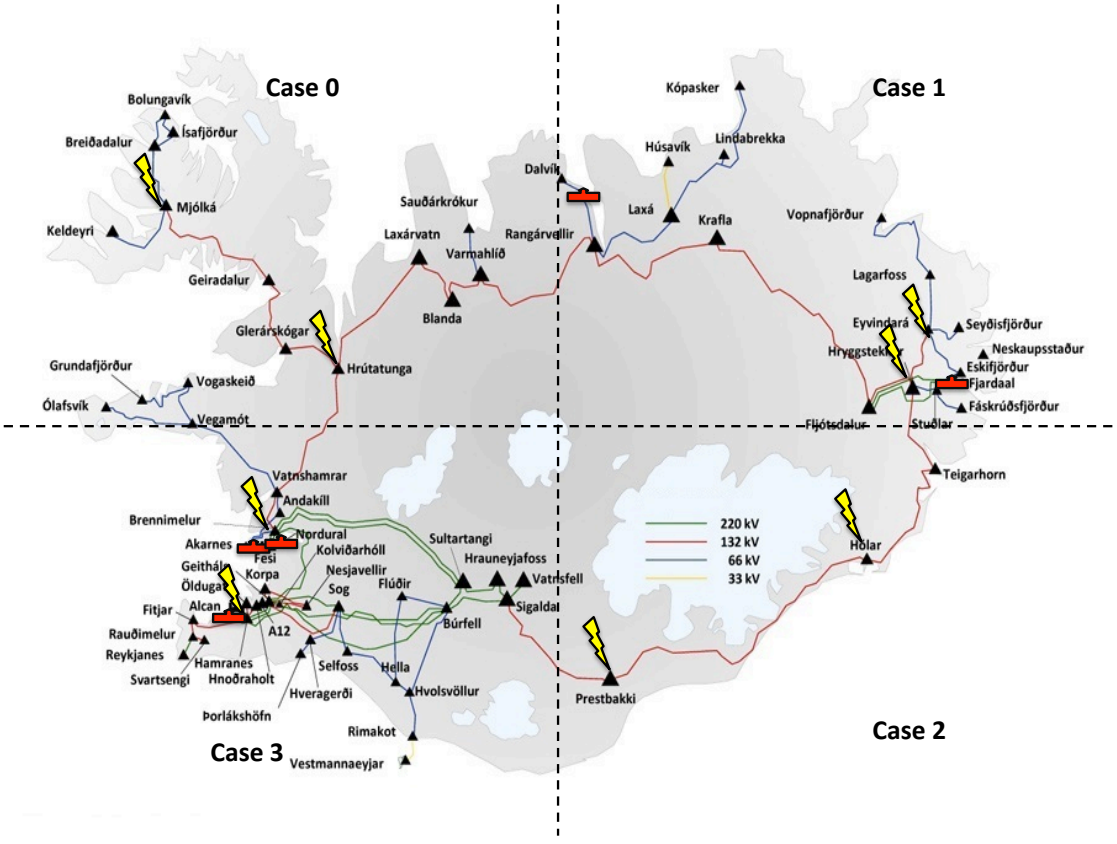

FIGURE 4.4: *Quadrants used in analysis of EES for four case studies across Iceland.*

Attachment of energy storage devices occurs at `transformer` and `meter` objects within the .GLM code. Since `transformer` objects contain variables for nominal voltage, real

and reactive power, it makes sense for them to act as the connection points for EES technologies that specifically control voltage and PQ in measured amounts. For example, the transformer at Mjólka is one of eight tested EES connection points.

The rationale behind choosing the four individual locations, aside from the perceived benefits of optimizing power flow, is each quadrant poses a risk for signal instabilities, power outages, voltage oscillations, high rates of energy consumption, and other instances of weakness. Each quadrant in fact poses its own unique problems. The Northwest quadrant (Case 0) experiences the highest amount of severe weather events that are most often responsible for frequent winter blackouts across the Westfjords. The nature and magnitude of these grid-compromising storms can be found in chapter 2.3. It should also be noted that all four quadrants are at risk of extreme weather-related grid disturbances.

The Northeast quadrant (Case 1) has the second highest energy consumption by heavy industry in all of Iceland, giving rise to widespread voltage oscillations and reduced power quality in the area (Landsvirkjun, 2013B). Guðmundsson *et al.* (2006) describe the transmission system in eastern Iceland as relatively weak given the extensive power plants and aluminum smelters located there. In fact, the operation of the Kárahnjúkar hydropower plant and heavy industry has a protracted impact on the 132 kV bus with which they connect, placing pressure on the Fljótsdalur and Hryggstekkur substations and affecting other loads in surrounding areas (Guðmundsson *et al.*, 2006). For this reason, Landsnet installed a dynamic VAr reactive compensator (also called a DVC) to improve system stability, increase voltage regulation, and ensure high power quality levels in the area.

In the Southeast (Case 2), 132 kV transmission lines Prestbakkalína and Sigöldulína are two of the longest cables between substations (Prestbakki, Hólar and Sigalda) in the entire grid, and despite a greatly reduced electricity demand in the Southeast quadrant, weakness does occur in the form of transmission line losses. Substations connecting these lines Hólar and Prestbakki can become taxed by loads and overwhelmed by generation in neighbouring quadrants (Landsnet, 2012A). Finally, the Southwest area of Iceland (Case 3) dominates the commercial and residential power-flows, as well as three of the five major power-intensive users: Century Aluminum, Rio Tinto Alcan, and Elkem. Landsnet (2013B) reports Brennimelur substation suffered an explosion and caught fire during a severe weather event that brought saline water and flash freezing in January 2012. Brennimelur has the single highest real power flowing through it measuring 632.6 MW (Orkustofnun, 2013). Slightly south of Brennimelur substation, the Hamranes 220 kV/132 kV transformer experiences some of the highest measured demands in the entire national grid (Landsnet, 2013A; Orkustofnun, 2013).

For these reasons, the eight EES attachment points have been carefully selected for parametric analysis testing inside the GCD transmission model.

4.8 GCD Prototypical Residential Model

Prototypical residential feeders were incorporated into the research as well to contribute fine-scale resolution to the grid and smarter community energy storage planning. These simulations were necessary for testing the impacts of EES on various levels of the Icelandic power system as part of the second research question. The residential feeders used in this experiment were originally designed by PNNL and GLD developers to provide researchers with an openly available set of generic distribution feeder models, which are representative of those seen in the United States (Schneider and Bonebrake, 2012). To account for the inconsistencies between American and Icelandic residential feeders, a distribution model that most closely matches Icelandic networks was chosen to alleviate the constraint of available data from electric utilities in Iceland. This feeder is a representation of a lightly populated urban area, composed of single and multi-family homes, moderate commercial loads, and light to medium industrial loads (large industrial loads are integrated in the transmission model). This feeder also supplies a university and a nearby domestic airport. Approximately 25% of the circuit-feet are overhead lines while the remaining 75% are underground lines. The majority of loads are located relatively near the substations, and finally this is an 11 kV feeder with a peak load of approximately 6,700 kVA, averaging 1600 kVA (Schneider and Bonebrake, 2012; Orkustofnun, 2013). A visualization of this generic feeder is shown in Figure 4.5 and Figure 4.6, which was created by Michael A. Cohen (2013) using Graphviz in GridLAB-D^{TM} and a ruby script for translating .GLM files. In these figures, the origin points of each object is arbitrary and without any true physical location (unlike the IceOpt transmission model). Refer to Table 4.2 for the object's legend.

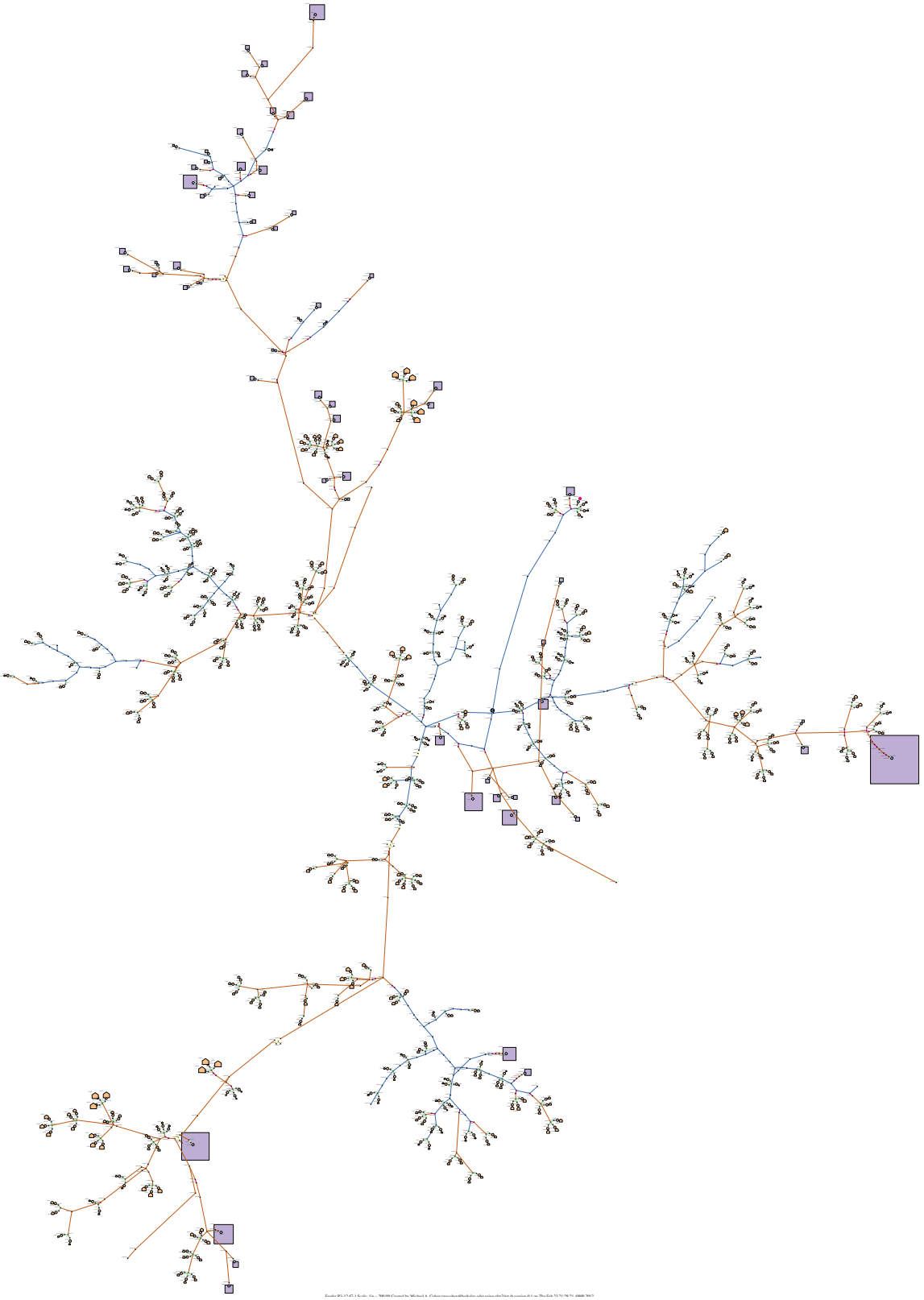

FIGURE 4.5: *Visualization of the residential feeder used in baseline and EES simulations (Cohen, 2013).*

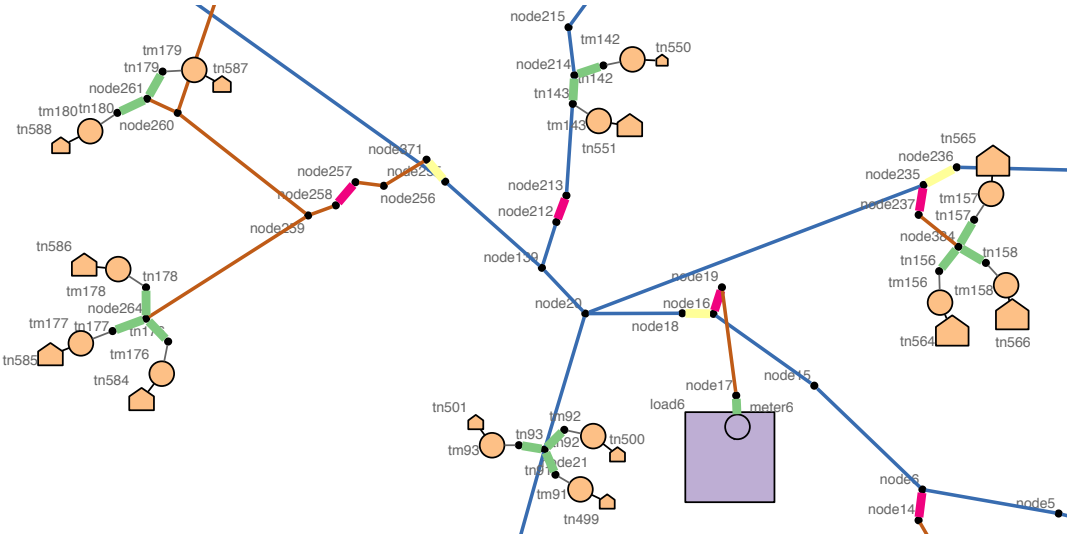

FIGURE 4.6: *Close-up of generic feeder used for residential simulations (Cohen, 2013).*

TABLE 4.2: *The object legend for the residential feeder visualizations.*

GridLAB-D object	Graph representation	Notes
Overhead line	Thin blue line	Length is roughly to scale
Underground line	Thin brown line	
Node, triplex node	Black dot	
Swing bus node	Magenta double octagon	Looks like a bullseye
Triplex node with real power demand	Orange house	Area is proportional to peak real power demand (same scale as load)
Capacitor	Green double circle	
Fuse	Short magenta line	
Load	Lavender square	Area is proportional to peak real power demand (same scale as triplex node)
Meter	Lavender circle	
Recloser	Short gray line flanked by magenta	
Regulator	Short gray line flanked by green	
Switch	Short yellow line	
Transformer	Short green line	
Triplex line	Thin gray line	
Triplex meter	Orange circle	

One may think of the residential feeder simulations as the experimental calibration before beginning simulations on the manually scripted, larger transmission model scenarios. Through the procedures of this thesis, the residential feeder simulations proved to be imperative in the debugging of the transmission model, improving its accuracy and therefore the final results. The apparent lack of residential feeder data (i.e. at the metered household level) in Iceland represents a significant data gap in this research; employing a prototypical feeder was the simplest and most effective solution.

4.9 Procedure, Assumptions and Data Gaps

The unavailability of Landsnet power flow data for their substations and power-intensive customers represents a constraint in the transmission model that was partially solved in two parts: (1) statistically scaling all five industrial loads in the model to meet 80% of electricity consumption; and (2) applying a reference schedule for power flows. For the first solution, considering heavy industry comprises 80% of all electricity consumption in Iceland, it is therefore plausible to state of the 17.7 TWh of electricity produced in 2012, approximately 14.0 TWh represents the demand of power-intensive industry (Landsvirkjun, 2013B). This is consistent with reports from Orkustofnun (2012) and the Ministry of the Environment. The electricity market in Iceland is therefore split into three parts:

1. Industrial loads (80%)
2. Commercial loads (15%)
3. Residential loads (5%)

The five major industrial loads selected in the model are the five most productive and energy-intensive aluminum smelters in Iceland: (1) Rio Tinto Alcan, (2) Alcoa, (3) Century Aluminum, (4) Becromal, and (5) Elkem. Their locations can be seen on Figure 4.3. Each plant uses roughly 2.8 TWh per year based on this first assumption.

$$17.7\,TWh * 80\% = 14.2\,TWh \textit{ consumed by 5 industrial loads} \tag{4.10}$$

$$\frac{14.2}{5} = 2.8\,TWh \textit{ electricity consumed by each industrial load} \tag{4.11}$$

... and for all remaining loads

$$17.7\,TWh * 20\% = 3.5\,TWh \textit{ consumed by all remaining loads} \tag{4.12}$$

Of course, this is a rough approximation since larger industrial sites such as Alcoa consume more electricity than smaller production plants like Elkem, however, the absolute industrial consumption remains the key while each individual load remains relatively consistent. Furthermore, PQ power measured at each industrial load was available for the simulations, which in effect partially compensates for this assumption. The above calculations are taken into account in the transmission model by using a multiplier function on power flow schedules for each load. Load files were originally written for commercial and

residential entities, but can be scaled up or down based on load size, therefore the industrial loads and large distribution feeders attached to the transmission system needed to be scaled according to the load's player files using the `base_power_schedule.value`(x) multiplier function. Player files are load schedules that contain standard load flow data varied by time, and are therefore responsible for causing the fluctuations of data in GridLAB-D^{TM} simulations. Player files are also capable of variable scaling and being weighted to match desired load characteristics (Schneider and Bonebrake, 2012). By scaling industrial loads to match 80% of electricity demand, while all other loads are scaled to 20%, the ratio for industrial loads versus remaining commercial and residential loads becomes equivalent to x multipliers 14.2 and 3.5, respectively (see equations 4.10 and 4.12).

Another important assumption involves the power-flows of heavy industry, an equivalent number of industrial loads to account for 80% of the generation side output. Aluminum smelters are clients of Landsvirkjun and Landsnet, and for this reason their information on power-flows and hourly energy consumption are private and were not made accessible for use in this study. As a result of this data gap, a standard player file for industrial power-flows was available which detailed consumption levels of the plants and basic heating and cooling schedules. Though these data are not exact, they do provide a good estimate of industrial consumption patterns and additional detail to the power system model. Player files and schedules were adjusted to match Icelandic seasonal variation, explained further in chapter 5.2.1.

Part of the procedure for running simulations within GridLAB-D^{TM} was setting the NR solver variable to iterate 100 times over in each of the residential and transmission model simulations. This iteration value was not selected arbitrarily, because the more iterations that are run brings the number of unknown variables in the power system closer towards 0. Theoretically, we could execute an infinite number of iterations to find a perfect representation of the model, however, it is assumed that the process has worked sufficiently with NR $\times$ 100 given the relaxed convergence tolerance with the 10 times ε variable (specified in chapter 4.5).

Lastly, there are minor uncertainties in latitude and longitude coordinates for `node` and `link` objects, set to $\pm$ .005 degrees. Transmission lines also appear as straight lines in the GCD IceOpt model when in reality they a more sinuous, however, their physical layout in the GCD model has no bearing on the accuracy of our results.

Chapter 5

Results and Post-Processing

Voltage, real and reactive power flow plots form the basis of these results and present new findings for the impacts of electricity energy storage in an energy market with 100% renewable generation. EES attachments to residential and transmission networks are performed using the GridCommand^{TM} parametric analysis tool. Post-processing of the output files takes place within the GridCommand^{TM} plotting interface (essentially MATLAB Plots), and allows for the assessment of the following EES performance metrics: (1) voltage control, (2) peak-shaving, (3) power quality, (4) energy arbitrage, (5) UPS, and (6) consumer-side time-shifting; each applied on residential and transmission scales of the Icelandic power system.

5.1 Performance Metrics

Six performance metrics are assessed based on the ability of EES to stimulate reductions in the baseline voltage, baseline real power, and baseline reactive power. Reductions below a predetermined threshold setpoint allows for the measurement of the degree of success resulting from EES actions. Thresholds for real and reactive power are herein presented as integrals of both the baseline curve and the resulting curves from the additions of EES. Thresholds for voltage are defined by the deviation from the mean annual voltage. If the actions of EES cause a shift below the threshold setpoint, then the performance metric is considered to be solved. Furthermore, for certain power events there is a quantity of energy that will be reduced by EES action, even if the threshold is not met (Wade *et al.*, 2010). For example, take a situation where baseline power flow is running at 250 MW, and the EES system causes a shift down to 227 MW, not crossing the hypothetical 220 MW threshold but still producing a significant improvement nonetheless.

For the purpose of this study, the lowest EES density that crosses below the threshold is deemed most efficient and to be the optimal condition.

Table 5.1 outlines the performance metrics for voltage and power, along with their respective thresholds for each model: residential and transmission. Real power thresholds are derived from 10% reduction targets from the real power baseline integrated over three days. Reactive power thresholds are also derived from the EES' ability to reduce reactive power flows by 10% below the baseline integrated over three days. Voltage thresholds are calculated differently, derived from the EES' ability to maintain voltage within 1% of the average annual voltage (found to be 11.1 kV in the residential feeder, and 33.1 kV in the transmission system). Choosing the setpoints for voltage and power in the two models involved identifying the needs of the Icelandic utilities, system weaknesses gathered from performance reports (Landsnet, 2012B), the timestamps of the simulations, and play to the strengths of the energy storage technologies selected for our study. This experimental design ensures a way of better assessing the effects of EES in the power system by means of quantitative analysis.

TABLE 5.1: Thresholds setpoints for real and reactive power are expressed as integrals over three days, using 10% reduction targets from the baseline. Voltage is expressed as the mean voltage over three days with variance limits of 1%.

	Li-ion CES in Residential Model	NaS EES in Transmission Model	Performance Metrics
Thresholds for Voltage	11.1 ± 0.11 kV	33.1 ± 0.34 kV	Voltage control, quality
Thresholds for Real Power	197.92 MW	2.05 x10^6 MW	Peak-shaving, energy arbitrage, UPS, consumer-side time-shifting
Thresholds for Reactive Power	2.44 MVAr	2.98 x10^4 MVAr	Power quality, peak-shaving, UPS

When results indicate power or voltage curves operate below its thresholds, the lowest EES density that produces the curve will suggest optimal battery densities and configurations. Tables 6.1, 6.2 and 6.3 in the discussion and analysis chapter summarizes the findings using this approach.

5.2 Complex Resource Deployment Scenarios

Each simulation run in GridLAB-D^{TM} generated .CSV output files for post-processing in GridCommand^{TM}. Once the output files were created they were placed into GCD's plotting interface for comparisons between "baseline data" (model without new infrastructure) and the impacts EES solutions introduce to the system. A breakdown of how simulations were divided follows:

1. Li-ion CES battery solutions:
   (a) Residential feeder to gather baseline data (without EES)
   (b) Residential feeder with the addition of Li-ion CES
2. NaS EES battery solutions:
   (a) Transmission model to gather baseline data (without EES)
   (b) Transmission model with the addition of NaS batteries

5.2.1 Complex Resource Scenario One: Li-ion CES Battery Solutions

Currently, there are numerous available CES schemes that implement some form of grid optimization and other energy storage benefits. For the purposes of this first analysis, an openly available CES scheme is utilized on the residential feeder. The parameters for the CES batteries and BMS are provided in Table 5.2. Figures 4.5 and 4.6 illustrate the scale and layout of the residential feeder tested for CES enhancement. Again, this serves as an approximation to an Icelandic residential feeder, and is less precise than the transmission system reproduced for this paper, however since Landsvirkjun (2013) and Orkustofnun (2013) account for residential electricity use to be in the 5% range of Iceland's total consumption, the prototypical model employed here still indicated the improvements CES can have on the distribution level despite its seemingly insignificant share of Iceland's electricity demand.

Two types of simulations were run on these residential feeders: (a) one baseline simulation, and (b) four distinct CES simulations of varied densities or concentration of batteries in the system. The parametric analysis wizard in GridCommand^{TM} has a built-in function for varying the amount (density as a percentage) of EES integrated into the system. In this case, CES_D20 represents a 20% density of CES in the feeder and is equivalent to 150 installed batteries; this being half the number of batteries integrated than CES_D40, a density of 40% and roughly 300 batteries, for instance. The minimum number for CES density parameters was set at 10%, while the maximum set at 40%, with an inclusion rate of 10. Therefore, parametric analysis attaches CES at four different densities: 10, 20, 30, and 40. GridCommand^{TM} has another function for selecting one of two EES configurations, either (a) clustering the CES technologies around a specific point in the grid, or (b) evenly distributing the batteries at the predefined densities. For the simulations in this section, all CES batteries are programmed to be evenly distributed across the feeder (clustering of EES will occur in the transmission model). Battery and BMS parameters are all designed for managing the electricity of a small number of households for each battery. Finally, once the simulations were plotted

and ready for post-processing, the optimal density of CES in the residential feeder is then mathematically derived using GCD's plotting interface and calculation toolbars.

TABLE 5.2: Parameters for CES batteries and BMS controller objects used in the residential feeder.

CES Battery:	Battery_capacity	45 kWh	
	Battery_size	HOUSEHOLD	
	Battery_type	Li-ion	
	Nominal_voltage	11 kV	
	Rated_power	45 kW	Maximum power used by device.
	Reserve_State_of_charge	0	
	Round_trip_efficiency	0.90	
	State_of_charge	1.0	
CES Controller:	Charge_setpoint	600 kW	Charging occurs when demand is below limit.
	Peak_shaving_setpoint	1000 kW	Tells controller when to switch batteries on.
	Fixed_charge_rate	0.5 kW	
	Fixed_discharge rate	1 kW	
	Islanded_mode	FALSE	The feeder is attached to others.
	Max_charge_rate	1	
	Max_discharge_rate	1	
	Max_discharge_rate_reactive	1	
	Peak_shaving_method	LOAD_FOLLOWING	Discharges when feeder regulator is above the peak_shaving_setpoint value.
Inverter:	Generator_mode	SUPPLY_DRIVEN	
	Generator_status	ONLINE	
	Inverter_efficiency	0.9	
	Inverter_type	FOUR_QUADRANT	
	Phases	ABCN	
	Rated_power	45 kW	
Parametric Analysi	Density	10%, 20%, 30%, 40%	Density-dependent parameter, varies 4 times.
	Name	CES	Community energy storage.

N.B. During the islanded mode of operation the CES control system continuously adjusts output active and reactive powers in order to keep the energy balance and maintain voltage close to their nominal values. Islanded mode is enabled in the IceOpt transmission model simulations.

Figures 5.1 and 5.2 illustrate the baseline real and reactive power flows, respectively, in the distribution feeder for 2012. Power fluctuations in both these figures are derived from real data on a slightly different schedule from seasonal variations in Iceland, which tend to exhibit maximum power flows during winter months November to April, and lesser power flows characteristic of summer months May to October. Therefore, the schedules needed to be offset to account for this annual variation using the standard player files for loads. In GLD, the player's values can be used as a schedule transform, allowing specific data sets to be played to the objects in the grid without the memory overhead of the schedule. In other words, the players were adjusted by shifting their time values by half a year and placing what would have been peak summer months to be peak winter months in order to reflect more accurately Icelandic seasonal power flows. This kind of data alteration does not compromise the integrity of the results because player files are designed to be flexible and scaled up or down. Furthermore, since EES simulations are tested on only three days of the year and considering the main goal of this thesis is to demonstrate the impacts of implementing EES technologies in Iceland's power system,

Figures 5.1 and 5.2 are simply intended to give the reader a more indicative idea of how the distribution feeder functions on an annual basis.

The aforementioned player schedules are based on real load flow or power consumption data, and each schedule is imported as a file in the code of every simulation that was run through GLD. Together, the real data along with the player files are responsible for causing the power and voltage fluctuations on an hourly, daily, and monthly basis as seen in Figure 5.1 and 5.2. Baseline curves for power and voltage fluctuations are defined as any curves resulting from simulations run without the addition of EES.

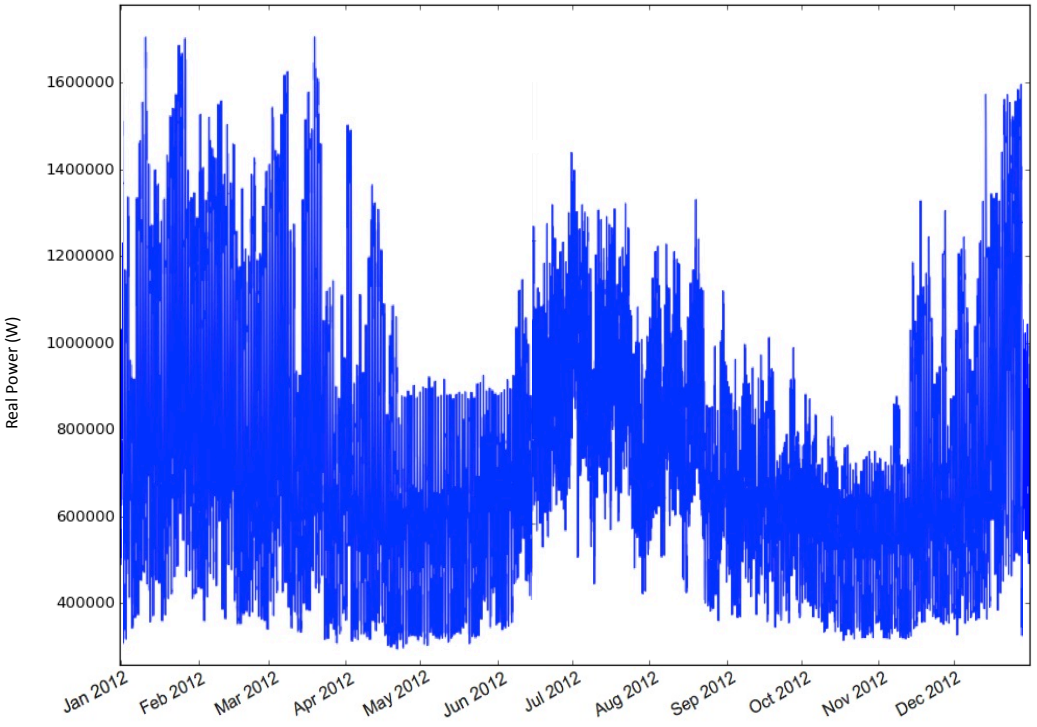

FIGURE 5.1: *Baseline power flows in a prototypical residential feeder over 2012.*

In Figure 5.3, natural voltage fluctuations within the baseline feeder over the course of the year are shown. This plot did not require the same data schedule offset as the power flow figure because feeder voltage remains relatively consistent throughout the year. Changes made to the nominal voltage of the prototypical feeder .GLM file can be seen along the y-axis of Figure 5.4, where voltage is plotted with kV units. Nominal voltages within the .GLM were scaled up from 7 kV to 11 kV to match residential output voltages to homes in Iceland, before they are scaled down to 230 V for household appliance use. This is a common 11 kV residential feeder.

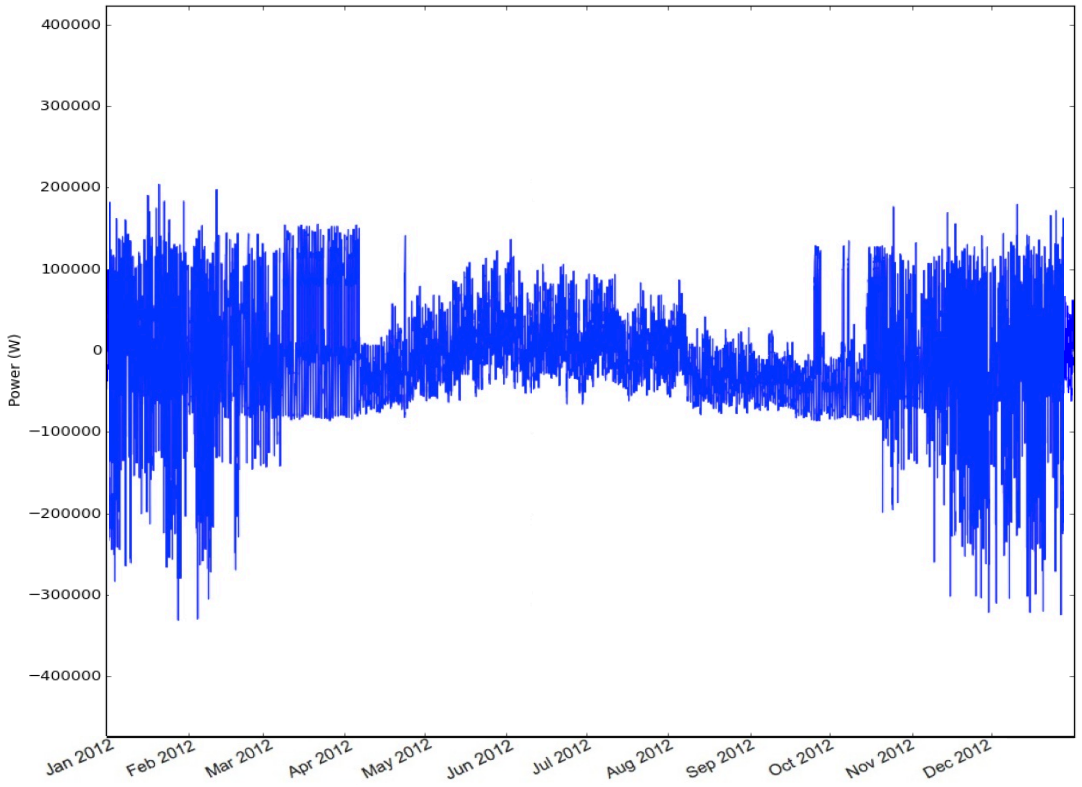

FIGURE 5.2: *Baseline reactive or imaginary power for residential feeder in 2012.*

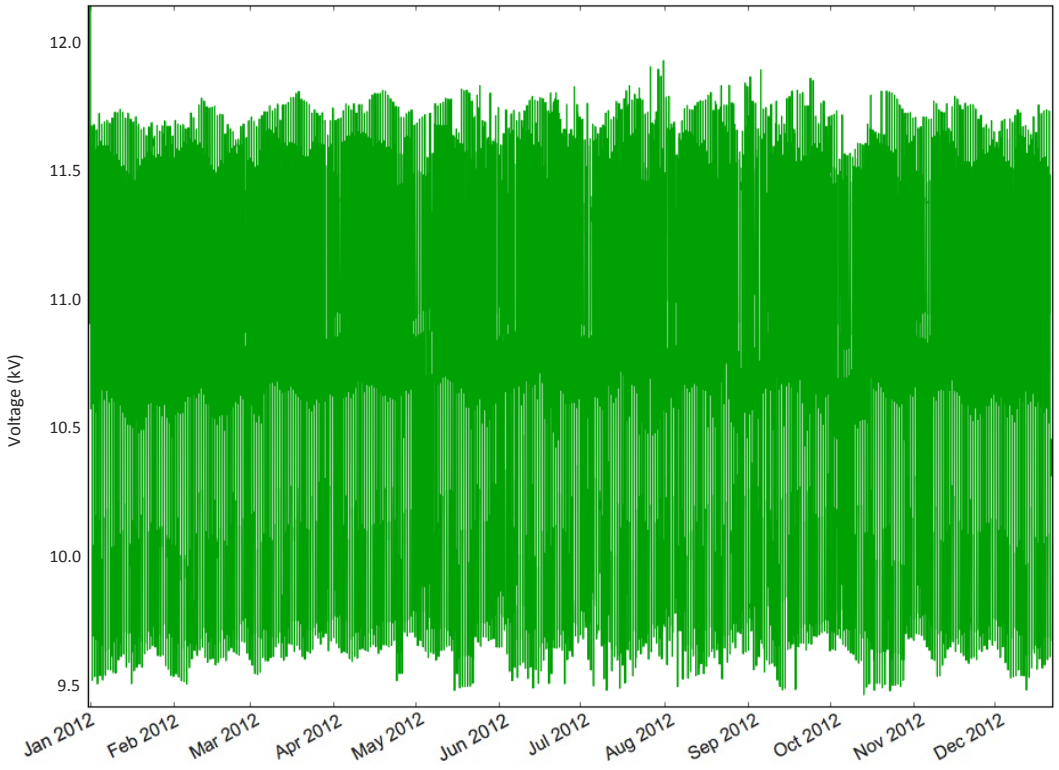

FIGURE 5.3: *Baseline voltage fluctuations over the course of 2012 in the residential feeder.*

The results in Figure 5.4 depict the baseline real power flows from Figure 5.1 on a three-day time period, offering a close-up of power peaking at 1287 kW between 16:00h and 20:00h, with a minimum of 438 kW from 00:00h until 5:00h. Mean real power in the feeder is 8539 kW, standard deviation is 2550 kW over these 3 days.

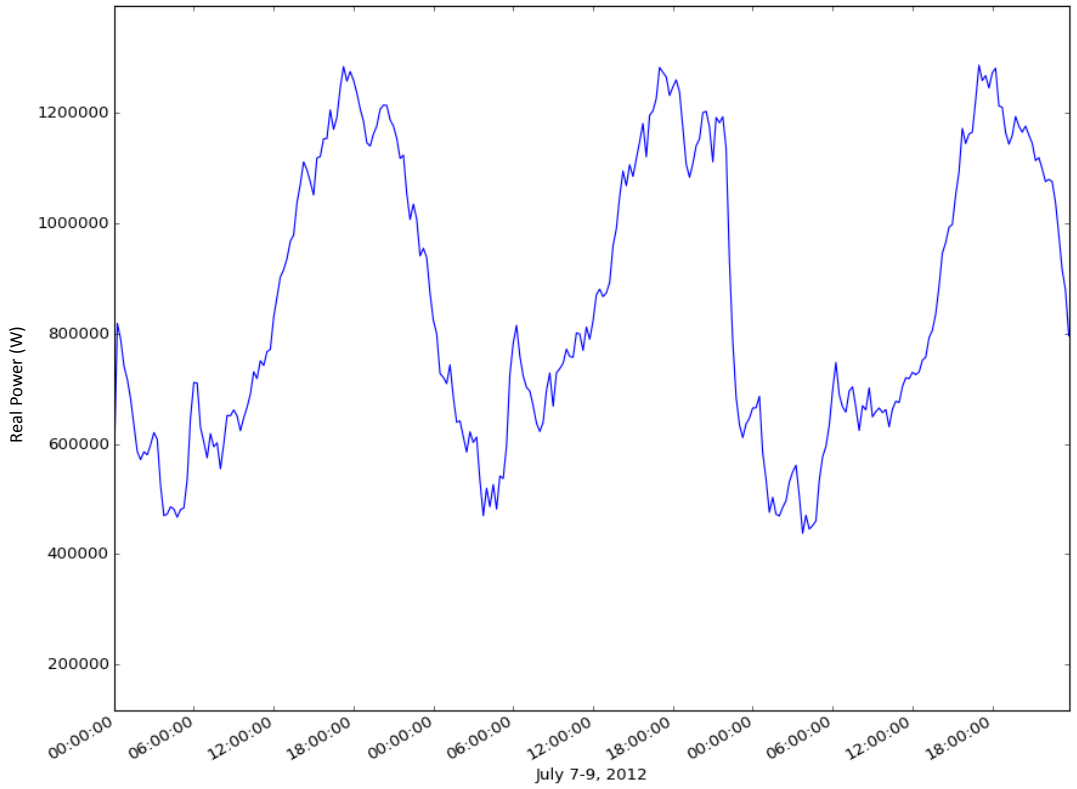

FIGURE 5.4: *Real power flow across the entire feeder over a three-day timescale in July.*

Results in Figure 5.5 depict baseline voltage fluctuations on a three-day time period, the mean voltage of the curve is 11.20 kV, and standard deviation is 6.10. Although less of a trend appears here than in power flows, voltage spikes in the baseline are still seen around the same times as peak power in the late afternoon and evenings.

The following plots illustrate the valuable impacts CES have on the same distribution feeder. As per Table 5.2, the batteries are in load-following mode, sensing power at the transformer level, and monitored using a BMS centralized controller object. The most significant improvements to the load flows of this feeder are seen in voltage control and peak-shaving when voltage spikes between 18:00h and 20:00h. Figure 5.6 compares CES at densities 10%, 20%, and 30%, excluding density 40% because Figure 5.7a indicates no gainful improvements between lower densities 30% and 40%. Therefore, increasing the CES density to 40% would produce little to no enhancements and work against achieving grid optimization with storage. Figure 5.7b illustrates the negligible difference between densities 30% and 40%.

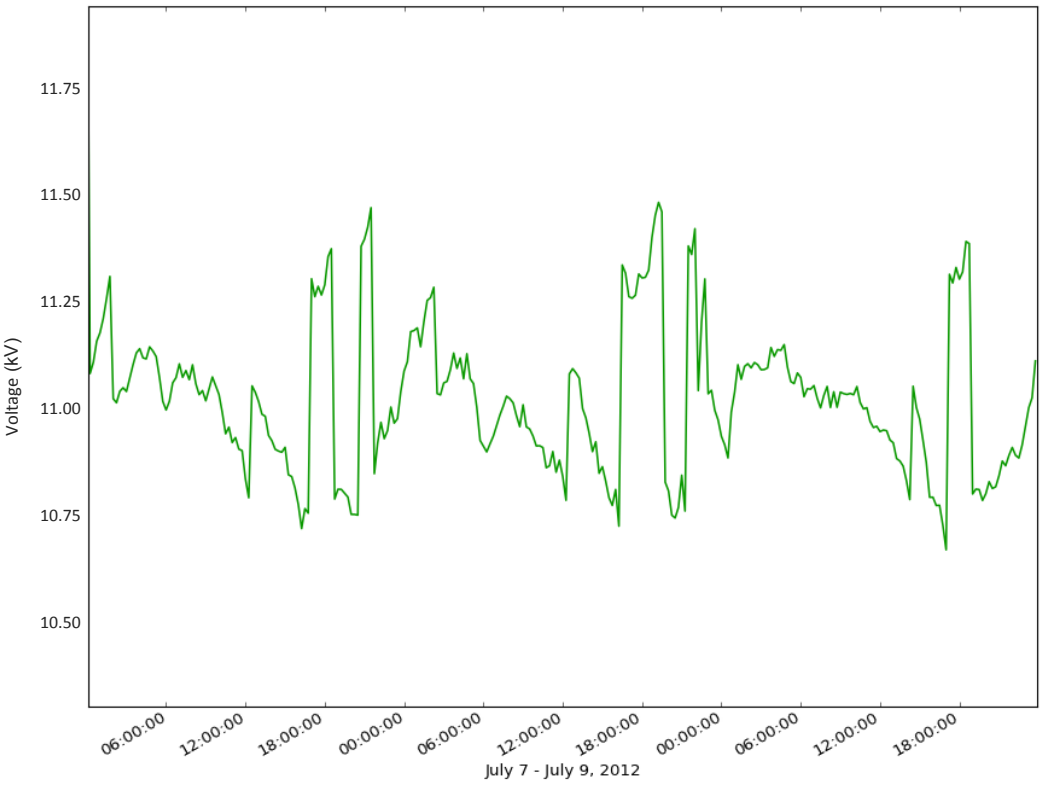

FIGURE 5.5: *Feeder voltage exhibits a more characteristic fluctuating tendency.*

The next series of plots depict the effects of CES on power flows, both real and reactive, in the residential feeder. Peak-shaving is the main performance metric to be determined from the results. Following the Li-ion battery and BMS parameters set in Table 5.2, the battery systems begin charging at 600 kW (600,000 W on the y-axis in Figure 5.8) obeying the charge setpoint at 600 kW in the parameters table. Figure 5.8 also shows the BMS batteries gradually turning on at 1000 kW in order to further reduce real power towards the peak-shaving setpoint. CES with density 40 has the greatest impact on real power peak reduction. Figure 5.9 explicitly shows the charge and discharge cycles beneath the real power flow curves.

Figures 5.10 and 5.11 integrate the areas beneath the baseline real power curve (without energy storage) and the CES_D30 real power curve, respectively. This function provides the total amount of real power in the feeder at the time. The integrated value for the baseline curve totals 219.91 MWh of real power within the entire feeder over the three-day simulation period. The integrated value for the new feeder with a 30% density of CES evenly distributed throughout totals 196.45 MWh, much less real power than the baseline curve over three days. Finally, CES_D40 offers the greatest improvement in power reduction, though such a high density of energy storage may not be the most realistic option for the residential feeder. The design of this experiment also stipulates that the lowest density to bring about a 10% reduction from the baseline would be

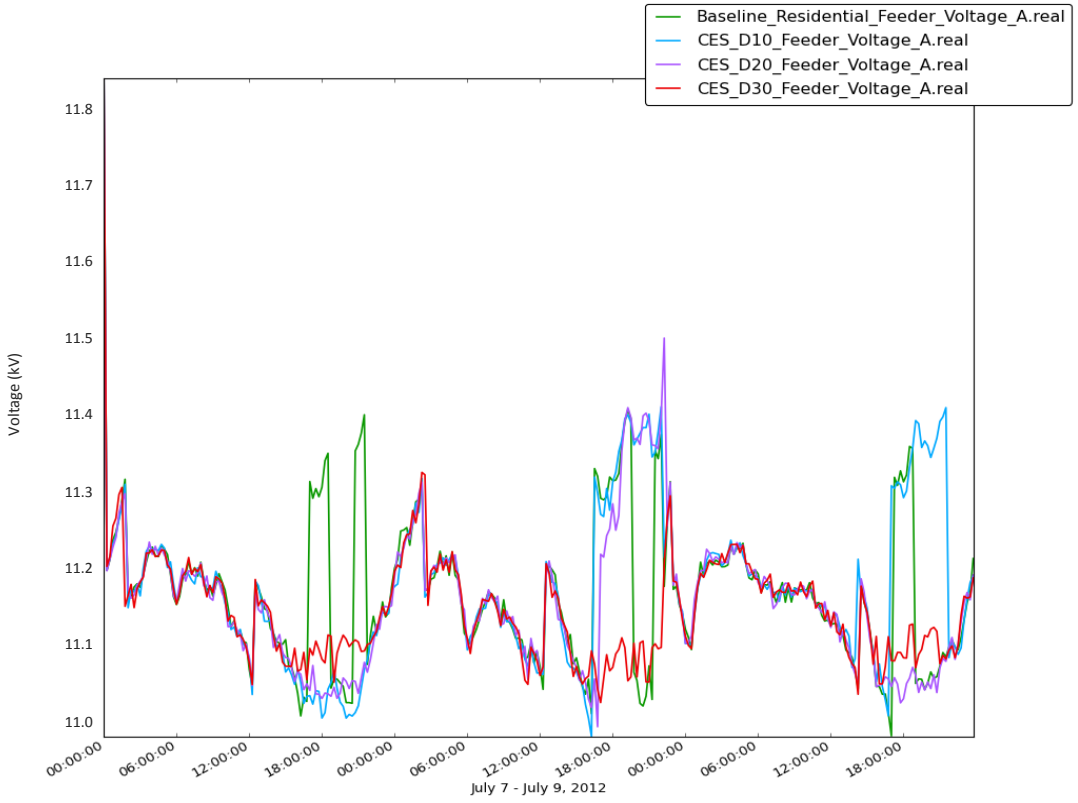

FIGURE 5.6: *CES at varied densities working to maintain voltage at a more desirable level. As the voltage curve spikes near 18:00h the CES system works to stabilize the fluctuations. Densities 30% and 40% are more effective in voltage regulation than the lower densities.*

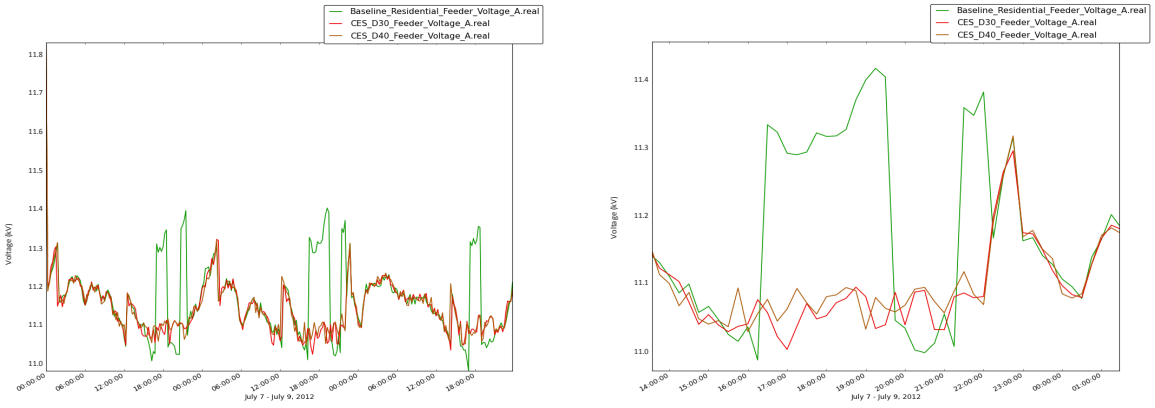

FIGURE 5.7: *CES comparison between densities 30 and 40. A close-up of voltage regulation is shown in Figure 5.7b shows clearly there is little improvement between densities 30% and 40%, suggesting the 30% density is the optimal CES concentration for this residential feeder.*

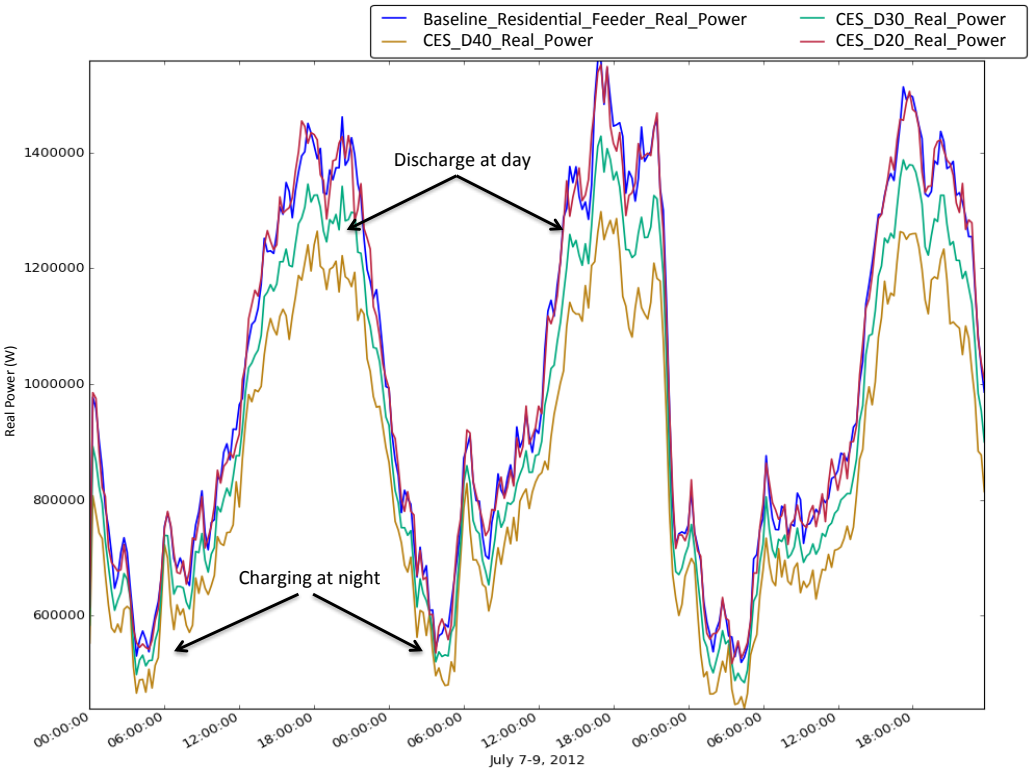

FIGURE 5.8: *CES reducing real power flows to enhance peak-shaving during max demand.*

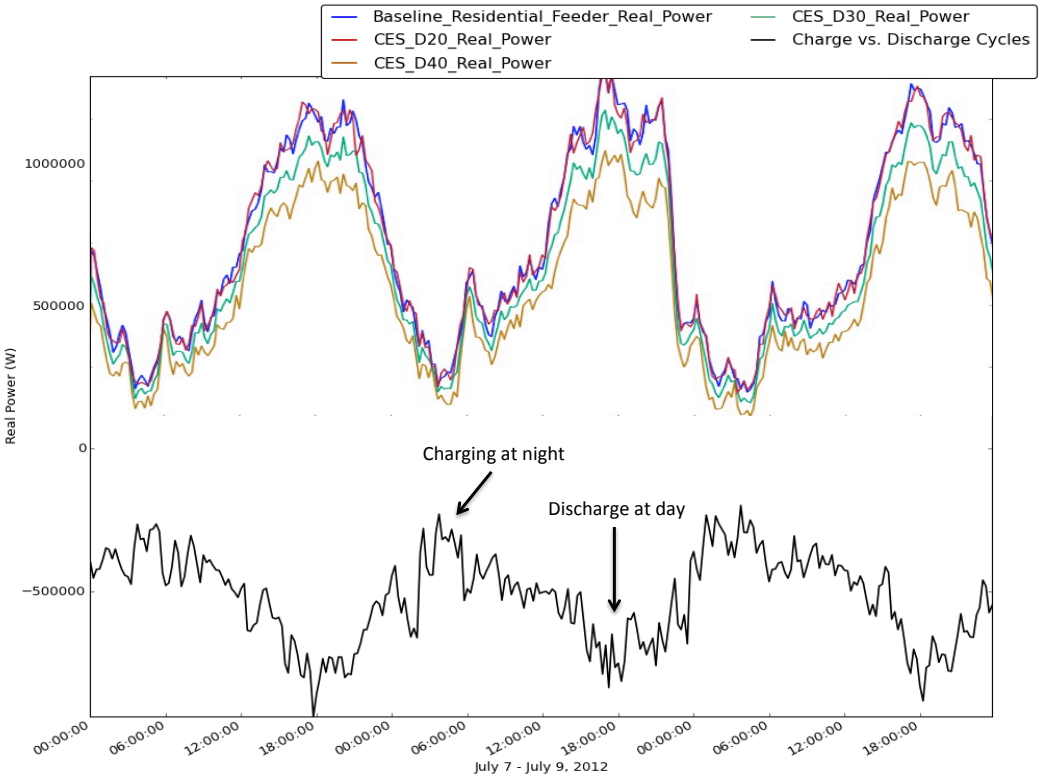

FIGURE 5.9: *CES supplementing real power flows over the three days, with its charge and discharge cycles shown coinciding with the rise and fall of real power within the feeder.*

selected, which in this case would be CES_D30. Nevertheless, the real power flow for CES_D40 was integrated to yield a total of 186.62 MWh beneath the curve and is shown in Figure 5.12.

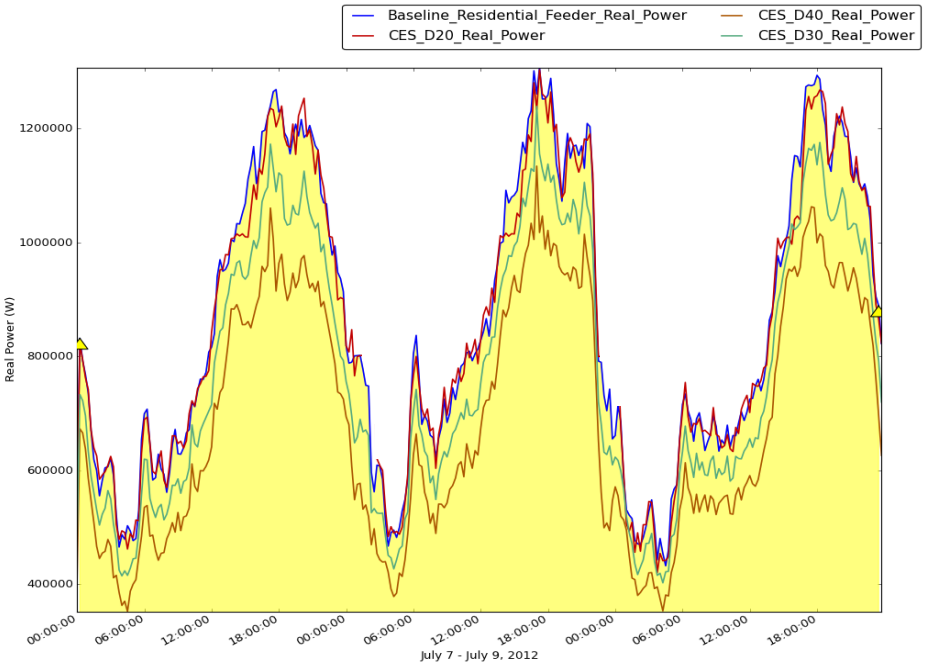

FIGURE 5.10: *Integrated power flow beneath baseline curve equals 219.91 MWh.*

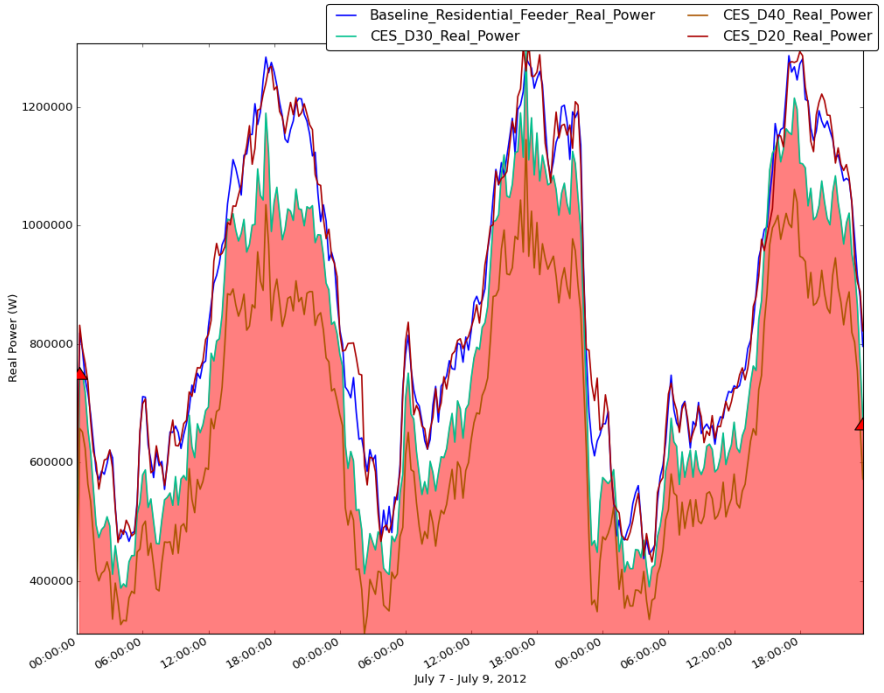

FIGURE 5.11: *Integrated power flow of CES_D30 real power curve equals 196.45 MWh.*

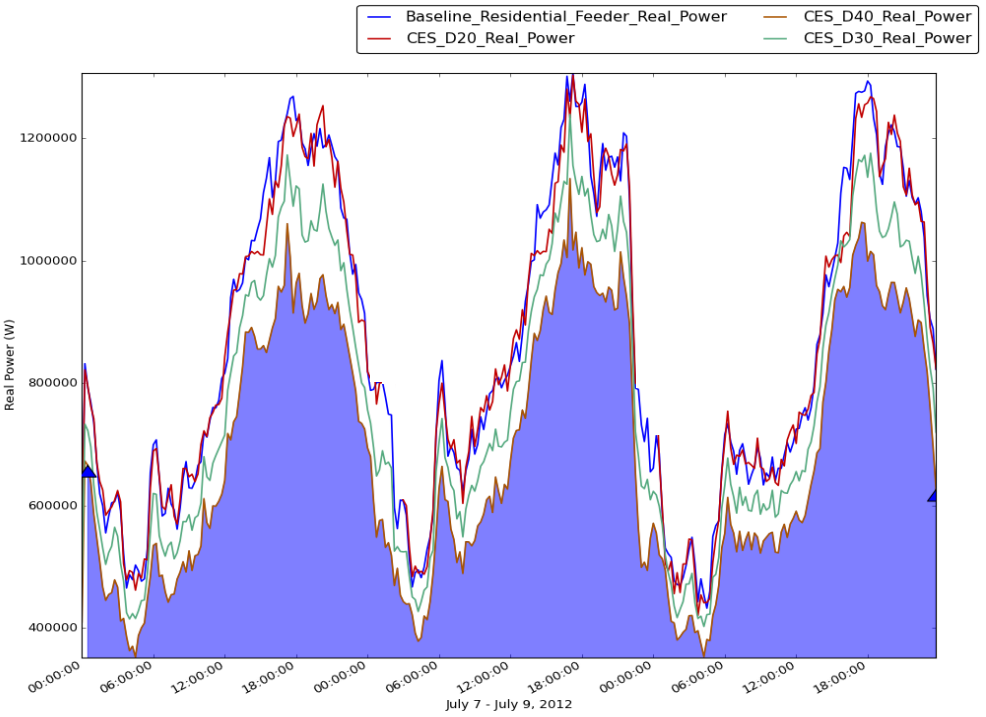

FIGURE 5.12: *Integrated power flow of CES_D40 real power curve equals 186.62 MWh.*

Results in Figures 5.13 and 5.14 suggest CES exerts effective reduction in reactive (or imaginary) power as it peaks each day in this sequence as well. Figure 5.13a plots baseline real power and reactive power control with CES for a comparison. Figure 5.13b brings the real power baseline down to the reactive power baseline. The integrated reactive power using CES_D30 is 1.22 MVAr, and CES_D40 is down at 0.61 MVAr, while the integrated reactive power of the baseline curve is much higher at 2.71 MVAr. See Appendix D for integrations.

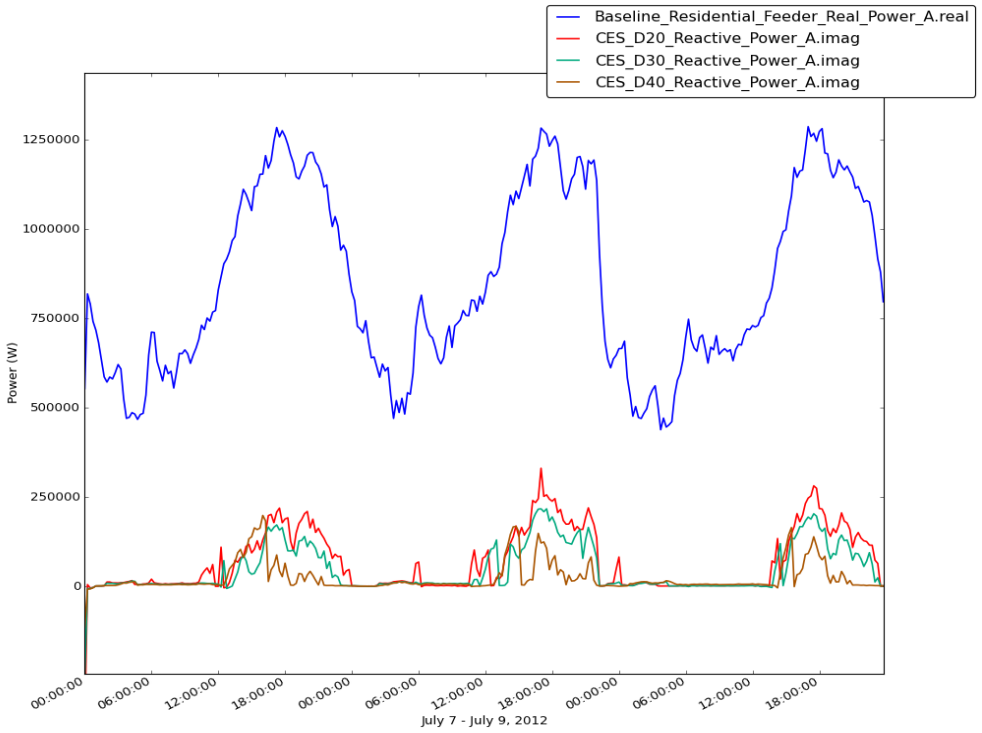

FIGURE 5.13: *Baseline real power plotted against reactive power below from three different CES density installments.*

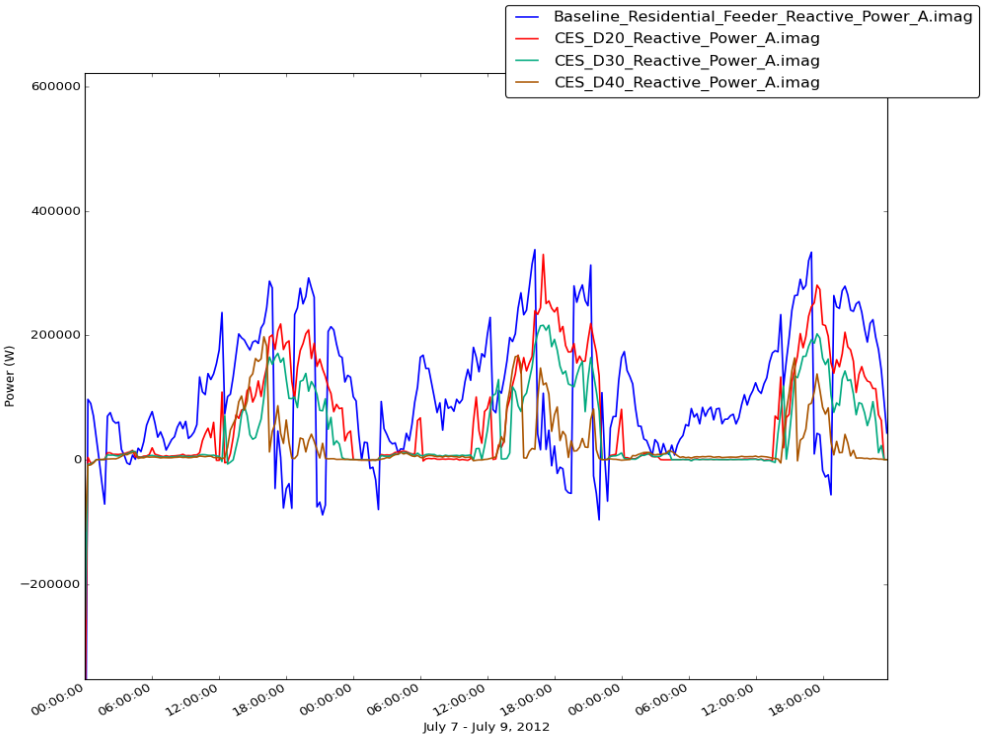

FIGURE 5.14: *Real power baseline is brought down to the reactive level for better comparison between baseline and EES curves.*

5.2.2 Complex Resource Scenario Two: NaS Battery Solutions

In this group of simulations, first the optimal density of energy storage is found employing the same techniques as the previous section on the Icelandic transmission network. This involves comparing real, reactive power and voltage curves for various EES densities that are evenly distributed across the grid using the GridCommand™ parametric analysis tool. Once the best EES density for the grid is identified, the second part of results in chapter 5.2.2 places NaS batteries clustered in targeted locations in each quadrant while keeping the EES density constant at the optimal level. In this way, varying EES attachment points in the transmission model is the second phase for pinpointing optimized conditions; therefore, configuration of energy storage in the IceOpt model was the key to the trials of this section.

Important changes have been made to the EES parameters and BMS controller object that better suit this much larger capacity grid. Table 5.3 outlines the parameters for the IceOpt simulations to first determine the optimal battery density. The density of NaS batteries are once again a measure of the concentration of battery systems evenly distributed in the feeder, which are set to 40%, 50%, 60%, and 70%. Noting that densities 60% and 70% are fairly unrealistic and yield almost identical results, they are nevertheless shown because the lower densities 40% and 50% had little to no effect on power and voltage. These matters are more closely explained in the discussion and analysis chapter.

TABLE 5.3: *Parameters for NaS batteries and BMS controller objects used in the IceOpt transmission model.*

	Variables	Parameters	Notes
NAS Battery:	Battery_capacity	10 MWh	
	Battery_size	LARGE	
	Battery_type	NaS	
	Nominal_voltage	33 kV	
	Rated_power	10 MW	Maximum power used by device.
	Reserve_State_of_charge	0	
	Round_trip_efficiency	0.90	
	State_of_charge	1.0	
NAS Controller:	Charge_setpoint	600 MW	Charging occurs when demand is at this limit.
	Peak_shaving_setpoint	1200 MW	Tells controller when to switch batteries on.
	Fixed_charge_rate	0.9 MW	
	Fixed_discharge rate	1 MW	
	Islanded_mode	TRUE	The grid is not attached to others.
	Max_charge_rate	1	
	Max_discharge_rate	1	
	Max_discharge_rate_reactive	1	
	Peak_shaving_method	LOAD_FOLLOWING	Discharges when regulator is above the peak_shaving_setpoint value.
Inverter:	Generator_mode	SUPPLY_DRIVEN	
	Generator_status	ONLINE	
	Inverter_efficiency	0.9	
	Inverter_type	FOUR_QUADRANT	Quadrant concept describes grid sectioning.
	Phases	ABCN	
	Rated_power	10 MW	
Parametric Analysi	Density	40%, 50%, 60%, 70%	Density-dependent parameter, varies 4 times.
	Name	NAS Battery	Large-scale transmission level storage.

Figure 5.15 is the result of real power flow simulated for all of 2012, using the same timestamp and schedule as the residential simulations. Figure 5.16 shows reactive power

flows for the year, and Figure 5.17 illustrates voltage fluctuations on an annual basis. If these figures look similar to those plotted in chapter 5.2.1. using the residential feeder, that is because both codes share the same timestamp, scheduling and player files. For keeping results consistent, the same three-day simulation was used: July 7-9, 2012 for the national grid.

Results in Figure 5.15 and 5.16 show important unit changes to the y-axis label, which is scaled up from W to kW since this is a much larger, national power system with far more power than the residential feeder modeled in the previous section. The same can be said for the voltage scale between residential and transmission systems, in Figure 5.17, the y-axis is scaled up from 11 kV to 33 kV to match the output nominal voltage from the Landsnet grid.

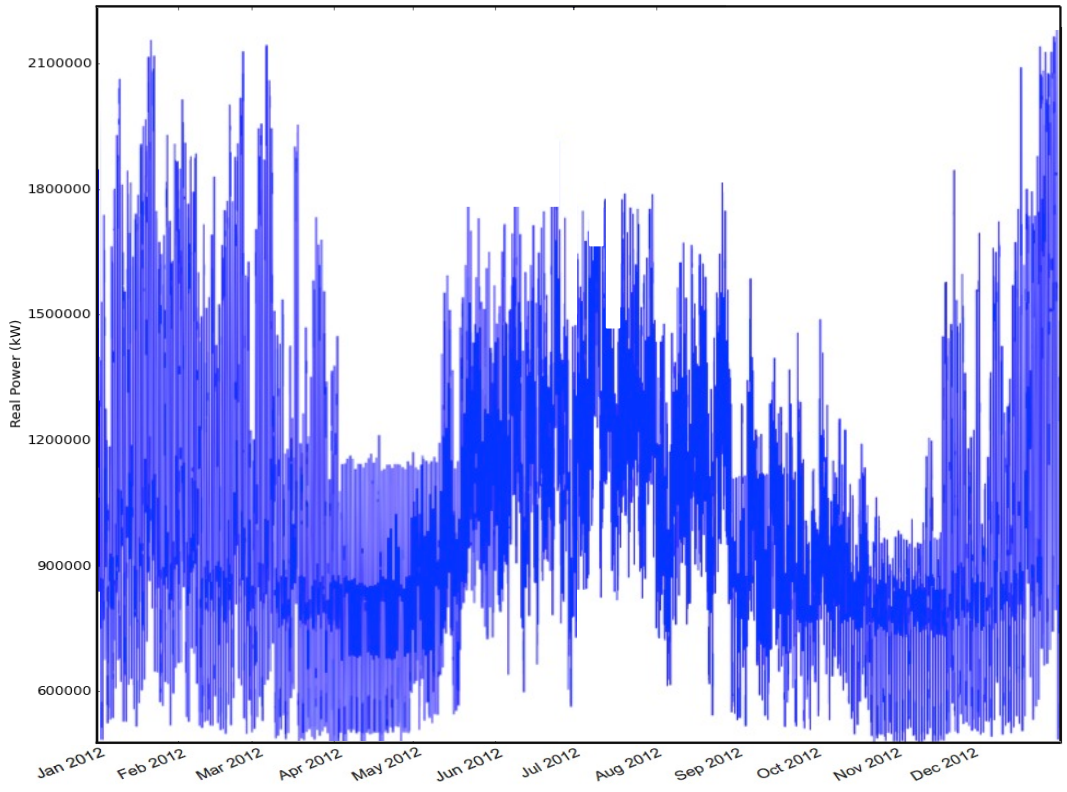

FIGURE 5.15: *Annual baseline real power flow for the Icelandic power system model.*

Figure 5.18 shows real power flow over the same three-day period. The large voltage spike in Figure 5.19 is most likely attributed to program error, considering it occurs at an off-peak hour.

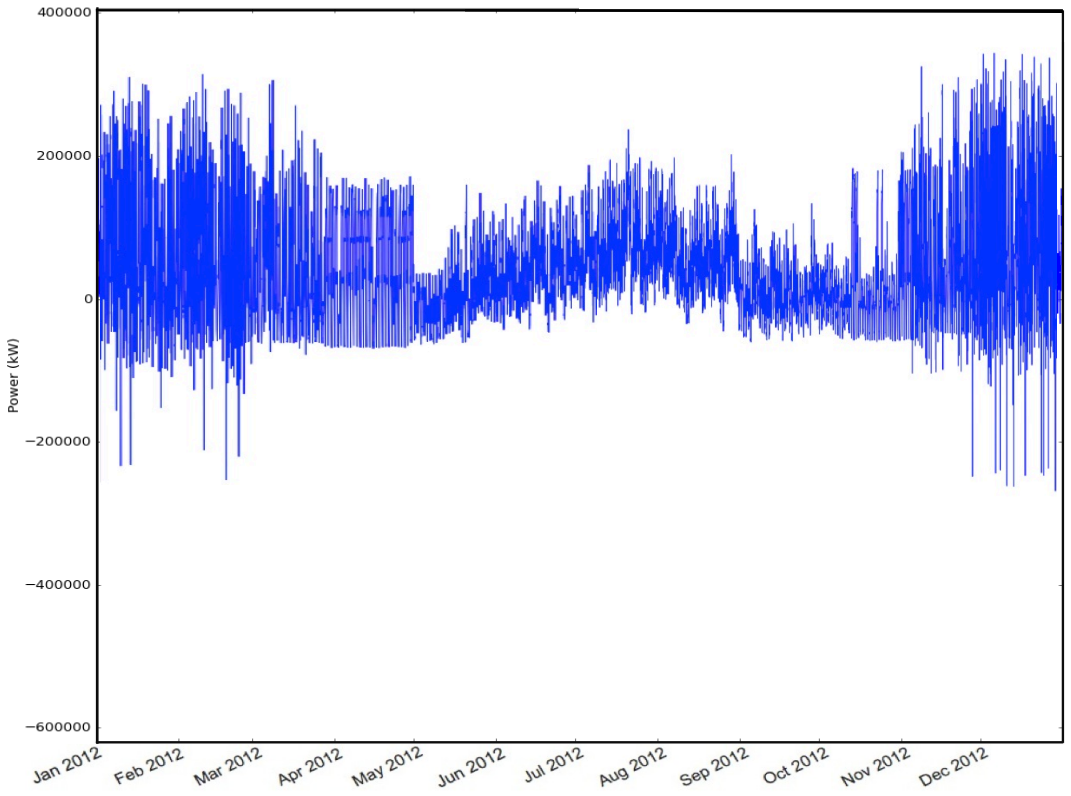

FIGURE 5.16: *Annual baseline reactive power for the Icelandic model.*

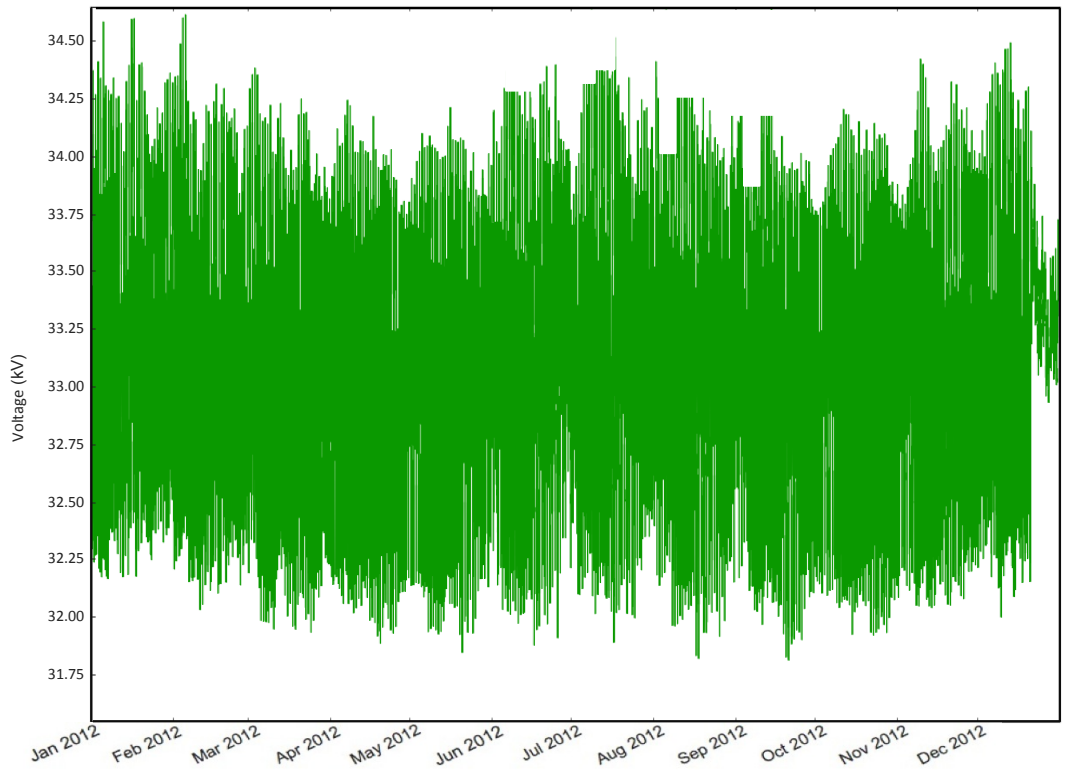

FIGURE 5.17: *Annual baseline voltage fluctuation in the Icelandic model.*

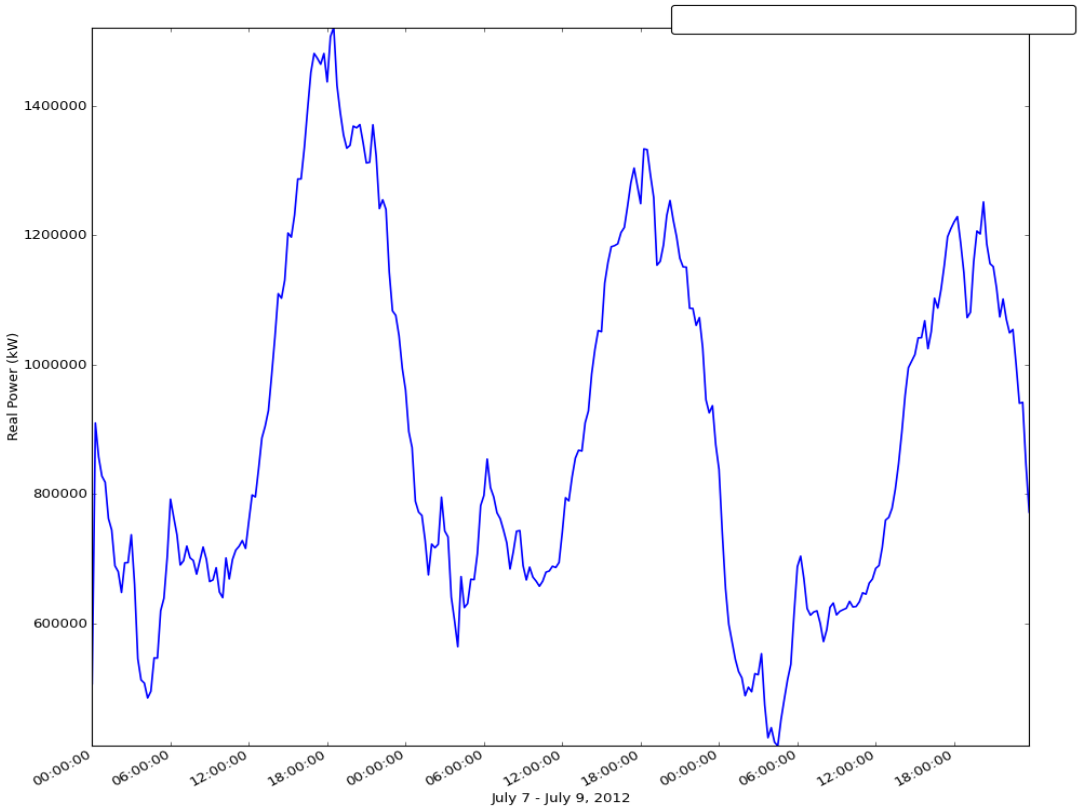

FIGURE 5.18: *Power flow across the Icelandic power system over a three-day timescale in July.*

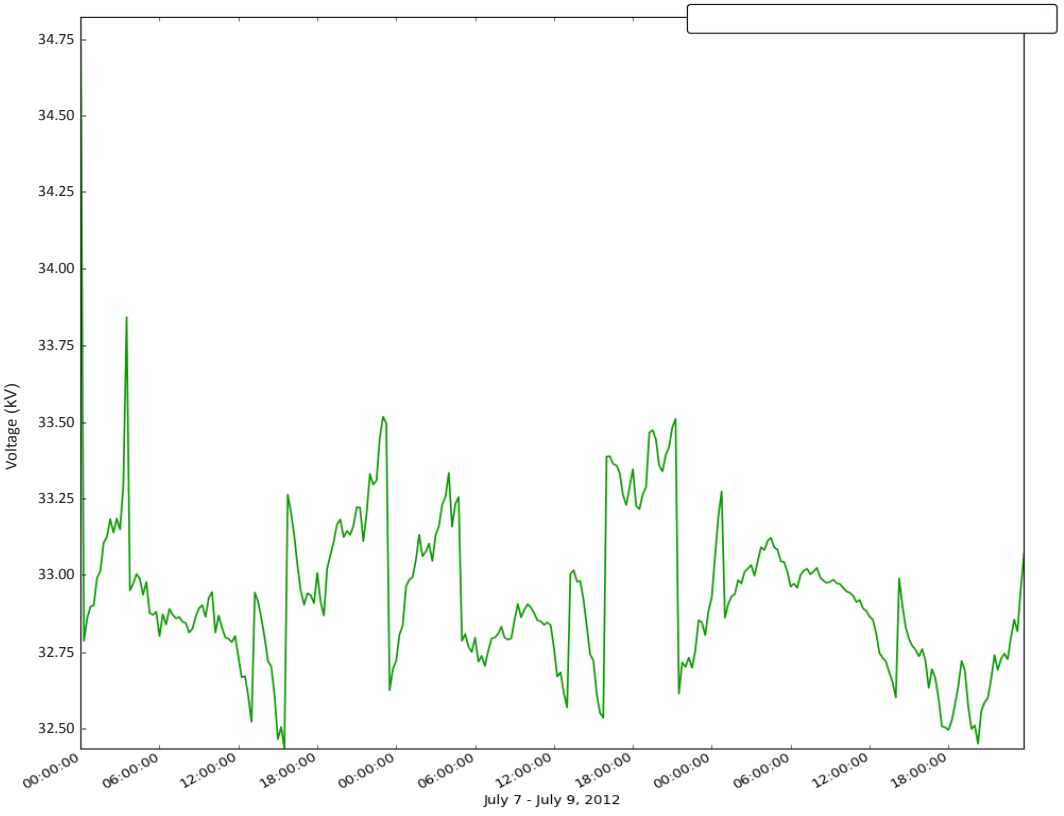

FIGURE 5.19: *Baseline voltage running throughout the transmission model.*

Results in Figure 5.20 and 5.21 demonstrate NaS integration's ability to regulate voltage within the grid. Much like the CES plots, higher densities have a greater propensity for reducing voltage fluctuations. Figure 5.21 shows only densities 50% and 60% because the difference between density 60% and 70% is deemed insignificant. The behaviour of NaS_D40 is unexpected, and believed to be attributed to the battery system attempting to adjust in response to the baseline voltage spike at the onset of the simulation on July 7.

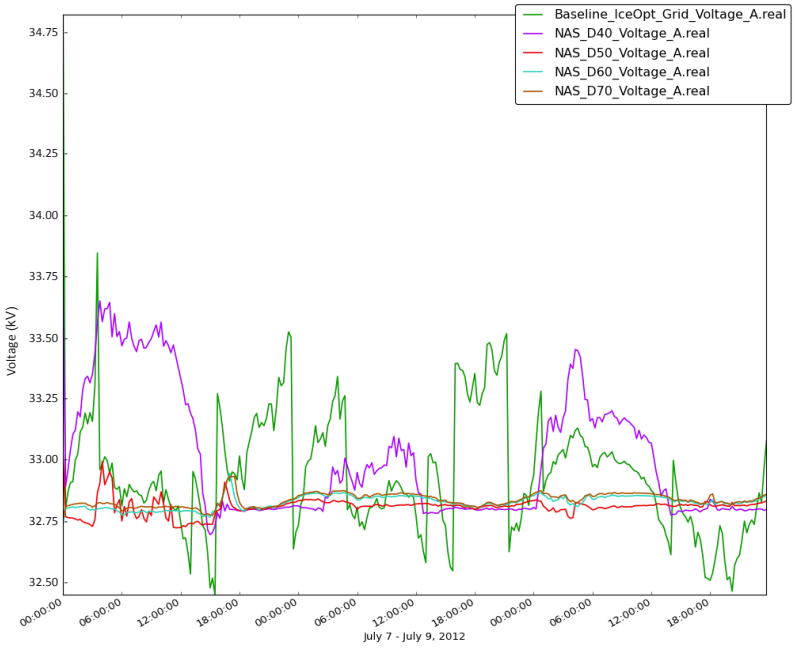

FIGURE 5.20: *All tested densities of NaS voltage curves plotted with baseline voltage.*

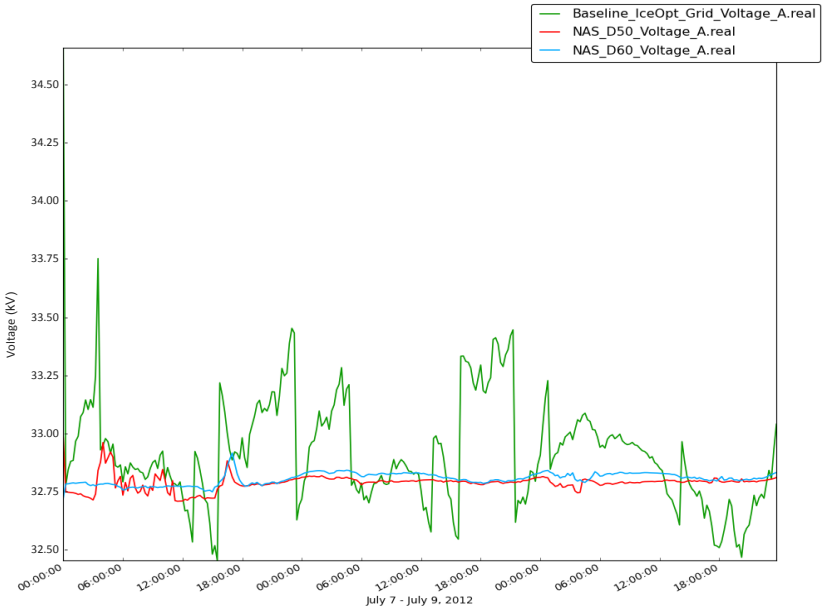

FIGURE 5.21: *Voltage curves for baseline and densities 50 and 60 only.*

The next series of plots investigate the effects of evenly distributed NaS batteries at different densities on the real power baseline. Figure 5.22 shows all EES densities and baseline data. There are four phases defined in each simulation of the electricity system: phases A, B, C, and N, or neutral. Real power curves for densities 60% and 70% are believed to drop below the baseline throughout the course of the simulation due to the A phase (A.real) plotted in Figure 5.22, and also possibly because these two EES densities are so large. The plot in Appendix E was performed for real power flows using the B phase (B.real) and shows different results. Real power curves for densities 60% and 70% do not continually reside below the baseline curve in this B phase plot, suggesting that phase selection is also critical in assessing the impacts of EES technologies in distribution networks.

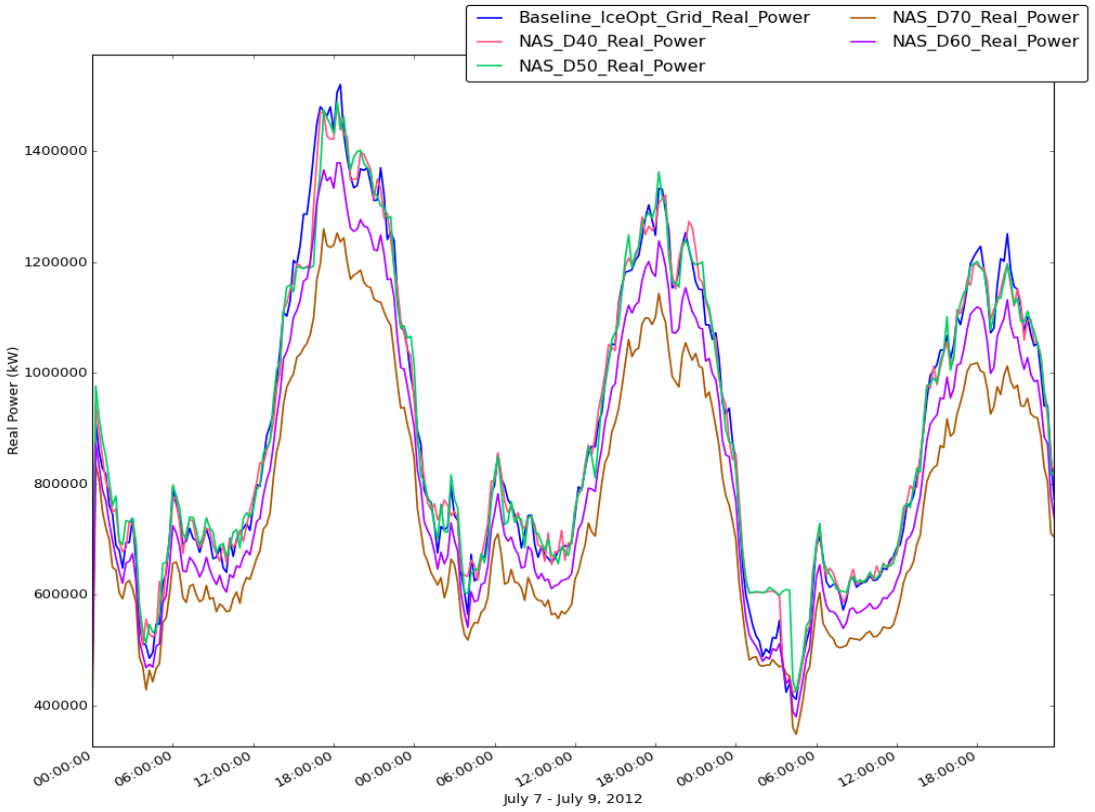

FIGURE 5.22: *Real power flow comparisons between baseline and increasing NaS densities.*

Figures 5.23, 5.24, and 5.25 are integrated beneath the selected curve to quantify how much real power is removed from the Icelandic grid with the addition of various EES densities. Baseline real power within the power system over the three selected days in July totals 228 GWh when integrated. In comparison, NAS_D60 reduces real power to 204 GWh, and NAS_D70, the highest density tested, reduces real power even further totaling 194 GWh within the grid over three days when integrated.

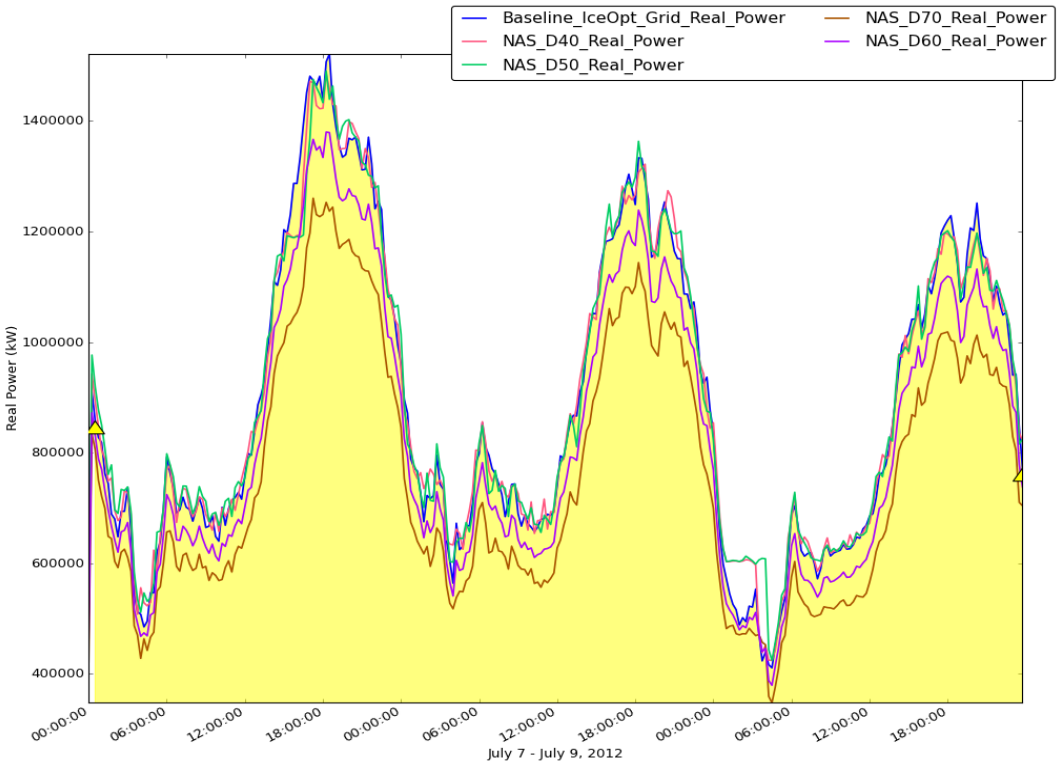

FIGURE 5.23: *Integration of the baseline real power flow curve, equals 228 GWh.*

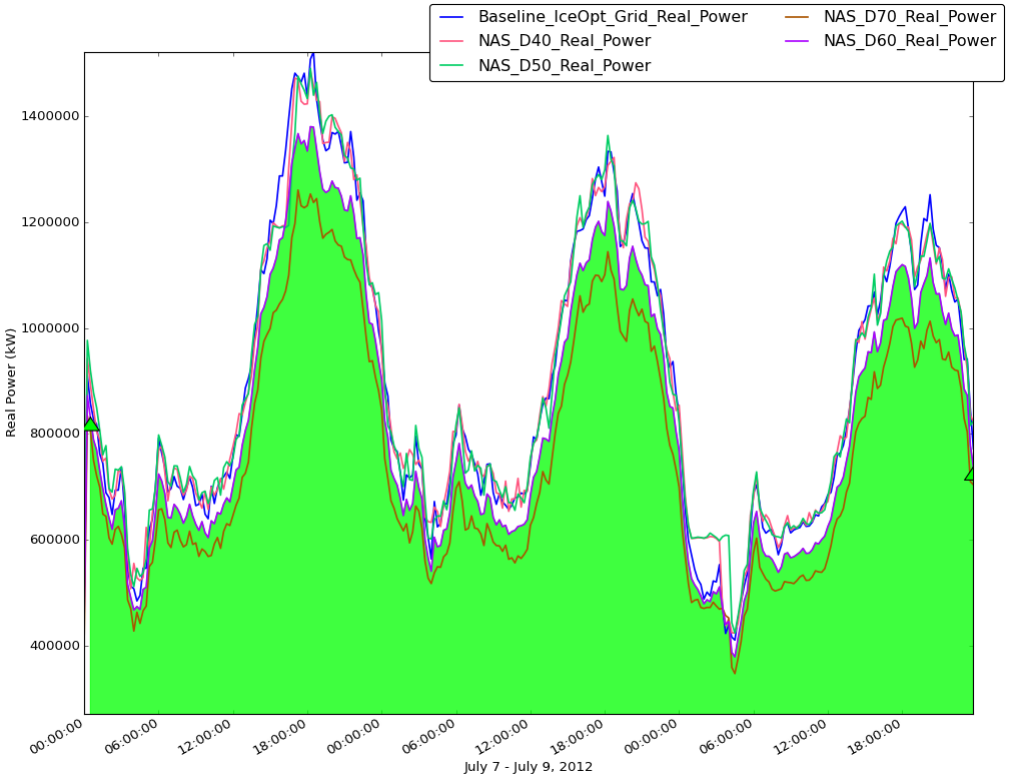

FIGURE 5.24: *Integration of the NaS_D60 real power flow curve, value equals 204 GWh.*

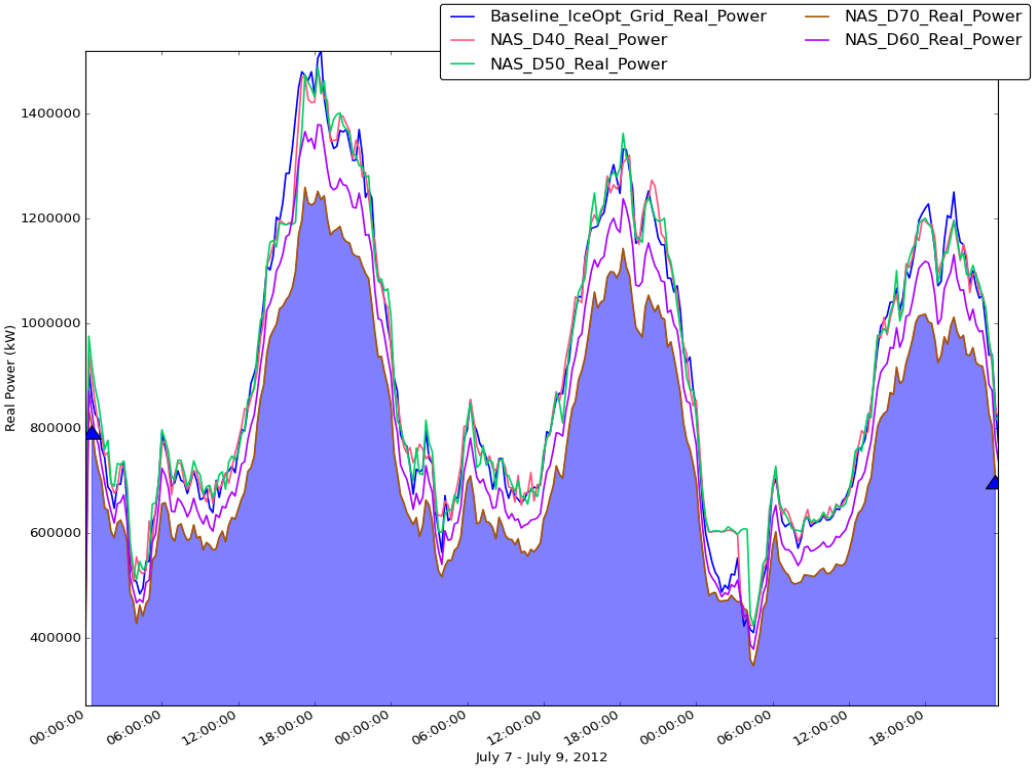

FIGURE 5.25: *Integration of NaS_D70 real power flow curve, value equals 194 GWh.*

Plotting reactive power shows new interesting trends in its performance metrics for the IceOpt model. Figure 5.26a shows the baseline real power flow along with the reactive power flows of all NaS densities tested. Figure 5.26b brings the baseline down to the reactive level to give a better indication of reactive power control with the addition of NaS. Figure 5.26c compares the two lowest EES densities 20% and 40%, while Figure 5.26d shows reactive power in the B phase (as opposed to A).

There is a clear nonconformity seen in the plots with NAS_D40 in the A phase. It appears to be minor feedback caused by the initial voltage spike seen in the baseline on July 7, just before 6am. What makes the reactive power plot in 5.26b truly odd is that the lower density, NAS_D20, appears more adept at stabilizing reactive power in the grid. This was the only phase and plot to show this abnormality, therefore it was included as part of the results along with the B phase plot to stress the importance of avoiding NAS_D40 as the optimal EES density for which to test our four simulations at various configurations in the IceOpt model.

Four conceivable EES configurations were tested; Table 5.4 details each location-specific configuration across quadrants of the Icelandic grid. Landsnet performance reports from 2011-2013 helped narrow down the possible combinations by identifying system weaknesses. EES systems were easily added to the IceOpt model using GridCommand^{TM} and its simple "add new technology" function. This allowed the connection of NaS batteries

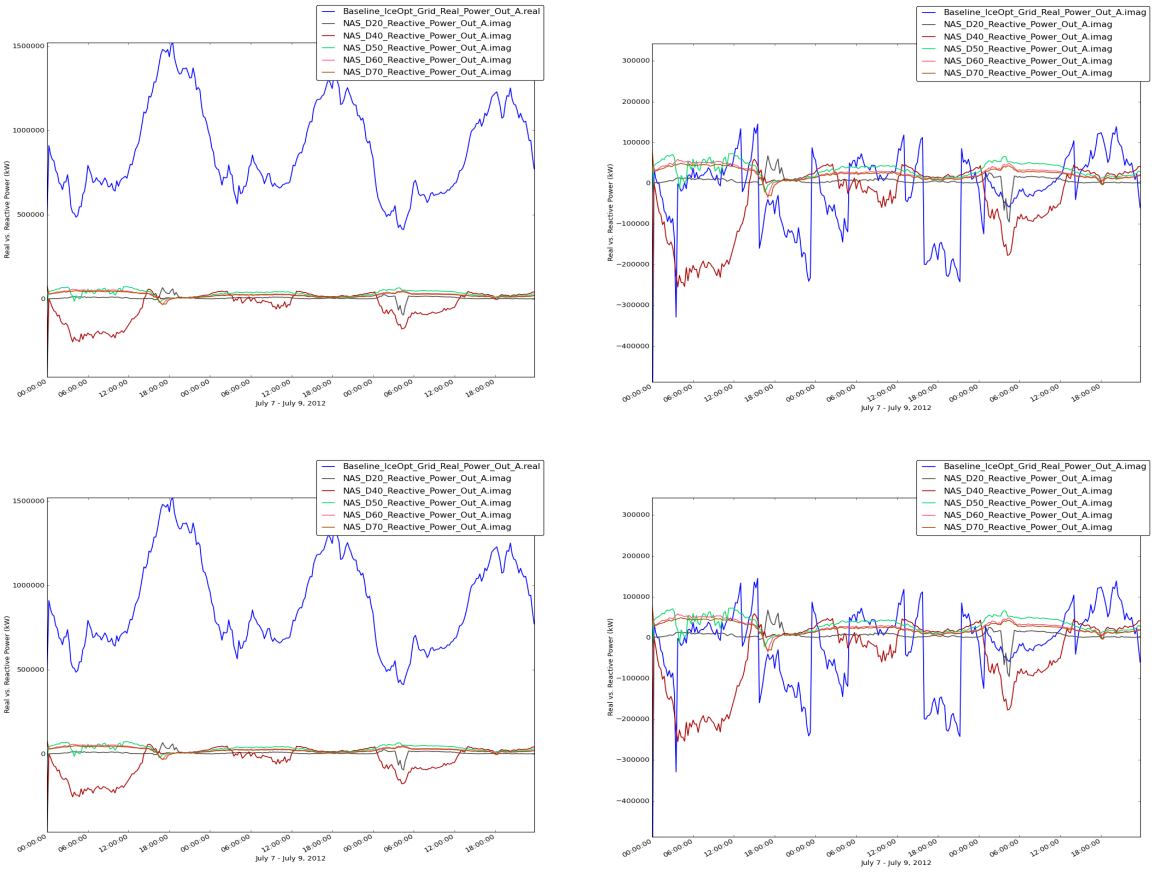

FIGURE 5.26: *Reactive powers of all NaS simulations plotted with the baseline reactive and real power.*

directly to user-defined transformer or substation objects in the model. The following results in Figure 5.27 and 5.28 illustrate how EES when clustered (instead of evenly distributed) at different electric substations within the grid reveal different benefits or drawbacks for energy efficiency, emergency storage, power quality, control and peak reduction.

Finally, it should be noted for all four configurations that add NaS batteries to their specific locations do so under the same parameters as those from Table 5.4, kept constant at density 60%. All results are further explained for their significance to the study and relevance to the future development of the Icelandic power system in the discussion and analysis chapter.

TABLE 5.4: *Configurations tested in the simulation by attaching EES at specific locations.*

Configurations	Quadrant	Substations/Transformers
Config_1	Q1	Mjolka
	Q2	Hryggstekkur
	Q3	Holar
	Q4	Hamranes
Config_2	Q1	Mjolka
	Q2	Hryggstekkur
	Q3	Holar
	Q4	Brennimelur
Config_3	Q1	Hrutatunga
	Q2	Fljotsdalur
	Q3	Prestbakki
	Q4	Hamranes
Config_4	Q1	Hrutatunga
	Q2	Fljotsdalur
	Q3	Prestbakki
	Q4	Brennimelur

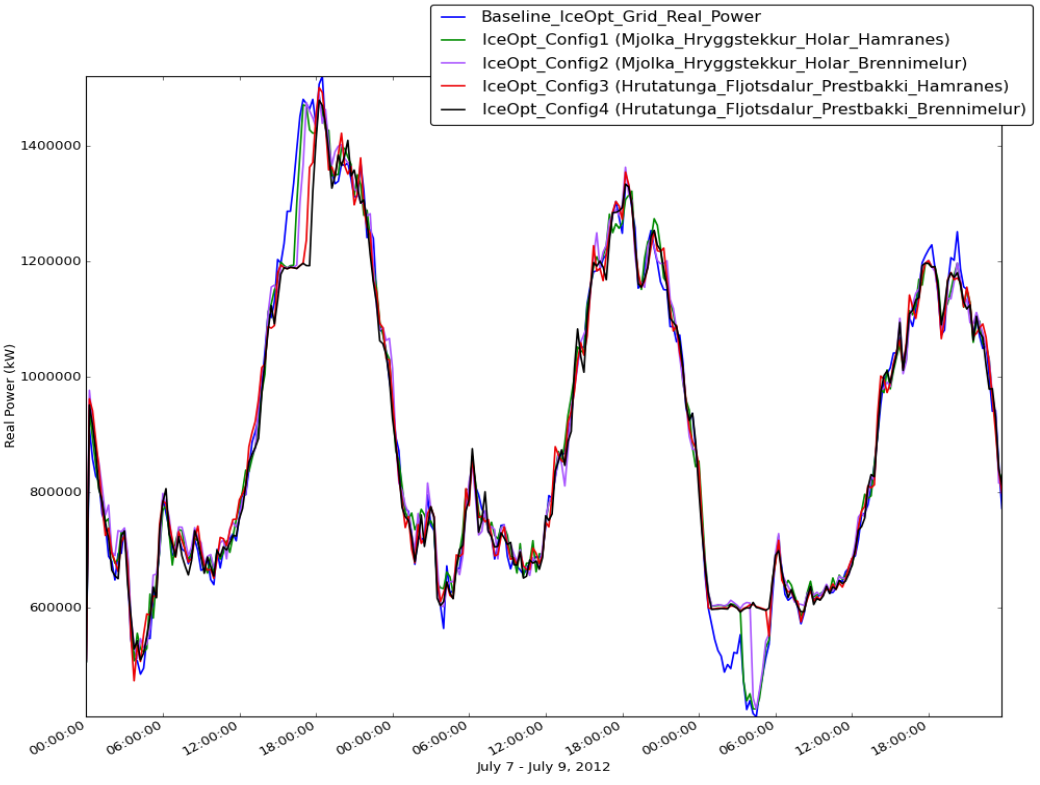

FIGURE 5.27: *Configurations plot for all four combinations of clustered NaS EES batteries and baseline real power.*

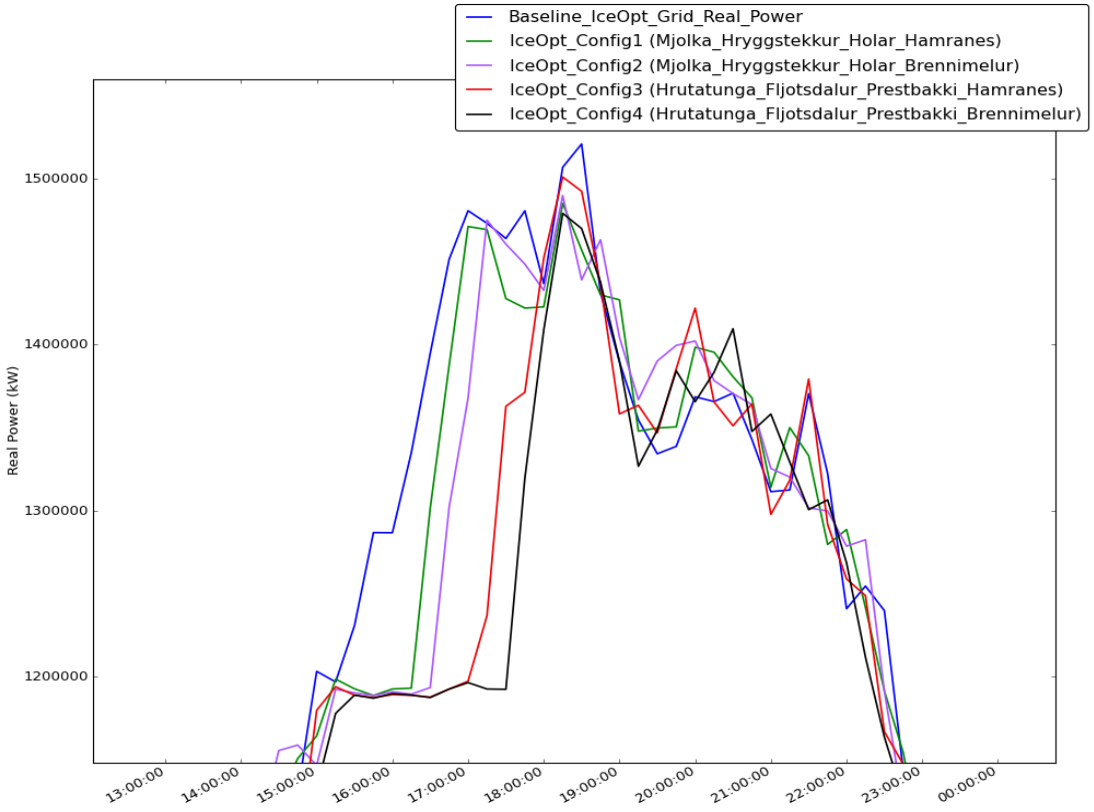

FIGURE 5.28: *Close-up view of real power peak reduction from the baseline using different NaS configurations.*

Chapter 6

Discussion and Analysis

Research results support the initial hypotheses that high-capacity energy storage will have significant improvements on power quality, peak-shaving, and voltage control, either by way of discharging electricity in controlled amounts to reduce real/reactive power, or by smoothing out voltage fluctuations. The two complex resource deployment scenarios tested are Li-ion CES in a residential feeder and NaS EES in the transmission system. Next we dissect the findings from each scenario with special emphasis on optimal battery conditions and the six EES performance metrics: (1) voltage control, (2) peak-shaving, (3) power quality, (4) energy arbitrage, (5) UPS, and (6) consumer-side time-shifting. Tables 6.1, 6.2, and 6.3 provides a summary of results for achieving grid energy storage optimization in Icelandic transmission and residential networks. Indicating which performance metrics are provided when threshold setpoints are solved, we determine optimal EES densities and the most ideal EES configurations discovered for each of the two scenarios. Each table is divided into three parts: real power, reactive power, and voltage, respectively.

TABLE 6.1: **Real Power Summary Table** – *Threshold for residential EES is 197.92 MWh. Threshold for transmission EES is 205 GWh. Integrals of real power flows below these thresholds are considered to be solved, and capable of providing the performance metrics listed.*

	Residential EES			Transmission EES		
	Simulation	Integral	Threshold	Simulation	Integral	Threshold
EES Densities	Baseline	219.91 MWh	No	Baseline	228 GWh	No
	CES_D10	219.34 MWh	No	NAS_D40	225 GWh	No
	CES_D20	219.25 MWh	No	NAS_D50	221 GWh	No
	CES_D30	196.45 MWh	Solved	NAS_D60	204 GWh	Solved
	CES_D40	186.62 MWh	Solved	NAS_D70	194 GWh	Solved
Performance Metrics	Peak-shaving, power quality, energy arbitrage, UPS, consumer time-shifting			Peak-shaving, power quality, energy arbitrage, UPS, consumer time-shifting		
Configuration	Evenly Distributed			Clustered, Configuration #4		
Optimal Conditions	CES_D30, Evenly distributed			NAS_D60, Clustered, Configuration #4		

TABLE 6.2: **Reactive Power Summary Table** – *Threshold for residential EES is 2.44 MVAr. Threshold for transmission EES is 2.98 $\times 10^4$ MVAr.*

	Residential EES			Transmission EES		
	Simulation	Integral	Threshold	Simulation	Integral	Threshold
EES Densities	Baseline	2.71 MVAr	No	Baseline	3.31 x10^4 MVAr	No
	CES_D10	1.85 MVAr	Solved	NAS_D40	2.99 x10^4 MVAr	No
	CES_D20	1.75 MVAr	Solved	NAS_D50	1.14 x10^4 MVAr	Solved
	CES_D30	1.22 MVAr	Solved	NAS_D60	1.07 x10^4 MVAr	Solved
	CES_D40	0.61 MVAr	Solved	NAS_D70	1.05 x10^4 MVAr	Solved
Performance Metrics	Peak-shaving, power quality, UPS			Peak-shaving, power quality, UPS		
Configuration	Evenly distributed			Clustered configuration #4		
Optimal Conditions	**CES_D10, Evenly distributed**			**NAS_D50, Configuration #4**		

TABLE 6.3: **Voltage Summary Table** – *Threshold for residential EES is 11.1 kV ± 0.11. Threshold for transmission EES is 33.1 kV ± 0.33. Standard deviations are shown as well.*

	Residential EES				Transmission EES			
	Simulation	Mean	σ	Threshold	Simulation	Mean	σ	Threshold
EES Densities	Baseline	11.30 kV	6.10	No	Baseline	33.49 kV	5.77	No
	CES_D10	11.26 kV	6.00	No	NAS_D40	33.44 kV	6.24	No
	CES_D20	11.22 kV	5.53	No	NAS_D50	33.16 kV	0.83	Solved
	CES_D30	11.12 kV	3.85	Solved	NAS_D60	33.13 kV	0.83	Solved
	CES_D40	11.11 kV	3.89	Solved	NAS_D70	33.11 kV	0.64	Solved
Performance Metrics	Voltage control, quality				Voltage control, quality			
Configuration	Evenly distributed				Clustered configuration #4			
Optimal Conditions	**CES_D30, Evenly distributed**				**NAS_D50, Configuration #4**			

In the case where thresholds are met by more than one density, it is common practice to choose the lower of the densities, especially if the lower density yields the same results as a density with more batteries. For instance, CES_D30 and CES_D40 both accomplish the same voltage reduction below the set threshold, with nearly identical mean and standard deviation values, therefore CES_D30 is selected for achieving optimal conditions as it requires less battery installation than CES_D40.

From the first summary table, we find that real power in the residential model is sufficiently reduced below the 10% threshold with a CES density of 30% incorporated into the feeder. The transmission model of the Icelandic power system crosses below the threshold once NaS batteries with a density of 60% are added to the grid. Solving these performance metrics will only then provide the benefits of peak-shaving, improved power quality, UPS, energy arbitrage, and consumer-side time-shifting for real power. Finally, the CES is evenly distributed in the residential feeder, and the NaS at 60% density is eventually clustered using the optimal configuration #4, consisting of Hrútatunga, Fljótsdalur, Prestbakki and Brennimelur substations.

From the reactive power summary table, CES at 10% density managed to solve the setpoint in the residential feeder. However, since this density cannot solve the real power threshold, the optimal density for the residential feeder remains at 30% CES. In the transmission model, a similar result is reached whereby the lower density 50% manages to reduce reactive power below the threshold. Once again, because 50% density NaS is incapable of solving real power threshold, the optimal density for the Icelandic transmission system remains to be 60%. This dichotomy presents an interesting anomaly in the results, suggesting that the EES systems tested here are more efficient at regulating reactive power (and to a degree voltage) using lower EES densities; on the other hand real power requires higher EES densities for peak-shaving and so on. Reactive power performance metrics provided when solved include power quality, UPS and peak-shaving of reactive power in both residential and transmission systems.

Finally, the voltage summary table expresses its comparisons using mean values and standard deviations. It also supports CES density 30% for maintaining voltage within the 1% limit for the 11.1 kV residential feeder. NaS with density 50% is found to be capable of reducing the baseline voltage from 33.49 kV towards a more desirable 33.16 kV, with a slight standard deviation of 0.83. Under the same rationale for EES density selection as the reactive power scenario, while NAS_D50 offers sufficient voltage regulation it cannot meet the performance requirements as NAS_D60 when it comes to real power, and therefore the transmission system still favours NaS batteries at 60% density as its best option for grid optimization, deployed in the Configuration 4 clustered arrangement.

Next we investigate with more detail into the analysis of each complex resource scenario for the residential feeder and transmission model.

6.1 Complex Resource Scenario One: Li-Ion CES Battery Solutions

Through the addition of Li-ion community energy storage to a residential feeder similar to that of a generic urban feeder in Reykjavík, baselines for both voltage and power were stabilized according to user-defined battery parameters and density. The optimal CES density in the residential feeder is determined to be 30%, equivalent to 225 individual 45 kWh Li-ion batteries, set with the same BMS and battery parameters from Table 5.2. Charging and discharging setpoints were determined based on baseline power flows, intended to improve the functionality of the CES in the feeder. By tailoring the BMS and battery parameters to meet the demands of the baseline power and voltage, for instance, choosing 600 kW as the charging setpoint and 1200 kW as the discharging setpoint, the efficiency of the simulated feeder is enhanced beyond the baseline once the right density of batteries are added.

The annual baseline power flows in the residential feeder for 2012 simulate the characteristic high energy consumption during winter months November to March, with a significant drop-off in consumption throughout the summer months April to October. All simulations of CES integration were scheduled using a timestamp occurring in early July because the three days (July 7 to July 9) signify fairly moderate, uniform consumption in the feeder. Reactive power flows echo the same seasonal variation tendencies as the real power flow on an annual basis – though with a much greater stability (low variance) through the spring and summer months – refer to Figure 5.1. Voltage maintained a steady fluctuation with no seasonal variation. CES simulations reproduced expected results. Real power in the residential feeder crosses below the threshold of 197.92 MWh with the addition of CES density 30%, which has a real power flow totaling 196.45 MWh when integrated over three days. This represents a difference of 1.47 MWh between the threshold and CES_D30 three-day integral, but a much larger 23.46 MWh reduction from the baseline real power integral. Of course, the simulation testing CES density 40% reduces real power flow even further to 186.62 MWh over three-days, however, because the 30% density of CES solves the 10% reduction target, and is the lowest density to do so, it is deemed to be the optimal EES condition for solving real power flows in the residential feeder. Performance metrics satisfied only when the threshold has been solved include first and foremost peak-shaving, and improved power quality, UPS, and consumer-side time-shifting. These are all useful EES applications and match the benefits of the medium discharge time energy storage technologies – most commonly known as the batteries group – refer to Table 3.1.

Reactive power and voltage thresholds have been outlined along with their optimal densities in chapter 6.0, however there is a very significant trend to be underscored in the CES residential simulations. That is, reactive power and voltage fluctuations are more effectively mitigated with lower CES densities, giving rise to the dichotomy between reactive power and voltage when compared with real power; whereby real power requires higher CES densities to accomplish peak reduction. Interestingly, another explanation as to why reactive power and voltage were both satisfied using lower density CES might be linked to the graphical correlation between the baselines of reactive power and voltage curves; it is an inverse relationship about the x-axis. The two curves almost mirror each other. This may suggest volt-VAR optimization devices are a feasible approach to improving voltage and power quality performance metrics as well. VVOs can be modeled in GLD and GCD, however were beyond the scope of this paper for modeling purposes, as the primary focus here is energy storage.

6.2 Complex Resource Scenario Two: Large-scale NaS Battery Solutions

Retrofitting the Icelandic power system with large-scale, 10 MWh NaS batteries at a density of 60% solved the real power threshold limit. Results support the notion of applying different configurations of EES at 60% density in the Icelandic transmission system does in fact provide slightly improved impacts on EES performance metrics over other, less effective arrangements of the batteries. Of all four arrangements tested, the best at achieving medium scores in the performance metrics was found to be Configuration 4, constituting EES attachments at Hrútatunga, Fljótsdalur, Prestbakki, and Brennimelur substations. The second most effective arrangement of EES in the Icelandic power system turned out to be Configuration 3, followed by Configuration 2, and lastly the least effective was Configuration 1. The order of effectiveness was determined by each configurations' shift away from the real power baseline, which can be seen graphically. Figure 6.1 illustrates the varying degrees of success each configuration has on real power peak reduction, along with detailing their EES systems' collective charge and discharge times. In this plot, Configuration 4 clearly establishes the most predominant discharging and charging cycles, fully charging at the 600 MW setpoint, and the greatest shift away from the real power baseline once the 1200 MW discharging setpoint is met.

This simulation produced unexpected results as well, however, whereby the first peak in the three-day period sees stored energy dispatch performed, while the second peak does not portray any significant peak-shaving of real power despite crossing above the 1200 MW discharge setpoint. Another deceiving intricacy is seen on July 7 prior to

6:00am when EES charging cycles are expected to be activated. One explanation for this behaviour is the batteries are believed to be already fully charged from the onset of this three-day simulation, therefore they forgo the initial charging process and dispatch the preliminary stored electricity once the first peak occurs around 1:00pm on July 7. Along the same line of reasoning, once the batteries have discharged all their stored energy on the first peak in real power, the transmission system does not drop below the 600 MW charging setpoint for long enough to fully recharge the EES. As a result of this minimal charge cycle the night previous, the second peak in real power does not experience any substantial stored energy dispatch, and peak-shaving therefore cannot occur. Finally, on the eve of July 8th and morning of July 9$^{\text{th}}$, the real power baseline drops sufficiently below the charging setpoint (see "charging point" in Figure 6.1), allowing the batteries to charge to near full capacity for the stored energy to be dispatched during the third peak in the series, which explains the full peak-shaving event on July 9$^{\text{th}}$. The arrangement in

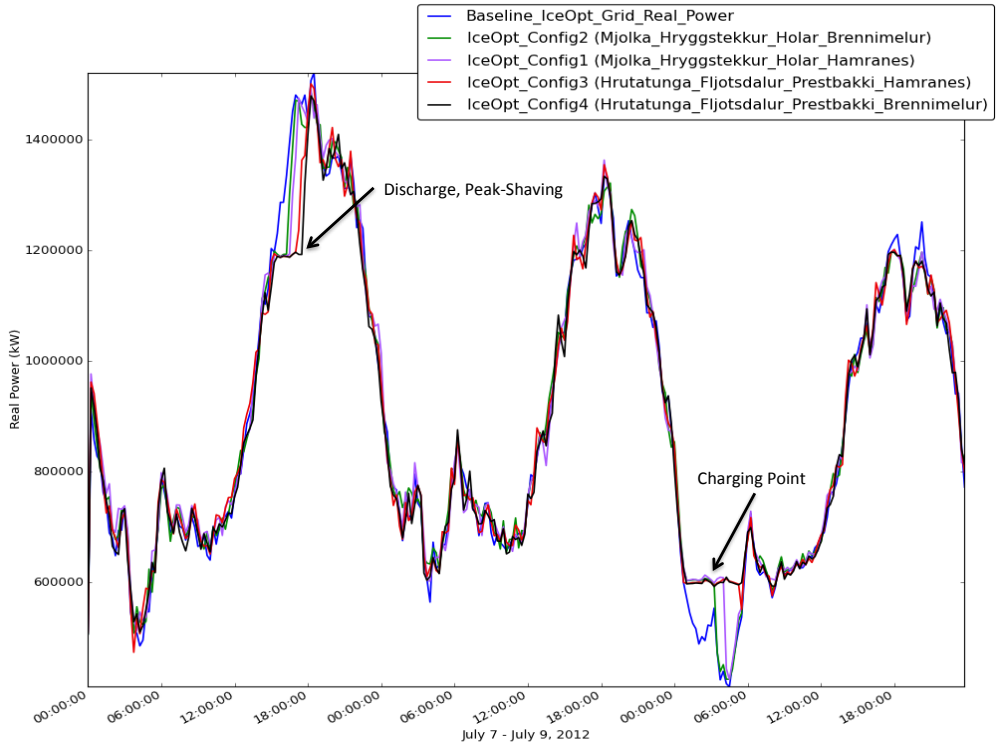

FIGURE 6.1: *Configurations 1-4 simulated over three days. NaS density is at 60%.*

Configuration 4 featured 2 clustered 10 MWh NaS batteries per cluster at each location for a combined 20 MWh capacity in each quadrant, and produced the most beneficial results for Landsnet's grid in terms of peak-shaving and optimization. However, in Figure 6.2, a close-up emphasizes that all configurations' ability for peak-shaving is somewhat short-lived, enduring approximately half of the peak demand event in the real power flow, thus falling short of achieving high scores in the performance metrics. Figure 6.2 shows sub-optimal conditions, and the dashed line indicates what the ideal EES

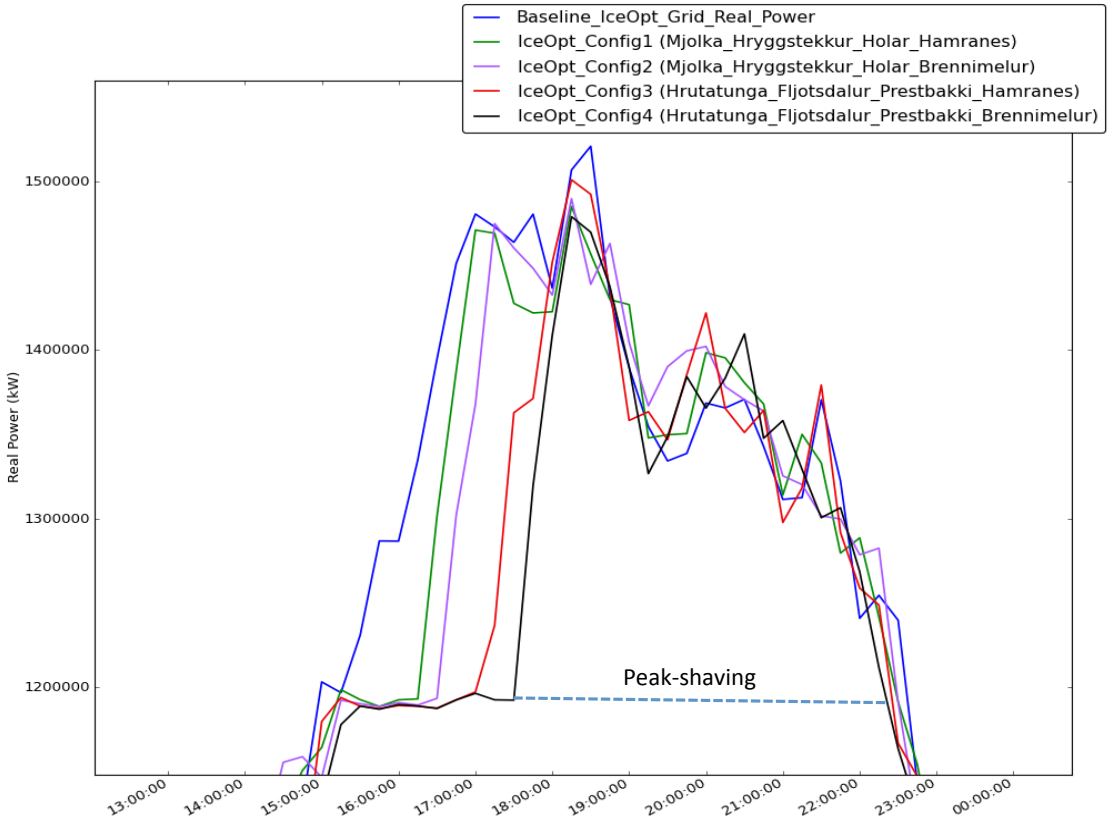

FIGURE 6.2: *Ideal real power flow impact.*

configuration would produce for the highest peak-shaving score in performance metrics. Real power curves in these configuration plots (Figures 6.1 and 6.2) are also very closely correlated with the baseline curve, overlapping for much of the simulation until the peak-shaving setpoints and charging setpoints are reached. This result strays from the figures that strictly plot NaS density comparisons, where the baseline curves became further separated from the higher density curves throughout the majority of the three day period.

Configurations within the Icelandic power system are believed to favour one location over another because EES functionality generally depends on location-specific factors such as power and voltage magnitudes, proximity to large load centres in the grid, and current infrastructure (i.e. transmission cables, capacitors, substations, transformers, and so on). For instance, Brennimelur appears to be better suited to improving EES performance metrics in Configuration 4 than Hamranes substation in Configuration 3, despite these two locations both residing in the same Southwest quadrant (Case 3). Referring to the tables in Appendix C, Brennimelur passes nearly double the real and reactive power flows than that of Hamranes, therefore the magnitudes of these demands placed on Brennimelur increase its EES suitability and performance metrics score. This may partially explain why Configuration 4 sees a greater shift away from the baseline

real power in Figure 6.2 when compared to Configuration 3, noting that the last location in each configuration is changed from Hamranes in Configuration 3 to Brennimelur in Configuration 4.

During the time when simulations were being tested, a transmission trial with 30% NaS density was initially designed for the experiment. However, this density of EES caused the same fuse in the grid to blow, repeatedly forcing GridLAB-D^{TM} to terminate the simulation. This is likely a response to a user error within the transcription of the IceOpt code written for this study, and is curious considering higher densities of NaS solutions did not pose the same peculiar problem (of blowing fuses). Results with 30% density were disregarded as well because higher density EES installments were having a less than expected impact on voltage and power control. The fuse guilty of blowing is attached near the Hryggstekkur bus. This could also explain why EES configurations involving Hryggstekkur produced poor real power peak-shaving – see Configurations 1 and 2 in Figure 6.2. This is especially true when comparing Hryggstekkur and Fljótsdalur substations (Case 1).

Comparing the performance metrics for Hrútatunga and Mjólka substations, we see improved peak-shaving using the Hrútatunga connection resulting from location-specific and voltage-related factors. Hrútatunga substation is attached directly to the 132 kV ring network across the country and situated in the Northwest quadrant (Case 0); it connects to Mjólka substation in the Westfjords to the larger ring network. Hrútatunga operates at 132 kV whereas Mjólka operates at 66 kV further away from the main network. Therefore, if Mjólka substation experiences an outage or disruption, energy stored in the battery system at Hrútatunga can be dispatched to alleviate these grid instabilities. Conversely, if the EES system was connected at Mjólka, its range for emergency voltage and power response towards the main network would be limited in effective area by its proximity away from the larger grid due to its more northern position.

Prestbakki and Hólar substations are distant from one another in the grid but have similar technical specifications and substation infrastructure. Therefore, they exhibit similar influence on performance metrics in their respective configurations. This might imply the Southeast quadrant (Case 2) is the easiest to solve, as long as there is EES in this quadrant, the system weaknesses should be reduced regardless of attachment point between these two sites.

One final comment on EES arrangements, while the power and voltage improvements offered from evenly distributed EES across the grid (as seen in Figure 5.22), evenly distributing batteries in the Icelandic power system requires far more batteries and is far less feasible than integrating EES at targeted areas of weakness within the grid. This is

so not only because clustering requires less batteries, but less grid rearrangements, and is therefore considered to be more practical and less expensive.

6.3 Putting It All Together: Connecting Scenarios

Rahman *et al.* (2012) notes the performance of EES technologies for various applications are highly dependent on spatial orientation and grid connectivity. Therefore, two arrangements for energy storage were considered in this study: (1) Large-scale storage at the transmission level; and (2) Small-scale storage at the distribution level.

Worldwide, the use of stored energy for real time optimization of the GT&D system has been fairly limited to the extent of pumped hydro storage, and in a few instances LA, Li-ion or NiCd batteries (Rydberg, 2011; Electric Power Research Institute, 2010). However, recent commercial advancements in EES technologies have provided new competing storage alternatives, and answers to many RE intermittency problems (at the generation level) as well as load variation and energy balance problems (at the transmission, distribution levels). Today, small neighbourhoods are serving as ideal testing grounds for EES configurations. This small-scale energy storage at the distribution level is very important for smoothing demand side variability in PQ power and voltage frequency regulation, thereby alleviating stress on the electric grid.

Other studies suggest having energy stored on the local level may offer greater benefits on the transmission scale, which mostly agrees with the results from this project (Rahman *et al.*, 2012). Configuring EES on small-scales throughout any grid will certainly improve power quality, reduce line conductor losses, and help prolong the use of transmission lines and infrastructure – this was a major finding from the simulations run on the residential feeder retrofit with community energy storage. Perhaps in future studies, power systems analysis can be run for the entire Icelandic transmission system with the attachment of residential models to the larger transmission grid for investigating how exactly increased CES capacity at the small-scale can improve grid optimization at the large-scale, and to what extent. These kinds of studies of interconnecting electric models are already well underway in the United States with the PNNL and U.S. Department of Energy's Smart Grid Investment Grant (SGIG) Project.

Chapter 7

EES Recommendations to Iceland

Considering the various configurations and leading EES technologies available, the task at hand was finding the best means of integrating energy storage for the Icelandic power system. Based on the remarkable RE contributions the country uses for electricity generation (100% from geothermal and hydropower combined), there are some important aspects to consider given these sources: (1) the controllability of geothermal and hydropower plants, (2) geothermal and hydropower are not intermittent, and (3) pumped hydro storage requires energy to drive water to a higher elevation (Pálmason, 2010; Rahman *et al.*, 2012). As Iceland continues to explore the inclusion of wind turbine projects (both on and offshore), it is expected the flexibility of hydropower could potentially increase the value of wind generation (Landsvirkjun, 2013B). Integrating wind and hydroelectric generation into a hybrid system is a new concept that offers a renewable means of powering pumped storage on-site at these hydropower plants. For instance, Landsvirkjun is now operating two wind turbines (2 MW total) in Hafið at the Búrfell hydropower plant in order to provide power to pump water from the lower reservoir to the upper reservoir – see Figure 7.1 (Pálmason, 2010). The hydroelectricity not used to drive pumps is diverted back into the electricity grid. This project is designed to reduce the construction (size) of a new reservoir and to increase electricity production (capacity) efficiency without adding extra hydropower turbines (Pálmason, 2010; Atlason and Unnthorsson, 2014).

Tables 3.2 and 3.4 in chapter 6 demonstrated VRB and NaS batteries are the best-suited EES options for improving power quality and integrating renewable sources such as wind at the transmission or generation scale. Therefore, to ensure there is energy in order to pump water between reservoirs, a VRB or NaS battery system (noting high operating temperatures of NaS) at the wind-pump would be ideal for maintaining UPS at Búrfell, and possibly any other power stations to incorporate PHS and wind turbines.

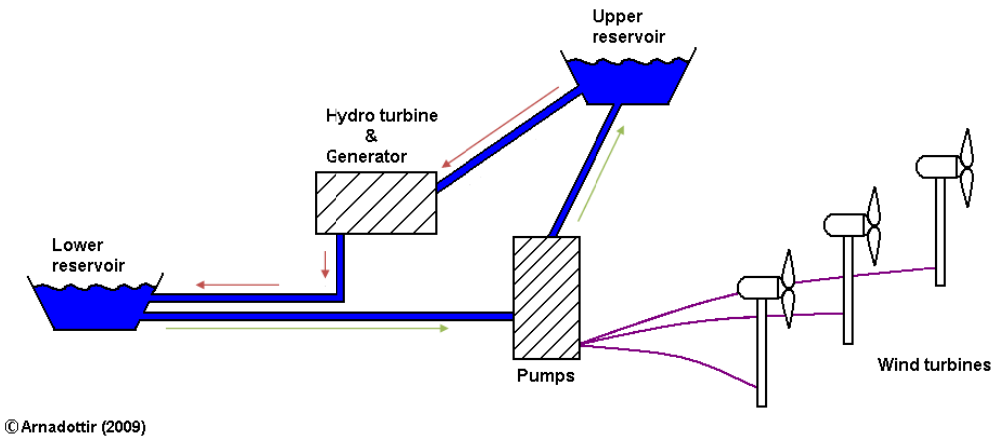

FIGURE 7.1: *Pumped storage system with wind turbines producing electricity to cycle water between reservoirs.*

Iceland has a single-defined electricity transmission system, but several regional distribution networks (Landsvirkjun, 2009). Landsvirkjun or Landsnet would be wise to install locally clustered, high-capacity EES systems along stress-points within the transmission grid. DSOs such as Orkuveita Reykjavíkur must start planning for future residential smart grids with small-scale, evenly distributed configurations of Li-ion battery CES for their distribution level markets. The interplay between energy storage on both small and large scales of the power system is believed to produce truly optimal nationwide grid conditions. Investments towards increased storage capacity to meet growing electricity demand from power intensive industries (i.e. aluminum smelters) would be better invested into EES storage at weak points along the grid for improving power quality, consumer-side time-shifting, energy balance, UPS, peak-shaving, and energy arbitrage. Even more impressively, and as an environmental student, the ability to store electricity would hopefully mean seeing less damming projects in Iceland's untouched highlands in conservation efforts, by reducing the necessity for increased generation capacity because the system would be maximizing their returns from the current power plants and its stored energy. More modeling using grid simulation software will be necessary to determine the precise placements of these devices to maximize energy efficiency, power quality and overall grid optimization at the generation level.

As with most commercial storage applications, these systems address demand charge management, reduce peak demand, and provide emergency backup power in case of outages and grid failures. Such a system automates the discharge of stored energy to optimize utility charge savings for customers. In Iceland, utilities often define their rates for larger consumers such as heavy-industry and even the University of Iceland campus, based less on the overall amount of electricity consumed, and more on electricity consumed during peak hours. Wind and other renewables can significantly offset the

overall amount of electricity used by organizations, but if a consumer's peak electricity demand is still high during the day, in late afternoon for example, the organization can be hit with high demand charges. Proposing new EES systems for regulating the amount of electricity that consumers need from the grid during peak periods will thereby reduce their exposure to exorbitant demand charges.

7.1 Summarizing Benefits of EES to Iceland

To summarize the major benefits of EES implementation in Iceland, we find that:

- Commercial and industrial customers save on their electricity bills by reducing peak demand:
  - Rising electricity prices are an area of concern in Iceland, however, advances in EES and demand response are paramount to controlling price variability in the future;
  - Utilities may reduce the operational cost of generating power during peak periods (reducing the need for peaking units that place added stress on Iceland's grid);
  - Investment in infrastructure delayed due to the flatter loads with smaller peaks.
- Possibility of integrating electric vehicles (EVs): A grid-to-vehicle (G2V) and vehicle-to-grid (V2G) system would be the first in the world in an effort to reducing Iceland's carbon emissions in its transportation sector. The ability to claim 100% RE powering its electric fleet would also be unmatched by any country in the world to date.
- Job creation in the energy storage field means a healthier economy: The Electricity Storage Association (ESA) estimates more than 100,000 incremental jobs will be created by 2020 (a 7-year period) in the energy storage sector, if investments into EES continues at today's pace (ESA, 2009; Rahman *et al.*, 2012).

7.2 EES Compatibility with Distributed Generation

GridCommand^{TM} allows for the deployment of distributed generation (DG) such as wind and solar PV for the testing of new complex resource scenarios. Other studies have evaluated and confirmed the benefits of adding EES combined with distributed generation,

especially for addressing RE intermittency and other difficulties with DG integration. Aside from being of benefit to distribution systems with distributed generation, energy storage can be applied to assist with and improve network operation, power quality, energy arbitrage, and offset peak power consumption to avoid higher rates for certain consumers (Wade *et al.*, 2010, Rahman *et al.*, 2012). The injection of ideal combinations of real and reactive power for voltage support and loss reduction were first assessed by Kashem and Ledwich (2007), who concluded that a battery-based storage system could provide a profitable solution for primary reserve capacity for frequency control. Distributed generation within Icelandic residential feeders would be a valuable aspect of future smart grid development, for various power applications and savings.

7.3 EES Compatibility with Electric Vehicles

Growing penetration of plug-in hybrid electric vehicles (PHEVs) in the future will require a much more dynamic electric infrastructure for compensating feedbacks between injecting and absorbing PQ power to and from the grid. (Roberts and Sandberg, 2011). GCD is also capable of simulating the addition of PHEVs as well as their impacts on PQ flows and voltage stability, however, these simulations are only credible when performed on small-scale residential feeders. Creation of a complex resource deployment scenario investigating the complementarity between EES and PHEVs in a large-scale power system would require a much more elaborate model beyond the capabilities of GCD's parametric analysis tool.

7.4 Future Developments of EES

Beginning with the U.S. Department of Energy "Grid 2030 Vision" Conference back in April of 2003, energy storage emerged as a top concern among industry professionals for the future of energy security worldwide (Roberts and Sandberg, 2011). In 2007, the DOE convened an Electricity Advisory Committee (EAC) to make recommendations for an energy road map including energy storage deployment in the U.S. grid over a ten-year period (Roberts and Sandberg, 2011). We suggest Iceland does the same as part of Orkustofnun's Master Plan for Energy Development, including further research into energy storage. Globally, other nations like Japan and Germany have been working to make larger amounts of energy storage a vital part of their energy plan. Japan has a near-term target of 15% storage in the grid; Germany meanwhile is planning 10% in comparison; and the U.S. at just over 2% deployment. Roberts and Sandberg (2011) state most countries already employ bulk energy storage today in the form of large PHS

facilities, which are generally located great distances from load centres and can do little to effect power quality and voltage frequency regulation (PHS is mostly used for off-peak base load leveling). Battery EES systems are in many ways the key to the future grid.

7.5 Continued Studies of Energy Storage in Iceland

Seeing the continuation of energy storage studies in Iceland would begin with peers and researchers further developing the code written for this thesis, (which will be made public as per open-source policies of GridLAB-D^{TM}), adding details to fill any data gaps to the IceOpt model. This will make future studies in grid optimization, technological advancements, and smart grid infrastructure in Iceland more robust and easier for those who wish to begin where this research leaves off.

The experiment was under time and budget constraints as well, therefore only eight locations for EES attachment were simulated on the transmission model out of literally hundreds of possible substations. It may also be worth investigating all possible 16 combinations in Table 4.1 as well to determine whether more efficient arrangements of EES are attainable.

One of the more exciting new frontiers open for both technical and economic research involves the proposed submarine HVDC cable connecting Iceland to parts of mainland Europe. Landsvirkjun appears to be looking at this option very closely – in the event this massive project gains approval, exploring the ideal role of added energy storage in Iceland to help buffer out additional demands from the newly connected European electricity market would become abundantly imperative (Hreinsson, 2013).

Chapter 8

Conclusions

A number of potential EES technologies exist and can be deployed for large or small-scale storage, however, each bearing their own strengths and weaknesses. Technical and economic comparisons between leading EES systems were used to distinguish two low cost and highly efficient batteries: vanadium redox batteries (VRB) and sodium sulfur (NaS). A third, lithium-ion (Li-ion) is showing signs of cost reduction as its development continues to progress (Rahman *et al.*, 2012).

Energy storage has a promising future in the Icelandic power system for both distribution and transmission sectors, and potentially for generation as well. Iceland does not currently require EES for intermittency problems in RE generation with the exception of two wind turbines at the Búrfell hydropower plant. However, peak reduction, UPS, consumer-side time-shifting, emergency power, infrastructure maintenance, and load energy balance can be all improved with the appropriate energy storage systems - answering the first research question addressing the numerous roles of EES. Two newly installed wind turbines at Búrfell hydropower station may also benefit from energy storage to ensure uninterrupted power supply for pumped storage operation. Furthermore, if Iceland chooses to become a major exporter of renewable energy to Europe (via submarine cables), EES will be vital for keeping a continuous external supply, energy arbitrage for controlling electricity pricing in the future which has been projected to rise in Iceland, and to satisfy demand while minimizing risks of stress and outages to its domestic grid – this concept does require more detailed analysis.

Results from this study have demonstrated the various roles of small-scale EES deployment in Iceland for improving power quality, voltage control, peak-shaving and energy arbitrage with low CES densities evenly distributed in light-urban and residential feeders similar to those in Reykjavík. The roles for large-scale EES in the transmission system are far more location-specific when clustered, and require relatively higher densities than

the residential scenarios. Performance metrics were assessed based on the ability of EES densities to solve predefined threshold setpoints and have shown storage can provide improved peak-shaving and load balancing in the IceOpt model. Recent studies suggest storing energy on smaller scales at the local level offer greater benefits than storage on the transmission scale. This research does reflect these findings, particularly because a much lower EES density of 30% solved thresholds for providing residential performance metrics, while a much higher EES density of 60% was required to solve thresholds in the transmission model. It is the author's opinion that as technological advancement in battery energy storage continue at their present pace, the effects of large-scale storage will be greatly enhanced with lesser batteries and lower density.

Configurations of EES are vital to achieving grid storage optimization on various levels of the Icelandic power system as well, as per the second research question. Testing multiple configurations of EES in the transmission system helped identify and confirm weaknesses within the grid; this study elucidated techniques for partially alleviating some of these constraints with the second resource deployment scenario and the IceOpt model. We found the most successful strategy for grid optimization in the transmission model consists of clustered NaS batteries with 10 MWh capacity operating in load-following mode to maximize peak reductions in real and reactive power. The fourth configuration tested included EES attachment across each quadrant at Hrútatunga, Fljótsdalur, Prestbakki, and Brennimelur substations, which translated to the most effective in terms of peak-shaving of real power flows. This indicates clustered configurations are also highly location-specific. Optimal EES densities in the IceOpt model are found to be either 50% or 60%, depending on intended purposes for energy storage actions. By many estimates, 60% EES density is considered to be unrealistic at this point in time. It would be wiser to install larger capacity NaS batteries at 40% or 50% density to regulate voltage and power flows in the Icelandic power system.

The most successful strategy presented for the residential feeder would be 150 evenly distributed 45 kWh Li-ion community energy storage batteries operated at the household level with a network density of 30%. One final important consideration for EES configurations is the comparison between clustered versus evenly distributed arrangements, which was found to favor even distribution, and is especially true for CES at the distribution level. On the transmission and generation scales, more testing to predict what configurations yield the greatest energy savings and efficiency from electricity storage is necessary and opens up several opportunities for future studies into EES in Iceland.

Grid simulation software such as GridCommand^{TM} and GridLAB-D^{TM} are emerging as the preferred means of simulating EES configurations. These programming environments allowed for an accurate representations of power flows (active and reactive power) in

Iceland, however produced some perplexing results with the higher density EES plots reducing power flows below the baseline. This was found likely to be attributed to phase selection of PQ power and EES technologies. GCD and GLD were nonetheless successful in solving both complex resource deployment scenarios by determining optimal grid storage conditions with the aid of threshold setpoints and EES performance metrics. When the country was divided into four quadrants to identify zones of instability, GCD also helped address the weaknesses within the grid by providing new and innovative ways for solving contingencies with several arrangements of energy storage. These two aspects of the study addressed the third and fourth research questions.

There appears to be general consensus on the need for energy storage systems in the modern electric grid. Given current trends toward increased renewable energy penetration, growing demands to improve power reliability and quality, along with the implementation of smart grids, EES has a bright future. Nevertheless, applications related to capacity, siting, configurations, performance parameters, storage applications, and so forth need to be further refined. Finally, materials research is contributing to the improvement of advanced batteries through work on nano-structured membranes with tailored electrolytes and electrodes, superpower capacitors, and hybrid flywheels (Rahman *et al.*, 2012). It is hoped new research will result in truly novel storage concepts in the near future and allow EES to be commonplace in many grids worldwide within 5 to 10 years (Yang *et al.*, 2011; Rahman *et al.*, 2012). Battery EES systems are in many ways the key to cleaner, efficient grids, however only once the price is right.

Chapter 9

References

ABB. (2012). *Energy storage: keeping smart grids in balance.* Energy Storage Overview.

Atlason, R. S., and Unnthorsson, R. (2014). *Energy return on investment of hydroelectric power generation calculated using a standardised methodology.* Renewable Energy, 66, pp. 364-370.

Batlle, C., and P. Rodilla. (2010). *A critical assessment of the different approaches aimed to secure electricity generation supply.* Energy Policy. 38(2010), pp. 7269–7290.

Carlon, T. (2012). *GridLAB-D Information Page.* Internet Source. Retrieved September 3, 2013, from http://www.gridlabd.org/

Chen, H., Cong, T.N., Yang, W., Tan, C., Li, Y., and Y., Ding. (2009). *Progress in electrical energy storage systems: a critical review.* Progress in Natural Science. 19(2009), pp. 291–312

Cohen, M.A. (2013). *GridLAB-D taxonomy feeder graphs.* Internet Source. Retrieved February 8, 2014, from http://emac.berkeley.edu/gridlabd/taxonomy_graphs/

Denholm, P., Kirby, B., and M. Milligan. (2010). *The role of energy storage with renewable electricity generation.* Technical Report, National Renewable Energy Laboratory.

Drevdal, E.N., Langset, T., and N.M. Espergren. (2011). *Appraisal of the Icelandic electricity market and regulation.* Conducted by the Norwegian Water Resources and Energy Directorate.

Electric Power Research Institute. (2010). *Electricity energy storage technology options: A White Paper primer on applications, costs, and benefits.* Technical Update. EPRI Inc. USA.

ESA. (2009). *Energy storage discharge times.* Energy Storage Association.

ESA. (2013). *Electricity storage technologies and future projections.* Energy Storage Association.

Eyer, J., and G. Corey. (2010). *Energy storage for the electricity grid: benefits and market potential assessment guide: a study for the DOE Energy Storage Systems Program.* Sandia Report. SAND2010-0815. Sandia National Laboratories.

Grave, K., Paulus, M., and D. Lindenberger. (2012). *A method for estimating security of electricity supply from intermittent sources: scenarios for Germany until 2030.* Energy Policy. Vol. 46(10), pp. 193–202

Guðmundsson, Þ., Nielsen, G., and N. Reddy. (2006). *Dynamic VAR Compensator (DVC) application in Landsnet grid, Iceland.* PSCE, IEEE. pp. 466–469, doi:1-4244-0178-X/06/PSCE.2006

Haarla, L., Koskinen, M., Hirvonen, R., and P.E. Labeau. (2011). *Transmission grid security: A PSA approach.* Power Systems. ISBN: 978-0-85729-144-8

Hreinsson, E.B. (2013). *Operations modeling in the Iceland hydro dominated power system.* Power Engineering Conference (UPEC), 2013 48th International Universities. pp.1–6, doi: 10.1109/UPEC.2013.6714916

Kaldellis, J.K., and D. Zafirakis. (2007). *Optimum energy storage techniques for the improvement of renewable energy sources-based electricity generation economic efficiency.* Energy. 32(2007), pp. 2295–2305. doi:10.1016/j.energy.2007.07.009

Kashem, M.A., and G. Ledwich. (2007). *Energy requirement for distributed energy resources with battery energy storage for voltage support in three-phase distribution lines.* Electric Power Systems Research 77, pp. 10-23.

Landsnet. (2011). *Annual Report: 2011.* Landsnet hf., Iceland

Landsnet. (2012A). *Energy balances: 2014 and power balances 2014/15 for Iceland.* Landsnet, hf., Iceland

Landsnet. (2012B). *Annual Report: 2012.* Landsnet hf., Iceland

Landsnet. (2013A). *Annual Report: 2013.* Landsnet hf., Iceland

Landsnet. (2013B). *Performance Report: 2012.* Landsnet hf., Iceland

Landsvirkjun. (2009). *Energy balances for 2012 and power balances 2012/13: for Iceland.* Internet Source. Retrieved October 21, 2013, from http://www.Landsvirkjun.is/uploads/703.pdf

Landsvirkjun. (2013A). *Búrfell power station. Landsvirkjun National Power Company.* Internet Source. Retrieved February 8, 2014, from http://www.landsvirkjun.com/Company/PowerStations/BurfellPowerStation

Landsvirkjun. (2013B). *Electricity generation in Iceland: Landsvirkjun's power-intensive customers. Landsvirkjun general presentation.* Internet Source. Retrieved February 9, 2014, from landsvirkjun.com/media/enska/about-us/Landsvirkjun_general_presentation.pdf

Lavine, M., Szuromi, P., and R. Coontz. (2011). *Electricity now and then: materials for grid energy.* Science. Vol. 334(18), pp. 921–929.

Lochet, A., G.Ö., Petersen, and B.B. Haraldsson. (2012). *Recent developments in the Icelandic energy market.* Energy Law in Iceland – the European Energy Handbook. pp. 187–192

Loftmyndir. (2013). *Interactive satellite map of national electric grid.* Retrieved from Landsnet. Loftmyndir ehf., Iceland. Internet Source. Retrieved November 11, 2013, from http://www.loftmyndir.is/k/kortasja.asp?client=lnet

METSCO. (2013). *Comparison of underground and overhead transmission options in Iceland (132 and 220kV).* METSCO Energy Solutions Inc., Independent Report Commissioned by Landvernd. Toronto. Canada.

Mork, B. (2000). *Newton-Raphson load flow formulation.* Michigan Technological University. USA.

Orkustofnun. (2011). *Report on regulation and the electricity market in Iceland.* The National Energy Authority (NEA) in Iceland. National Report Iceland.

Orkustofnun. (2013). *Raforkuspá: electricity forecast.* Internet Source. Available at: http://os.is/gogn/Skyrslur/OS-2013-02.pdf. Orkustofnun, National Energy Authority, Iceland.

Orkuveita Reykjavíkur. (2014A). *Load flow schedules for substations A1 to A12, January 1, 2012 to January 1, 2013.* Private datasets. Orkuveita Reykjavíkur, Iceland.

Orkuveita Reykjavíkur. (2014B). *Transformer and substation specifications, geographical layouts for substations A1 to A12.* Orkuveita Reykjavíkur. Iceland.

Orkuveita Reykjavíkur. (2014C). *Residential feeders information for homes in Reykjavík. Obtained through interviews with Guðleifur Kristmundsson and Rúnar Svavar Svavarsson.* Orkuveita Reykjavíkur, Iceland.

Pálmason, A.V. (2010). *Wind power pumped storage system for hydropower plants.* Master's thesis, Industrial Engineering, Mechanical Engineering, and Computer Science, University of Iceland, pp. 73.

Rahman, F., Rehman, S., and M. Arif Abdul-Majeed. (2012). *Overview of energy storage systems for storing electricity from renewable sources in Saudi Arabia.* Renewable and Sustainable Energy Reviews. 16(2012), pp. 274–283.

Roberts, B.P., and C. Sandberg. (2011). *The role of energy storage in development of Smart Grids. Institute of Electrical and Electronics Engineers.* IEEE Proceedings. 99(6) pp. 1139–1144.

Rydberg, L. (2011). *RTDS modeling of battery energy storage system.* Uppsala Universitet.

Sadoway, D.R., Bradwell, D.J., Kim, H., Aislinn, H., and C. Sirk. (2012). *Magnesium-Antimony liquid metal battery for stationary energy storage.* Journal of the American Chemical Society. 134(2012), pp. 1895–1897. dx.doi.org/10.1021/ja209759s

Schneider, K.P., and C.A. Bonebrake. (2012). *Evaluation of representative Smart Grid Investment Grant project technologies: Distribution automation.* Pacific Northwest National Laboratory, United States.

Wade, N.S., Taylor, P.C., Lang, P.D., and P.R. Jones. (2010). *Evaluating the benefits of an electrical energy storage system in a future smart grid.* Energy Policy. 38(7) pp. 7180–7188.

Yang, Z., Zhang, J., Kintner-Meyer, M.C.W., Lu, X., Choi, D., Lemmon, J.P., and J. Liu. (2011). *Electrochemical energy storage for green grid.* Chemical Reviews.

Appendix A. Capital costs and life cycles for the main EES technologies. Source: Yang *et al.*, 2011.

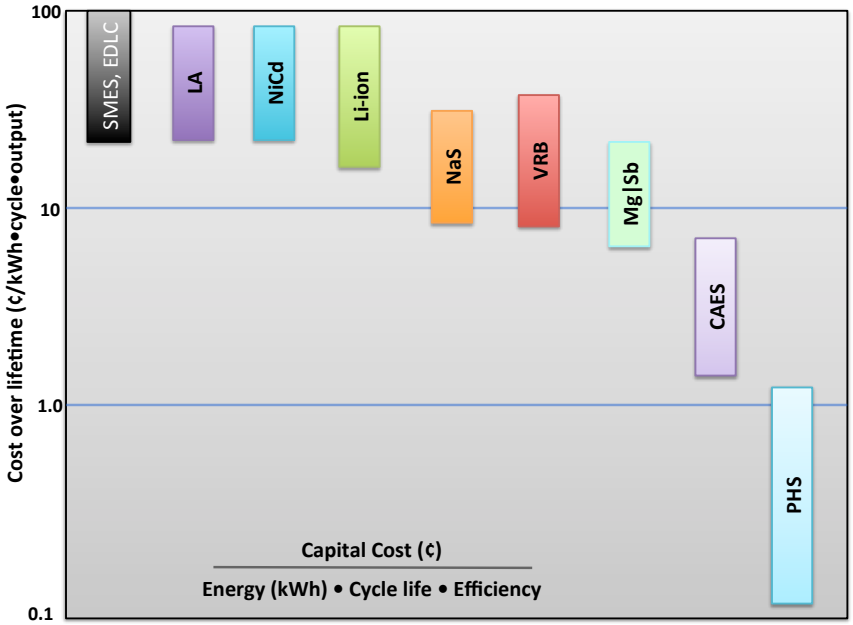

Appendix B. Single-line diagram of PSS/e file from Landsnet used in data acquisition phase of project. Buses (thick lines) are colour-coded, along with branches (thin lines), load centers (triangles) and power-generating machines (circles). For each, the same colour scheme applies: black (11 kV); yellow (33 kV); blue (66 kV); red (132 kV); and green (220 kV).

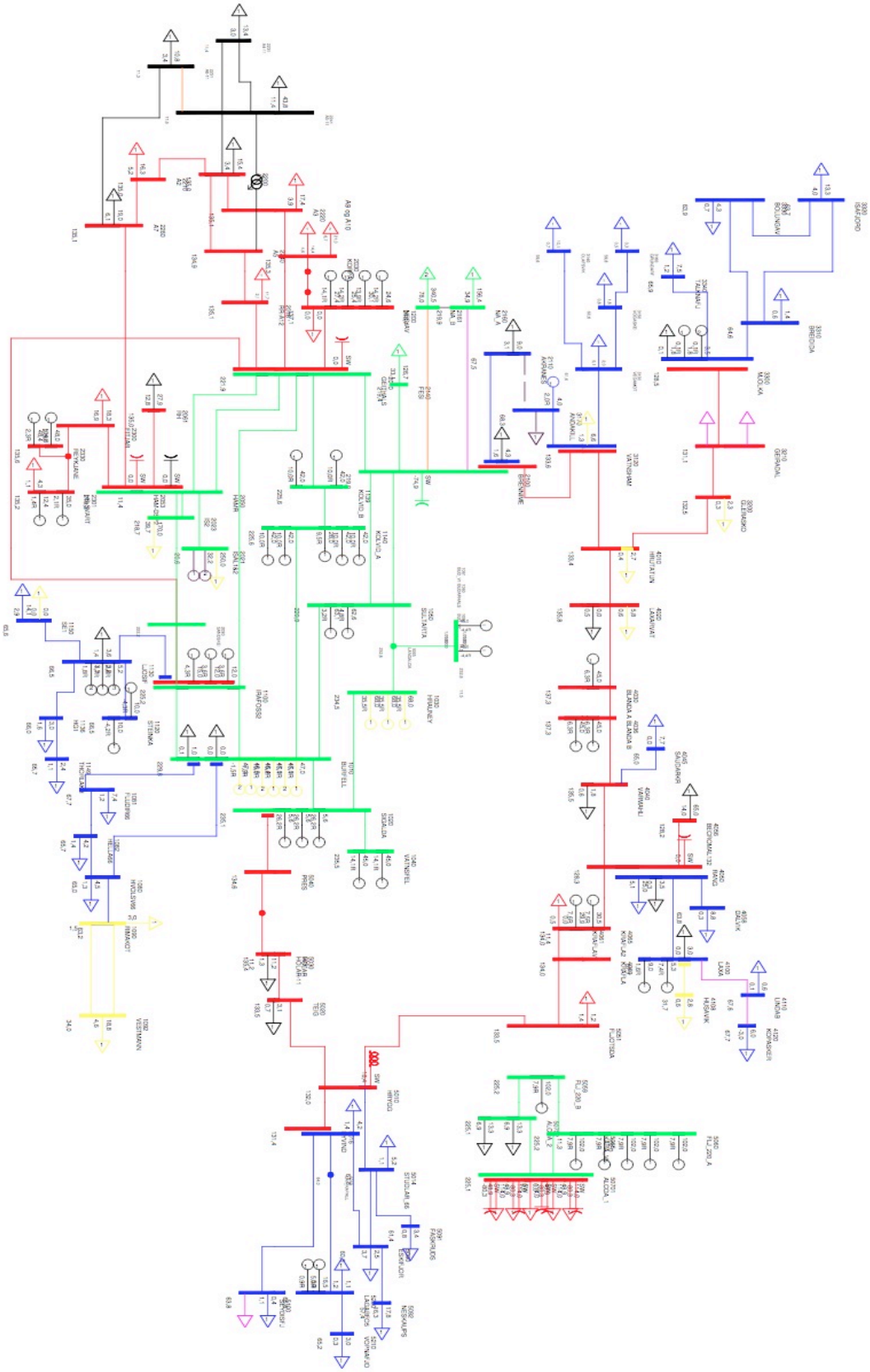

Appendix C. Bus data for power plants, buses, and loads sourced from Landsnet (2013). Substations are denoted with (SS), loads (L), industrial loads (IL), and power plants (PP). All *PQ* values are as of 2012 (Orkustofnun, 2013). There are 33 major loads defined in Iceland. Five of which are power-intensive industries: Alcoa, Becromal, Century Aluminum, Elkem, and Rio Tinto Alcan. The remaining 28 loads are major distribution feeders to municipalities, residential areas, and external commercial activity.

OBJECT	OBJECT TYPE	ID	LATITUDE	LONGITUDE	BUS VOLTAGE (KV)	P, REAL POWER (MW)	Q, REACTIVE POWER (MVAr)
AKRANES	L, PP, SS	2110	64° 18.960'	-22° 5.027'	66	12.3	4.7
ANDAKILL	L, SS	3170	64° 33.470'	-21° 4.398'	66	6.6	1.3
A12 (RR)	L, SS	2018	64° 18.960'	-22° 5.027'	66	183.2	49.8
ALCOA_1 ALCOA_2	IL, SS	50701 50702	65° 2.019'	-14° 6.021'	220 220	596.6	258.3
BECROMAL BECROMAL132	IL, SS	4055 4056	65° 42.192'	-18° 6.905'	11 132	65.0	14.0
BLANDA A BLANDAV1 BLANDAV2 BLANDAV3 BLANDA B	PP, SS	4030 4031 4032 4033 4036	65° 24.945'	-19° 49.168'	132 11 11 11 132	135.0	18.9
BOLUNGAV	L, SS	3330	66° 9.012'	-23° 14.943'	66	4.3	0.7
BRENNIME-220	SS	2100	64° 2.335'	-21° 4.468'	220	623.6	20.0
BREN-132 BRENN-11 BRENN-66	SS	2101 2103 2107	64° 2.335'	-21° 4.468'	132 11 66	5.1	0.3
BREIDIDA	L, SS	3310	66° 3.038'	-23° 30.939'	66	1.4	0.6
BUDARHALS BUD_V1 BUD_V2	PP, SS	1060 1061 1062	64° 14.078'	-19° 22.479'	220 11 11	90.0	8.8
BURFELL220	PP, SS	1010	64° 6.361'	-19° 50.071'	220	282.0	9.0
BURFELL-12 BURFELL-34 BURFELL-56 BUR66SP5 BUR11SP5 BUR66SP4 BUR11SP4	PP, SS	1011 1012 1013 1014 1015 1017 1018	64° 6.361'	-19° 50.071'	13.8 13.8 13.8 66 11 66 11	0.5	0.01
CENTURY_ALA CENTURY_ALB	IL, SS	2160 2161	64° 21.880'	-21° 4.625'	220 220	496.9	11.3
DALVIK	L, SS	4058	65° 58.232'	-18° 32.135'	66	8.8	0.3
ELKEM	IL, SS	2999	64° 45.022'	-21° 4.721'	220	126.7	33.1
ESKIFJOR	L, SS	5090	65° 4.548'	-14° 1.853'	66	2.5	3.7
EYVIND EYVIND66 EYV-DELT	L, SS	5016 5017 5018	65° 16.996'	-14° 25.436'	132 66 11	4.2	1.4
FASKRUDS	L, SS	5091	64° 55.806'	-14° 0.686'	66	3.4	0.8
FITJAR	L, SS	2300	64° 3.864'	-22° 38.246'	132	27.0	12.8
FLJOTSDA FLJ_11 FLJ_220_B FLJ_220_A	L, SS	5051 5052 5059 5060	65° 15.830'	-14° 23.627'	132 11 220 220	1.2	1.4
FLUDIR	L, SS	1081	64° 7.525'	-20° 1.950'	66	7.4	1.2
GEITHALS GE_132 GE_11SP1 GE_11SP2	BUS	2010 2011 2012 2013	64° 2.420'	-21° 57.346'	220 132 11 11	10.0	1.0
GEIRADAL	BUS, SS	3210	65° 29.581'	-21° 5.443'	132	6.1	0
GLERASKO GLERA-19 GLERAS-S	PP, SS	3200 3201 3202	65° 14.656'	-21° 37.615'	132 19 0.415	2.3	0.3

OBJECT	OBJECT TYPE	ID	LATITUDE	LONGITUDE	BUS VOLTAGE (KV)	P, REAL POWER (MW)	Q, REACTIVE POWER (MVAr)
HAMRANES220	BUS	2050	64° 2.567'	-21° 58.390	220	340.0	10.0
HAMRANES132	L, SS	2051	64° 2.567'	-21° 58.390	132	0.02	0.00
HAM-DSP1		2052			11		
HAM-DSP2		2053			11		
HELLA66	L, SS	1082	63° 49.988'	-20° 23.426'	66	4.2	1.4
HVERAGERDI	L, SS	1136	63° 44.931'	-20° 12.983'	66	3.0	1.6
HELLIS_V1	PP, SS	1141	64° 2.239'	-21° 24.033'	11	See KOLVID_A	See KOLVID_B
HELLIS_V2		1142			11		
HELLIS_V11		1143			11		
HELLIS_V3		1144			11		
HELLIS_V4		1145			11		
HELLIS_V5		1146			11		
HELLIS_V6		1147			11		
HNODRAHOLT	L, SS	XX	64° 2.637'	-21° 58.213'	132	2.7	0.4
HRAUNEY	PP, SS	1030	64° 11.385'	-19° 13.653'	220	204.0	106.5
HRAUNE12		1031			13.8		
HRAUNE22		1032			13.8		
HRAUNE32		1033			13.8		
HRUTATUNGA	BUS, L, SS	4010	65° 7.619'	-21° 3.792'	132	2.7	0.4
HRYGG	L, BUS, SS	5010	65° 1.259'	-14° 33.556'	132	0.8	0.01
HRYGG_66		5011			66		
HRYGG_11		5012			11		
HVOLSV66	L, SS	1080	63° 45.097'	-20° 13.576'	66	4.5	1.3
HUSAVIK	L, SS	4108	66° 2.844'	17° 20.596'	33	2.8	0.6
IRAFOSS	PP,				132	39.0	11.5
ISAFJORD	L, SS	3320	66° 4.401'	-23° 7.070'	66	13.3	4.0
KARA_V1	PP, SS	5061	64° 56.000'	-15° 47.821'	11	612.0	47.4
KARA_V2		5062			11		
KARA_V3		5063			11		
KARA_V4		5064			11		
KARA_V5		5065			11		
KARA_V6		5066			11		
KELDEYRI	L, SS	XX	65° 36.140'	-23° 4.687'	66	8.9	0.1
KOLVID_A	PP, SS	1139	64° 6.274'	-21° 42.312'	220	280	69.5
KOLVID_B		1140			220		
KORPA	L, SS	2030	64° 9.355'	-21° 45.503'	132	60.7	8.0
KORPA04		2036			0.400		
KOPASKER	L, SS	4120	66° 18.028'	-16° 26.847'	66	6.0	3.0
KRAFLA	PP, SS	4060	65° 42.184'	-16° 46.486'	132	60.4	15.1
KRAFLAV1		4061			11		
KRAFLAV11		4062			11		
KRAFLA-S		4063			0.415		
KRA11BJA		4064			11		
KRAFLA2		4065			132		
LANGALDA	BUS	1065	64.26700	-19.40441	220	XX	XX
LAGARFO5	PP, SS	5200	65° 30.434'	-14° 21.971'	66	22.9	7.1
LAGARFO1		5201			6		
LAGARFOSS		5202			11		
LAXA	PP, SS	4100	65° 49.245'	-17° 19.105'	66	3.0	0.0
LAXA-2		4101			11		
LAXA33		4102			33		
LAXA11		4104			11		
LAXA2		4105			6.3		

OBJECT	OBJECT TYPE	ID	LATITUDE	LONGITUDE	BUS VOLTAGE (KV)	P, REAL POWER (MW)	Q, REACTIVE POWER (MVAr)
LAXARVAT	PP, SS	4020	65° 37.504'	-20° 12.820'	132	5.8	1.1
LAXAVA-2		4021			11		
LAXAVA-4		4022			33		
LAXAV0-4		4023			0.415		
LAXARV-V		4025			6.6		
LINDAB	L, SS	4110	66° 4.324'	-16° 40.461'	66	0.6	0.1
LJOSIF	PP, SS	1130	64° 5.679	-21° 6.610	66	3.6	1.4
LSJO-VEL		1131			6.6		
MJOLKA	PP, SS	3300	65° 46.507'	-23° 9.981'	132	7.1	3.7
MJOLK-66		3301			66		
MJOLKVEL		3303			6.3		
MJODUMMY		3305			33		
NESKAUPS	L, SS	5092	65° 9.058'	-13° 41.019'	66	17.8	16.3
NESJAV	PP, SS	1200	64° 6.506'	-21° 15.452'	132	XX	XX
NESV-VEL 1		1201			11		
NESV-VEL 2		1202			11		
NESV-VEL 3		1203			11		
NESV-VEL 4		1204			11		
OLAFSVIK	L, SS	3140	64° 53.639'	-23° 42.663'	66	10.1	0.7
PRES	L, SS	5040	63° 47.256'	-18° 3.172'	132	2.2	0.1
PREST-19		5041			19		
PRESTB.4		5042			0.451		
PREST-D1		5043			11		
RANG	L, PP, SS	4050	65° 40.697'	-18° 8.619'	132	28.5	5.4
RANGARV5		4051			66		
RANGARV1		4052			6.6		
RANG-11		4053			11		
RANG-S		4054			0.451		
RAUDIMELUR	SS	2320	63° 57.683'	-22° 34.006'	132	3.0	0.1
REYKJANES	L, PP	2330	63° 59.893'	-22° 33.675'	132	4.3	1.1
REYKJAV1		2332			11		
REYKJAV2		2333			11		
REYKJAN_VEL3		2334			11		
REYKJAN_VEL4		2335			11		
RIMAKOT	L, SS	1090	63° 34.190'	-20° 10.149'	66	3.0	0
RIMAKOT		1091			33		
RIO_TINTO_AL	IL, SS	10000	64° 28.050’	-22° 17.012	220	420.0	71.9
RR-A5	L, SS	2017	64° 6.475'	-21° 46.976'	132	183.2	49.8
RR-A12		2018			132		
RH-A1-4		2061			132		
RH-11		2062			11		
11DELTA		4057			132		
RR-A6-10		2018			132		
SAUDARKR	L	4045	65° 44.679'	-19° 38.284'	66	7.7	0.0
SE1	L	1150	63° 56.398'	-20° 58.485'	66	14.1	2.9
SELFOSS-33		1151			33		
SEYDISFJ	L	5100	65° 15.621'	-14° 0.122'	66	0.4	1.1
SIGALDA	PP	1020	64° 10.380'	-19° 7.611'	220	16.8	7.8
SIGALD12		1021			10.5		
SIGALD22		1022			10.5		
SIGALD32		1023			10.5		
SIGALDA6		1024			132		
SIGHR11		1025			11		
STEINKA	PP	1120	64° 7.969'	-21° 1.721'	66	10.0	4.2

OBJECT	OBJECT TYPE	ID	LATITUDE	LONGITUDE	BUS VOLTAGE (KV)	P, REAL POWER (MW)	Q, REACTIVE POWER (MVAr)
STUDLAR_66	BUS / L	5014	65° 1.302'	-14° 15.517'	66	5.2	1.1
SULTARTA	PP	1050	64° 10.030'	-19° 37.287'	220	125.7	8.0
SULT-V1		1051			11		
SULT-V2		1052			11		
HS-SVART	PP	2301	63° 52.703'	-22° 25.963'	132	XX	XX
TEIGA	L / BUS	5020	64° 40.593'	-14° 21.031'	132	3.1	0.7
TEIGHO.2		5021			11		
TEIG-33		5022			33		
TEIGAR.4		5023			0.451		
TEIGA-D1		5024			11		
THORLAKH		1149	63° 51.350'	-21° 23.152'	66	2.4	1.1
VARMAHLI	L / BUS	4040	65° 33.180'	-19° 26.781'	132	1.8	0.6
VARMAHL4		4041			66		
VARMAHL2		4042			11		
VARMAHL0		4043			0.4		
VATNSFEL	PP	1040	64° 11.789'	-19° 2.051'	220	XX	XX
VATN-V1		1041			11		
VATN-V2		1042			11		
VATNSHAM	L / BUS	3120	64° 33.222'	-21° 42.570'	132	9.4	0.6
VATNS-66		3121			66		
VATNSH19		3122			19		
VATNSH-S		3123			0.415		
VEGAMOT	SS	3130	64° 51.027'	-22° 43.816'	66	2.0	5.1
VESTMANN	L	1092	63° 26.635'	-20° 15.921'	33	18.8	4.6
VOGASKEI	BUS	3150	64° 58.841'	-21° 49.552'	66	1.8	0.8
VOPNAFJO	L	5210	65° 45.309'	-14° 49.786'	66	3.0	0.3

N.B. Objects A1 to A12 are the twelve substations through which Landsnet supplies the DSO Reykjavík Energy. Step-down transformers at each substation bring voltage from 132 kV down to 66 kV, 33 kV, and 11 kV for distribution across the Reykjavík capital region. In the transmission model code written for this project, real and reactive (PQ) power measurements at the 12 substations are summed, totaling 183.2 MW real power and 49.8 MVAr reactive power.

Appendix D. IceOpt model integrations and calculations for determining thresholds, performance metrics and qualitative analysis of results.

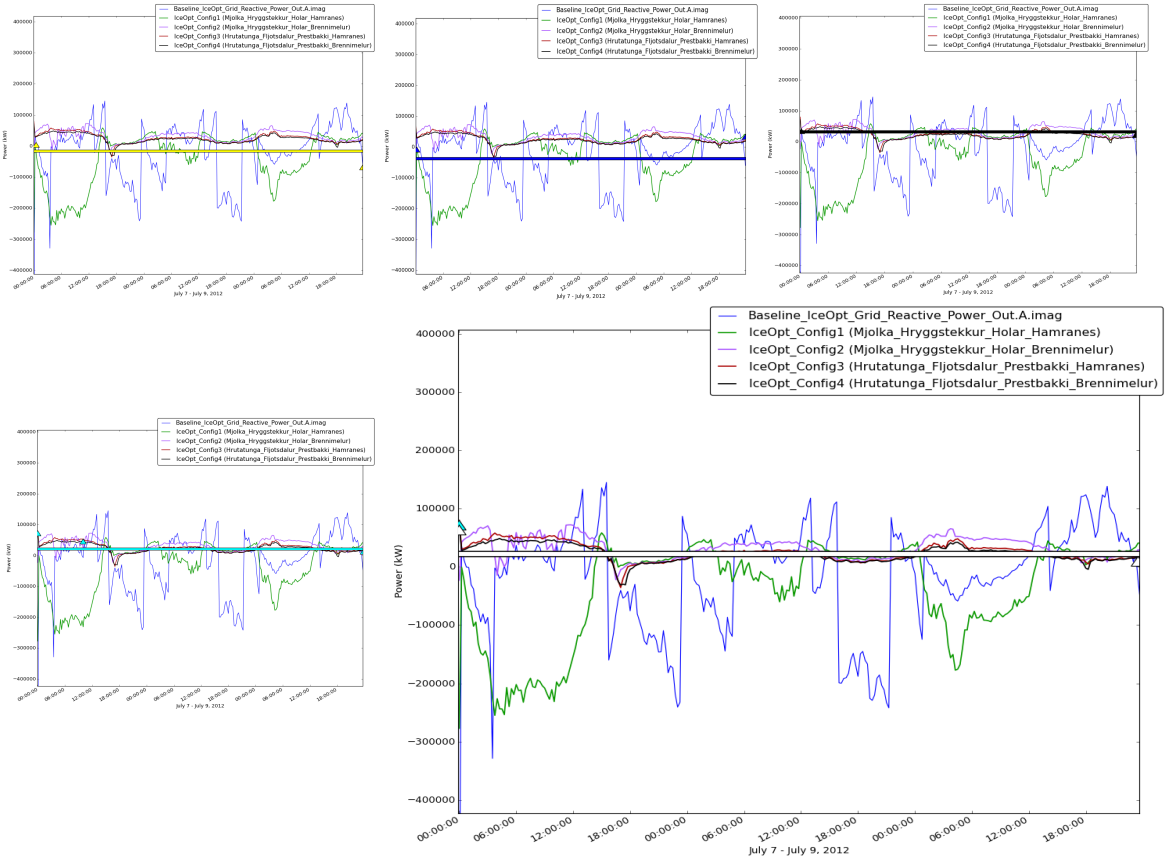

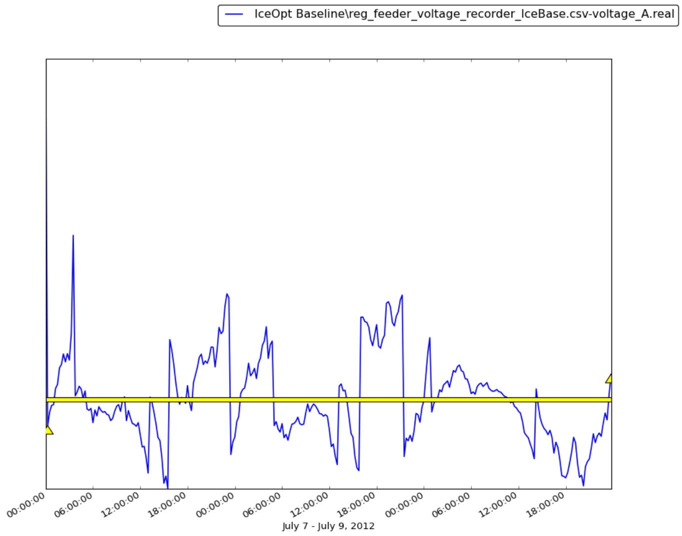
IceOpt Baseline\reg_feeder_voltage_recorder_IceBase.csv-voltage_A.real
00:00:00
06:00:00
12:00:00
18:00:00
July 7 - July 9, 2012

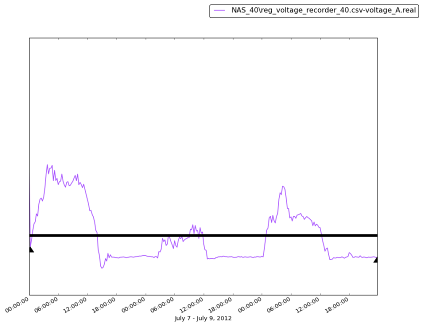
NAS_40\reg_voltage_recorder_40.csv-voltage_A.real
July 7 - July 9, 2012

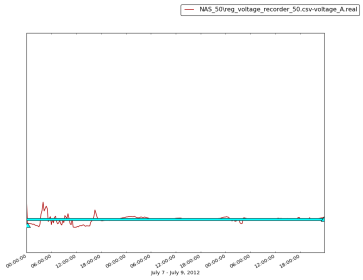
NAS_50\reg_voltage_recorder_50.csv-voltage_A.real
July 7 - July 9, 2012

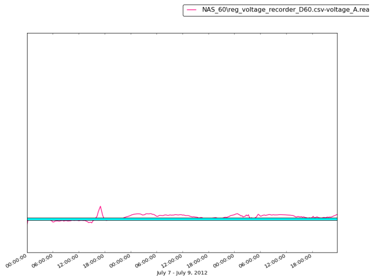
NAS_60\reg_voltage_recorder_D60.csv-voltage_A.rea
July 7 - July 9, 2012

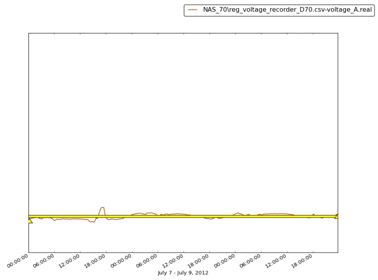
NAS_70\reg_voltage_recorder_D70.csv-voltage_A.real
July 7 - July 9, 2012

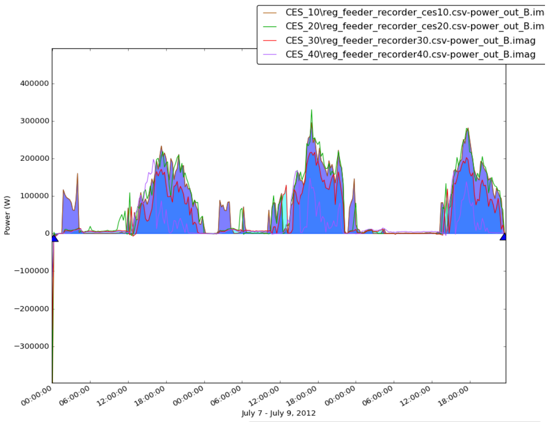
CES_10\reg_feeder_recorder_ces10.csv-power_out_B.im
CES_20\reg_feeder_recorder_ces20.csv-power_out_B.im
CES_30\reg_feeder_recorder30.csv-power_out_B.imag
CES_40\reg_feeder_recorder40.csv-power_out_B.imag
Power (W)
400000
300000
200000
100000
0
−100000
−200000
−300000
July 7 - July 9, 2012

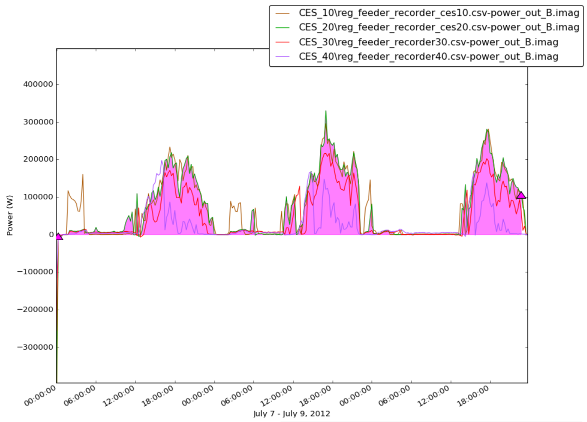
CES_10\reg_feeder_recorder_ces10.csv-power_out_B.imag
CES_20\reg_feeder_recorder_ces20.csv-power_out_B.imag
CES_30\reg_feeder_recorder30.csv-power_out_B.imag
CES_40\reg_feeder_recorder40.csv-power_out_B.imag
Power (W)
400000
300000
200000
100000
0
−100000
−200000
−300000
July 7 - July 9, 2012

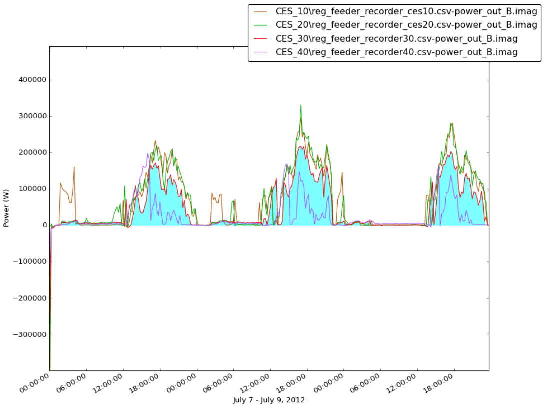
CES_10\reg_feeder_recorder_ces10.csv-power_out_B.imag
CES_20\reg_feeder_recorder_ces20.csv-power_out_B.imag
CES_30\reg_feeder_recorder30.csv-power_out_B.imag
CES_40\reg_feeder_recorder40.csv-power_out_B.imag
Power (W)
400000
300000
200000
100000
0
−100000
−200000
−300000
July 7 - July 9, 2012

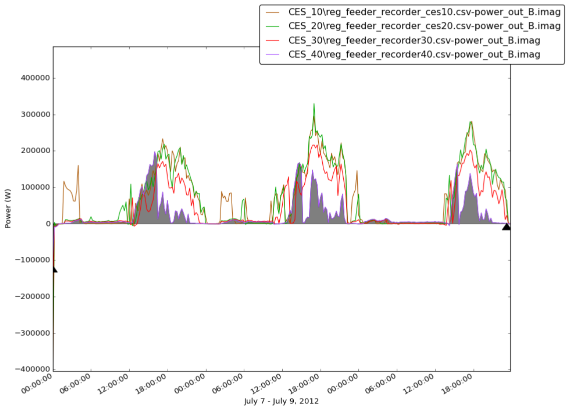
CES_10\reg_feeder_recorder_ces10.csv-power_out_B.imag
CES_20\reg_feeder_recorder_ces20.csv-power_out_B.imag
CES_30\reg_feeder_recorder30.csv-power_out_B.imag
CES_40\reg_feeder_recorder40.csv-power_out_B.imag
Power (W)
400000
300000
200000
100000
0
−100000
−200000
−300000
−400000
July 7 - July 9, 2012

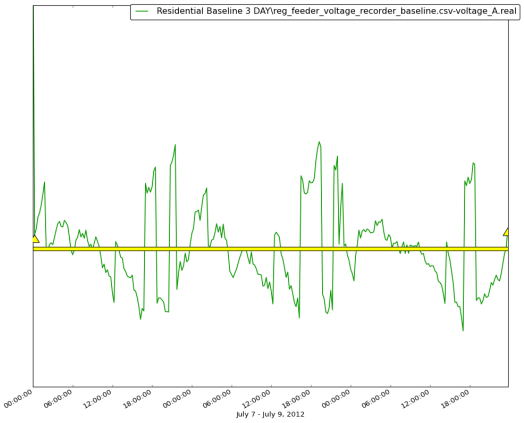
Residential Baseline 3 DAY\reg_feeder_voltage_recorder_baseline.csv-voltage_A.real
00:00:00
06:00:00
12:00:00
18:00:00
00:00:00
06:00:00
12:00:00
18:00:00
00:00:00
06:00:00
12:00:00
18:00:00
July 7 - July 9, 2012

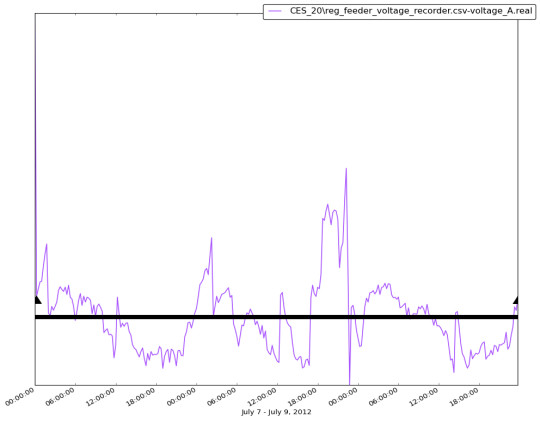
CES_20\reg_feeder_voltage_recorder.csv-voltage_A.real
00:00:00
06:00:00
12:00:00
18:00:00
00:00:00
06:00:00
12:00:00
18:00:00
00:00:00
06:00:00
12:00:00
18:00:00
July 7 - July 9, 2012

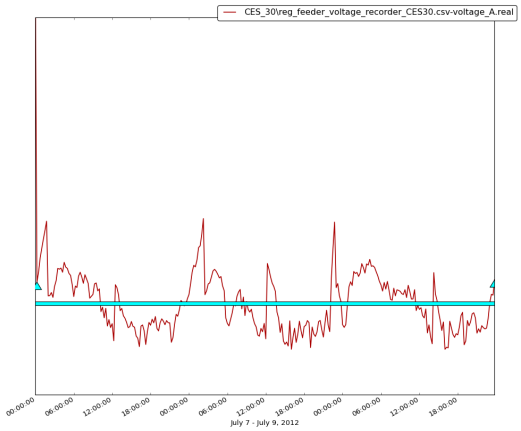
CES_30\reg_feeder_voltage_recorder_CES30.csv-voltage_A.real
00:00:00
06:00:00
12:00:00
18:00:00
00:00:00
06:00:00
12:00:00
18:00:00
00:00:00
06:00:00
12:00:00
18:00:00
July 7 - July 9, 2012

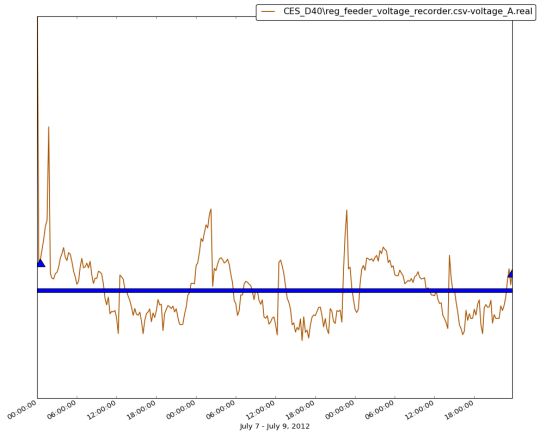
CES_D40\reg_feeder_voltage_recorder.csv-voltage_A.real
00:00:00
06:00:00
12:00:00
18:00:00
00:00:00
06:00:00
12:00:00
18:00:00
00:00:00
06:00:00
12:00:00
18:00:00
July 7 - July 9, 2012

Appendix E. Real power flow comparisons using the B phase (B.real) as opposed to the A phase (A.real) in Figure 5.22. This adjustment in phase selection does not show real power curves for densities 60% and 70% crossing below the baseline throughout the simulation.

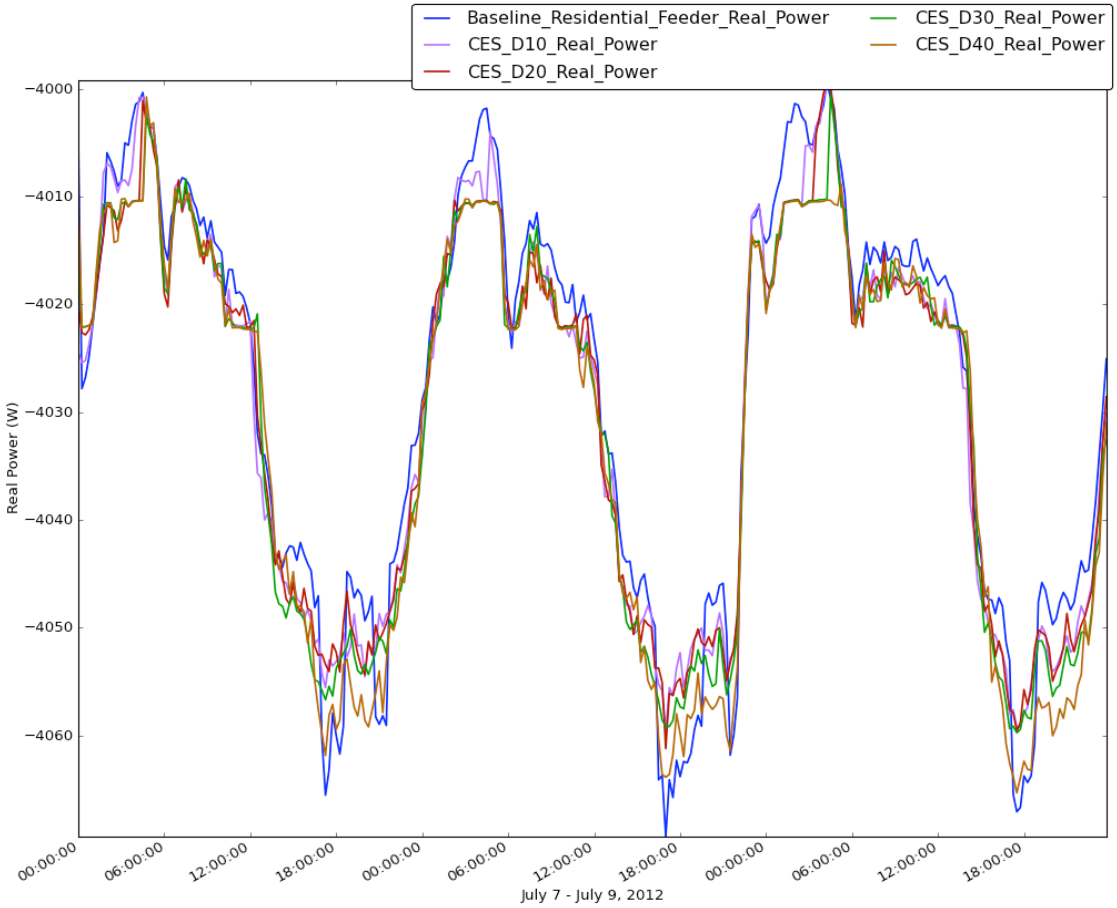

Disclaimer

This thesis was prepared as an account of work sponsored in part by Orkustofnun. Neither the Government of Iceland, the United States Government, nor any agency thereof, nor Battelle Memorial Institute, makes any warranty, express or implied, or assumes any legal liability or responsibility for the accuracy, completeness, or usefulness of any information, data, apparatus, product or process disclosed herein, or represents that its use would not infringe privately owned rights. Reference herein to any specific commercial product, process, or service by trade name, trademark, manufacturer, or otherwise does not necessarily constitute or imply its endorsement, recommendation, or favouring by any agency, Battelle Memorial Institute, the authors or the University of Iceland.

Under Contract OPP111320R2 from Battelle Memorial Institute.